Guidance of Nonlinear Nonminimum-Phase Dynamic Systems

Performance Report

Principal Investigator
Dr. Santosh Devasia
2252 Merrill Engineering Building
Department of Mechanical Engineering
University of Utah
Salt Lake City, Utah 84112
Tel: (801) 581 4613
Email: santosh@me.utah.edu

Administrative Contact for Grantee's Institution
Office of Sponsored Projects
1471 Federal Way
University of Utah
Salt Lake City, Utah 84112

Period: 3/1/97 - 11/14/97

Grant Number: NAG 2-1042

Summary

The first two years research work has advanced the inversion-based guidance theory for:

- systems with non-hyperbolic internal dynamics;
- systems with parameter jumps;
- systems where a redesign of the output trajectory is desired; and
- the generation of recovery guidance maneuvers.

Non-hyperbolic Internal Dynamics

Output tracking for nonminimum phase nonlinear systems with non-hyperbolic and near non-hyperbolic internal dynamics was developed. This approach integrated stable inversion techniques, that achieve exact-tracking, with approximation techniques, that modify the internal dynamics to achieve desirable performance [1]. Such modification of the internal dynamics was used (a) to remove non-hyperbolicity which is an obstruction to applying stable inversion techniques and (b) to reduce large preactuation times needed to apply stable inversion for near non-hyperbolic cases. This approach has been extended to nonlinear systems [2].

Systems with Parameter Jumps

The exact output tracking problem for systems with parameter jumps was considered [3]. Necessary and sufficient conditions were derived for the elimination of switching-introduced output transient. While previous works had studied this problem by developing a regulator that maintains exact tracking through parameter jumps (switches), such techniques are, however, only applicable to minimum-phase systems. In contrast, our approach is also applicable to nonminimum-phase systems and leads to bounded but possibly non-causal solutions. In addition, for the case when the reference trajectories are generated by an exosystem, we developed an exact-tracking controller which could be written in a feedback form. As in standard regulator theory, we also obtained a linear map from the states of the exosystem to the desired system state, which was defined via a matrix differential equation. The constant solution of this differential equation provided asymptotic tracking, and coincided with the feedback law used in standard regulator theory.

Work has been initiated to connect this work to the control of hybrid systems.

Output Trajectory Redesign

We studied the optimal redesign of output trajectory for linear invertible systems [4, 5]. The specified output trajectory uniquely determines the required input and state trajectories, that are found through inversion. These input-state trajectories exactly track the desired output, however, they might not meet acceptable performance requirements. For example, the required inputs might cause actuator-saturation during an exact tracking maneuver, for example, in the flight control of conventional take-off and landing aircraft. In such situations, a compromise is desired between the tracking requirement and other goals like reduction of internal vibrations and prevention of actuator saturation - the desired output trajectory

needs to be redesigned. We posed the trajectory redesign problem as an optimization of a general quadratic cost function, and solved it in the context of linear systems.

This theory is currently being extended to nonlinear systems, and will be applied to (a) the flight control of conventional take-off and landing aircraft and (b) to the guidance of the landing maneuvers for the Space Shuttle. Results will be submitted to the 1998 CDC and the 1998 AIAA Conference on Guidance and Navigation (and to the related journals).

Recovery Guidance Maneuvers for Linear Systems

We studied the development of recovery guidance maneuvers for linear systems which may have actuator-saturation or actuator rate-limits [6]. Note that if a fixed regulator is used to stabilize a desired state trajectory (guidance law), large initial tracking errors can lead to input saturation, which can result in performance deterioration. A method to modify the guidance law for recovering state-trajectory tracking (without violating input and state constraints) was developed. Although it may be usually feasible to find a satisfactory recovery guidance maneuver for a given initial tracking error, online development of recovery guidance maneuvers may not be computationally tractable. A technique was also developed to use precomputed recovery guidance maneuvers (for a finite set of initial tracking errors) to generate recovery guidance maneuvers for other initial errors. The technique was applied to an illustrative example with input-magnitude-limits and input-rate-limits.

The convexity arguments used in this work, along with our results for switched systems, will form the basis of future research into hybrid systems.

References

[1] S. Devasia. Output tracking with non-hyperbolic and near non-hyperbolic internal dynamics: Helicopter hover control. *AIAA J. of Guidance, Control, and Dynamics*, 20(3):573–580, 1997.

[2] S. Devasia. Stable inversion for nonlinear systems with nonhyperbolic internal dynamics. *Submitted to IEEE Trans. Automatic Control, and accepted to CDC 97*, 1997.

[3] S. Devasia, B. Paden, and C. Rossi. Exact-output tracking theory for systems with parameter jumps. *International Journal of Control*, 67(1):117–131, 1997.

[4] S. Devasia. Optimal output-trajectory redesign for invertible systems. *AIAA J. of Guidance, Control, and Dynamics*, 19(5):1189–1191, 1996.

[5] J.S. Dewey and S. Devasia. Experimental and theoretical results in output- trajectory redesign for flexible structures. *CDC 96, also submitted to ASME Journal of Dynamic Systems, Measurement and Control*, 1996.

[6] S. Devasia and G. Meyer. Recovery guidance maneuvers for linear systems with input and state constraints. *Submitted to AIAA Journal of Guidance, Control and Dynamics and to ACC 98*, 1997.

Appendix: Publications

SANTOSH DEVASIA

Department of Mechanical Engineering
U of Utah, SLC, UT 84112
Email: santosh@me.utah.edu

(801) 581 4613 (Work)
(801) 484 8246 (Home)

EDUCATION

- Doctor of Philosophy (December 1993)
  Mechanical Engineering, University of California, Santa Barbara (UCSB)
  Thesis: **Design, Dynamics and Control of Intelligent Structures**
  Major: Dynamic Systems, Controls and Robotics
  Minors: (1) Solid Mechanics and Structures (2) Mathematics
- Masters of Science (December 1990)
  Mechanical Engineering, University of California, Santa Barbara
- Bachelor of Technology (June 1988)
  Mechanical Engineering, Indian Institute of Technology, Kharagpur, India

AWARDS AND HONORS

- The University of California Special Regents Fellowship (1988-92).
- Conference on Decision and Controls (CDC) Best Student Paper Finalist Award (1994)
- Received the Deans Award for outstanding teaching assistant in Mechanical Engineering at UCSB (1992).
- Delco Electronics Corporation's Best Graduate Dissertation Award (1993).
- UCSB School of Engineering Dean's Fellowship (1993-94).
- The National Merit Scholarship for undergraduate study (1984-88).

FUNDING

Nonlinear Inversion-Based High-Speed/High-Precision
Tracking for Scanning-Probe-Based Nanotechnology (PI)
NSF Design and Manufacturing Division, DMI-9612300, 9/1/96-8/30/99, $168,599.

Guidance of Nonlinear Nonminimum Phase Dynamic Systems (PI)
NASA-Ames Research Center, NAG 2-1042, 3/1/96-2/28/98, $49934

Ultrasound Hyperthermia System for Cancer Therapy (Co-Investigator)
NIH-53716(2). 7/1/95-3/31/2000, Five Years, Annual Funding of $237,815.

TEACHING EXPERIENCE

Assistant Professor, Mechanical Eng. Department, U of Utah (Aug. 15, 1994--).

- Current Teaching Interests: Undergraduate and Graduate Courses in Linear and Nonlinear Controls, Integrated Design, Mechatronics, Dynamics, Structural Vibrations, and Finite Element Methods.

JOURNAL PUBLICATIONS

S. Devasia and G. Meyer, "Recovery Guidance Maneuvers for Linear Systems with Input and State Constraints" Submitted to AIAA Journal of Guidance, Control, and Dynamics, September, 1997.

M. Mattingly, R. B. Roemer, and S. Devasia "Optimal Actuator Placement for Large Scale Systems: A Reduced-Order Modeling Approach", Submitted to International Journal of Hyperthermia, July, 1997.

D. Croft and S. Devasia "Hysteresis and Vibration Compensation for Piezo Actuators", Submitted to AIAA Journal of Guidance, Control, and Dynamics, June, 1997.

S. Devasia "Stable Inversion for Nonlinear Systems with Nonhyperbolic Internal Dynamics," Submitted to IEEE Transactions on Automatic Control, June, 1997.

E.A. Bailey, A.W. Dutton, M. Mattingly, S. Devasia and R.B. Roemer "A Comparison of Reduced-Order Modeling Techniques for Application in Hyperthermia Control and Estimation," Submitted to International Journal of Hyperthermia, Oct., 1996.

J.S. Dewey, and S. Devasia "Experimental and Theoretical Results in Output-Trajectory Redesign for Flexible Structures," Submitted to ASME Journal of Dynamic Systems, Measurement, and Control, June, 1996.

M. Mattingly, E. A. Bailey, A. W. Dutton, R. B. Roemer, and S. Devasia "Reduced-order Modeling for Hyperthermia: An Extended Balanced-Realization-Based Approach," Accepted for Publication, IEEE Trans. on Biomedical Eng., 1997.

D. Croft, D. McAllister, and S. Devasia "High-Speed Scanning of Piezo-Actuators for Nanofabrication," Accepted to ASME Journal of Manufacturing Science and Engineering, May., 1997 (to appear in May 1998).

S. Devasia and B. Paden, "Exact Output Tracking for Nonlinear Time-Varying Systems," Accepted to IEEE Transactions on Automatic Control, Feb. 1997.

S. Devasia, B. Paden, and C. Rossi "Exact-Output Tracking Theory for Systems with Parameter Jumps," International J. of Control, Vol. 67 (1), pp. 117-131, May, 1997.

S. Devasia "Output Tracking with Non-Hyperbolic and Near Non-Hyperbolic Internal Dynamics: Helicopter Hover Control," AIAA Journal of Guidance, Control, and Dynamics, Vol. 20 (3), May-June, pp. 573-580, 1997.

S. Devasia, "Optimal Output-Trajectory Redesign for Invertible Systems," AIAA J. of Guidance, Control, and Dynamics, Vol. 19 (5), Sept.-Oct., pp. 1189-1191, 1996.

JOURNAL PUBLICATIONS

S. Devasia, D. Chen, and B. Paden, " Nonlinear Inversion-Based Output Tracking" IEEE Transactions on Automatic Control, Vol. 41 (7), pp. 930-942, July, 1996.

Ph. Martin, S. Devasia, and B. Paden, "A different look at output tracking: Control of a VTOL Aircraft," Automatica, Vol. 32 (1), pp. 101-107, January 1996.

S. Devasia, and E. Bayo, "Redundant Actuators to Achieve Minimal Vibration Tracking of Flexible Multibodies: Theory and Application," Journal of Nonlinear Dynamics , Vol. 6, pp. 419-431, 1994.

R. Ledesma, S. Devasia, and E. Bayo, " Inverse Dynamics of Spatial Open-Chain Flexible Manipulators with Lumped and Distributed Actuators," Journal of Robotics Systems, Vol. 11 (4), pp. 327-338, 1994.

S. Devasia, and E. Bayo, " Inverse Dynamics: Simultaneous Trajectory Tracking and Vibration Reduction with Distributed Actuators, "Journal of Dynamics and Control, Vol. 4, pp. 299-309, 1994.

S. Devasia, T. Meressi, B. Paden, and E. Bayo, " Piezo-electric Actuator Design for Vibration Suppression: Placement and Sizing, " AIAA Journal of Guidance, Control and Dynamics , Vol. 16 (5), pp. 859-864, 1993.

Output Tracking with Nonhyperbolic and Near Nonhyperbolic Internal Dynamics: Helicopter Hover Control

S. Devasia

Reprinted from

Journal of Guidance, Control, and Dynamics

Volume 20, Number 3, Pages 573–580

A publication of the
American Institute of Aeronautics and Astronautics, Inc.
1801 Alexander Bell Drive, Suite 500
Reston, VA 20191–4344

JOURNAL OF GUIDANCE, CONTROL, AND DYNAMICS
Vol. 20, No. 3, May–June 1997

Output Tracking with Nonhyperbolic and Near Nonhyperbolic Internal Dynamics: Helicopter Hover Control

Santosh Devasia*
University of Utah, Salt Lake City, Utah 84112

A technique to achieve output tracking for nonminimum phase linear systems with nonhyperbolic and near nonhyperbolic internal dynamics is presented. This approach integrates stable inversion techniques, which achieve exact tracking, with approximation techniques, which modify the internal dynamics, to achieve desirable performance. Such modification of the internal dynamics is used 1) to remove nonhyperbolicity, which is an obstruction to applying stable inversion techniques, and 2) to reduce large preactuation times needed to apply stable inversion for near nonhyperbolic cases. The method is applied to an example helicopter hover control problem with near nonhyperbolic internal dynamics for illustrating the tradeoff between exact tracking and reduction of preactuation time.

I. Introduction

PRECISION output tracking controllers are needed to meet increasingly stringent performance requirements in applications such as flexible structures, aircraft and air traffic control, robotics, and manufacturing systems. Although perfect tracking of minimum phase systems is relatively easy to achieve, output tracking of nonminimum phase systems tends to be more challenging due to fundamental limitations on transient tracking performance.[1] This poor transient performance has been mitigated by using preactuation in the stable inversion-based approaches for nonminimum phase systems.[2–5] However, the required preactuation time (during which most of the preactuation control effort is required) is large if the zeros of a linear system that lie on the open right-half of the complex plane are close to the imaginary axis. In the limiting case, with the zeros on the imaginary axis (nonhyperbolic internal dynamics), presently available inversion-based techniques fail because the preactuation time needed becomes infinite. We present a design technique for output tracking of linear nonminimum phase systems, which have nonhyperbolic and near nonhyperbolic nonminimum phase internal dynamics. This technique is then applied to an example helicopter hover control problem, and simulation results are presented.

Output tracking has a long history marked by the development of regulator theory for linear systems by Francis and Wonham[6] and the generalization to the nonlinear case by Isidori and Byrnes.[7] These approaches asymptotically track an output from a class of exosystem-generated outputs. Further, the Isidori–Byrnes regulator has been extended in Refs. 8 and 9 and computational issues have been studied in Refs. 10 and 11. Although nonlinear regulator design is computationally difficult, the linear regulator is easily designed by solving a manageable set of linear equations. A problem, however, with the regulator approach is that the exosystem states are often switched to describe the desired output; this leads to transient tracking errors after the switching instants. Such switching-caused transient errors can be avoided by using inversion-based approaches to output tracking.[4,12] Thus, it is advantageous to use inversion-based output tracking when precision tracking of a particular output trajectory is required.

Inversion, which is key to our approach, was restricted to causal inverses of minimum phase systems in the early works by Silverman[13] and Hirschorn[14] because these approaches lead to unbounded inverses in the nonminimum phase case. Di Benedetto and Lucibello[15] considered the inversion of time varying nonminimum phase systems with a choice of the system's initial conditions. Instead of choosing initial conditions, preactuation was used by noncausal stable inversion techniques developed in Refs. 2–5 and 16. Such noncausal inverses, which require preactuation, have been successfully applied to the output tracking of flexible structures[17,18] and aircraft and air traffic control.[19,20] However, the fundamental limitation of presently available inversion schemes is that they fail if the internal dynamics is nonhyperbolic. Even when the internal dynamics is hyperbolic, if the right-half-plane zeros of the system are close to the imaginary axis (the near nonhyperbolic case), then the required preactuation time tends to become unacceptably large. In summary, output tracking remains a challenge for nonminimum phase systems with nonhyperbolic or near nonhyperbolic internal dynamics.

There are several approximation-based output tracking techniques, where the central philosophy is to replace the internal dynamics with a dynamics that provides satisfactory behavior, and then to develop the controller based on the altered system.[21–23] The technique most relevant to this paper is developed by Gopalswamy and Hedrick,[23] where trajectory modifications are considered to stabilize the internal dynamics. This technique, however, requires hyperbolicity of the internal dynamics for computational purposes. The development of computational techniques for stable inversion (e.g., Ref. 16) motivates the present integration of the stable inversion scheme with approximation techniques, especially for systems with nonhyperbolic internal dynamics where the existing stable inversion techniques fail. However, instead of stabilizing the unstable internal dynamics, we only aim to modify the nonhyperbolic behavior with a small perturbation of the internal dynamics. Additionally, in nonminimum phase systems with near nonhyperbolic internal dynamics, the present approach allows a tradeoff between the precision tracking requirement and the amount of preactuation time needed to apply the stable inversion-based output tracking technique.

The approximate inversion-based technique is developed in Sec. II, and the technique is applied to a helicopter hover control example in Sec. III, where simulation results are discussed. Conclusions are in Sec. IV.

II. Stable Inversion

A. Inversion-Based Output Tracking Scheme

Here we describe how the inversion approach is used to develop output tracking controllers. Consider a linear system described by

$$\dot{\boldsymbol{x}}(t) = A\boldsymbol{x}(t) + B\boldsymbol{u}(t), \qquad \boldsymbol{y}(t) = C\boldsymbol{x}(t) \tag{1}$$

which has the same number of inputs as outputs, $\boldsymbol{u}(t), \boldsymbol{y}(t) \in \Re^p$, and $\boldsymbol{x}(t) \in \Re^n$. Let $\boldsymbol{y}_d(\cdot)$ be the desired output trajectory to be tracked. Then in the inversion-based approach, first, we find a nominal input-state trajectory $[\boldsymbol{u}_{\rm ff}(\cdot), \boldsymbol{x}_{\rm ref}(\cdot)]$ that satisfies the system equations (1) and yields the desired output exactly, i.e.,

$$\left.\begin{aligned} \dot{\boldsymbol{x}}_{\rm ref}(t) &= A\boldsymbol{x}_{\rm ref}(t) + B\boldsymbol{u}_{\rm ff}(t) \\ \boldsymbol{y}_d(t) &= C\boldsymbol{x}_{\rm ref}(t) \end{aligned}\right\} \qquad \forall t \in (-\infty, \infty) \tag{2}$$

Received Oct. 2, 1996; revision received Jan. 14, 1997; accepted for publication Jan. 28, 1997.

*Assistant Professor, Department of Mechanical Engineering. Member AIAA.

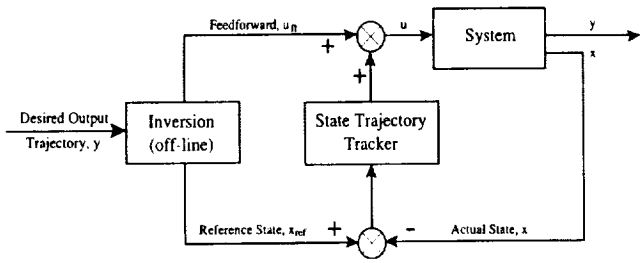

Fig. 1 Control scheme.

Second, we stabilize the exact-output yielding state trajectory $x_{ref}(\cdot)$ by using state feedback (see Fig. 1). Thus, $x(t) \to x_{ref}(t)$ and $y(t) \to y_d(t)$ as $t \to \infty$, and output tracking is achieved. It is noted that in this output tracking scheme, the reference state trajectory $x_{ref}(\cdot)$ and the feedforward input $u_{ff}(\cdot)$ are computed off-line. Whereas stabilization of the reference state trajectory can be easily achieved through standard techniques[24] such as state feedback of the form $K[x(t)-x_{ref}(t)]$, the main challenge is to find the inverse input-state trajectory $[u_{ff}(\cdot), x_{ref}(\cdot)]$, especially for systems with nonminimum phase dynamics. This paper addresses the off-line computation of the inverse input-state trajectory for a given desired trajectory, $y_d(\cdot)$.

B. Internal Dynamics

In this subsection, it is shown that finding the inverse input-state trajectory is equivalent to finding bounded solutions to the system's internal dynamics. Let the linear system (1) have a well-defined vector relative degree, $r := [r_1, r_2, \ldots, r_p]$. Then the output's derivatives are given as[25]

$$\frac{d^{r_k} y_k}{dt^{r_k}} = C_k A^{r_k} x + C_k A^{r_k - 1} B u \tag{3}$$

where C_k is the kth row of C and $1 \le k \le p$. In vector notation, let Eq. (3) be rewritten as

$$y^{(r)}(t) = A_x x(t) + B_y u(t) \tag{4}$$

where

$$y^{(r)} := \begin{bmatrix} \frac{d^{r_1} y_1}{dt^{r_1}} & \frac{d^{r_2} y_2}{dt^{r_2}} & \cdots & \frac{d^{r_p} y_p}{dt^{r_p}} \end{bmatrix}^T$$

$$A_x := \begin{bmatrix} C_1 A^{r_1} \\ C_2 A^{r_2} \\ \vdots \\ C_p A^{r_p} \end{bmatrix} \qquad B_y := \begin{bmatrix} C_1 A^{r_1 - 1} B \\ C_2 A^{r_2 - 1} B \\ \vdots \\ C_p A^{r_p - 1} B \end{bmatrix}$$

and B_y is invertible because of the well-defined relative degree assumption. Equation (4) motivates the choice of the control law of the form

$$u_{ff}(t) = B_y^{-1}\left[y_d^{(r)}(t) - A_x x(t)\right] \tag{5}$$

for all $t \in (-\infty, \infty)$. Substituting this control law in Eq. (4), it is seen that exact tracking is maintained, i.e.,

$$y^{(r)}(t) = y_d^{(r)}(t)$$

To study the effect of this control law, consider a change of coordinates T such that[25]

$$\begin{bmatrix} \zeta(t) \\ \eta(t) \end{bmatrix} = T x(t)$$

where $\zeta(t)$ consists of the output and its time derivatives

$$\zeta(t) := \left[y_1, \dot{y}_1, \ldots, \frac{d^{r_1 - 1}}{dt^{r_1 - 1}} y_1, y_2, \dot{y}_2, \ldots, \frac{d^{r_2 - 1}}{dt^{r_2 - 1}} y_2, \right.$$

$$\left. \ldots, y_p, \dot{y}_p, \ldots, \frac{d^{r_p - 1}}{dt^{r_p - 1}} y_p \right]^T$$

The system equation (1) can then be rewritten in the new coordinates as

$$\dot{\zeta}(t) = \hat{A}_1 \zeta + \hat{A}_2 \eta + \hat{B}_1 u \tag{6}$$

$$\dot{\eta}(t) = \hat{A}_3 \zeta + \hat{A}_4 \eta + \hat{B}_2 u \tag{7}$$

where

$$\hat{A} := T^{-1} A T := \begin{bmatrix} \hat{A}_1 & \hat{A}_2 \\ \hat{A}_3 & \hat{A}_4 \end{bmatrix} \quad \text{and} \quad \hat{B} := \begin{bmatrix} \hat{B}_1 \\ \hat{B}_2 \end{bmatrix} = T^{-1} B$$

In the new coordinates, the control law for maintaining exact tracking [Eq. (5)] can be written as

$$u(t) = B_y^{-1}\left[y_d^{(r)}(t) - A_\zeta \zeta_d(t) - A_\eta \eta(t)\right] \tag{8}$$

where

$$\begin{bmatrix} A_\zeta \\ A_\eta \end{bmatrix} := A_x T^{-1}$$

Note that the desired $\zeta(\cdot)$ is known when the desired output trajectory $y_d(\cdot)$ and the output's time derivatives are specified. This desired $\zeta(\cdot)$ is defined as $\zeta_d(\cdot)$. Inasmuch as the control law was chosen such that exact tracking is maintained, $y^{(r)}(t) = y_d^{(r)}(t)$, we also have $\dot{\zeta}(t) = \dot{\zeta}_d(t)$, and Eqs. (6) and (7) become

$$\dot{\zeta}(t) = \dot{\zeta}_d(t) \tag{9}$$

$$\dot{\eta}(t) = \hat{A}_3 \zeta + \hat{A}_4 \eta + \hat{B}_2 B_y^{-1}\left[y_d^{(r)}(t) - A_\zeta \zeta_d(t) - A_\eta \eta(t)\right] \tag{10}$$

This is the inverse system, and in particular, Eq. (10) is the internal dynamics. Solving the internal dynamics is key to finding the inverse input-state trajectories. If a bounded solution $\eta_d(\cdot)$ to the internal dynamics (10) can be found, then the feedforward input can be found through Eq. (8) as

$$u_{ff}(t) = B_y^{-1}\left[y_d^{(r)}(t) - A_\zeta \zeta_d(t) - A_\eta \eta_d(t)\right] \tag{11}$$

and the reference trajectory can be found as

$$x_{ref}(t) = T^{-1}\begin{bmatrix} \zeta_d(t) \\ \eta_d(t) \end{bmatrix}$$

Thus, a bounded solution to the internal dynamics (10) is required to find the inverse and to apply the output tracking scheme shown in Fig. 1.

C. Modified Internal Dynamics

Standard inversion schemes[13,14] that integrate (forward in time) the internal dynamics (10) lead to unbounded solutions because the internal dynamics is unstable for nonminimum phase systems. Noncausal inversion (e.g., Ref. 4) leads to a bounded but noncausal solution to the internal dynamics. Such stable inversion techniques are, however, not applicable to systems with nonhyperbolic internal dynamics. In this subsection a compromise between stable inversion and approximation-based inversion schemes is proposed. The key is to modify the internal dynamics by giving up exact output tracking, enough to remove the nonhyperbolicity, and then to apply stable inversion. Note that the system zeros are not being modified by output feedback (which is impossible): rather, the inverse system is perturbed to a nearby system, which has better behaved internal dynamics, for stable inversion. The difference between the proposed technique and other approximation techniques is that the internal dynamics is perturbed only to remove the nonhyperbolicity and not to stabilize the entire internal dynamics.

To change the nonhyperbolicity of the internal dynamics, an extra term, $v(t)$, is added to the control law (8) as follows:

$$u_{ff}(t) = B_y^{-1}\left[y_d^{(r)}(t) - A_\zeta \zeta(t) - A_\eta \eta(t) + v(t)\right] \tag{12}$$

With this modified control law, the inverse system [Eqs. (9) and (10)] becomes

$$\frac{\mathrm{d}}{\mathrm{d}t}\begin{bmatrix} e_\zeta(t) \\ \eta(t) \end{bmatrix} = \hat{S}\begin{bmatrix} e_\zeta(t) \\ \eta(t) \end{bmatrix} + G_y Y_d(t) + G_v v(t) \tag{13}$$

where $e_\zeta(t) := \zeta(t) - \zeta_d(t)$ is the error in the output and the output's derivatives,

$$\hat{S} = \begin{bmatrix} \hat{A}_1^* & 0 \\ \left(\hat{A}_3 - \hat{B}_2 B_y^{-1} A_\zeta\right) & \left(\hat{A}_4 - \hat{B}_2 B_y^{-1} A_\eta\right) \end{bmatrix}, \quad G_v = \begin{bmatrix} \hat{B}_1 B_y^{-1} \\ \hat{B}_2 B_y^{-1} \end{bmatrix}$$

$$G_y = \begin{bmatrix} 0 & 0 \\ \left(\hat{A}_3 - \hat{B}_2 B_y^{-1} A_\zeta\right) & \hat{B}_2 B_y^{-1} \end{bmatrix}, \quad Y_d(t) = \begin{bmatrix} \zeta_d(t) \\ y_d^{(r)}(t) \end{bmatrix}$$

$$\hat{A}_1^* := \mathrm{diag}[A_1, A_2, \ldots, A_p]$$

where each A_i is an $r_i \times r_i$ zero-matrix with ones on the elements above the main diagonal (for all $1 \le i \le p$).

Assuming that the original system (A, B) is controllable, we also have $(\hat{S}, G_v)$ controllable, and hence there exists a feedback of the form

$$v(t) = F\begin{bmatrix} e_\zeta(t) \\ \eta(t) \end{bmatrix} \tag{14}$$

such that the modified inverse system (13) is hyperbolic; i.e., all poles on the imaginary axis are moved. Note that this change to an hyperbolic system can be achieved through arbitrarily small F because nonhyperbolicity is not a structurally stable property. The hyperbolic system

$$\frac{\mathrm{d}}{\mathrm{d}t}\begin{bmatrix} e_\zeta(t) \\ \eta(t) \end{bmatrix} = (\hat{S} + G_v F)\begin{bmatrix} e_\zeta(t) \\ \eta(t) \end{bmatrix} + G_y Y_d(t)$$

$$:= S\begin{bmatrix} e_\zeta(t) \\ \eta(t) \end{bmatrix} + G_y Y_d(t) \tag{15}$$

is the modified inverse system. This modification of the internal dynamics can also be used to move unstable poles of the inverse system that may be close to the imaginary axis for reducing the required preactuation time. Next, stable inversion of the modified inverse system is carried out.[4]

D. Computation of the Inverse

We begin by decoupling the modified inverse system (15) into stable (z_s) and unstable (z_u) subsystems. Because the modified inverse system is hyperbolic, there exits a decoupling transformation U such that the modified inverse system (15) can be written as

$$\dot{z}_s(t) = S_s z_s(t) + G_s Y_d(t), \qquad \dot{z}_u(t) = S_u z_u(t) + G_u Y_d(t) \tag{16}$$

where

$$z(t) := \begin{bmatrix} z_s(t) \\ z_u(t) \end{bmatrix} = U\begin{bmatrix} e_\zeta(t) \\ \eta(t) \end{bmatrix} \tag{17}$$

To find bounded solutions to the unstable inverse systems, the boundary conditions that $z_s(-\infty) = 0$ and $z_u(\infty) = 0$ are applied to Eq. (16). This leads to unique bounded solutions to the modified inverse system by flowing the stable subsystem forward in time and flowing the unstable system backward in time as

$$z_{s,d}(t) = \int_{-\infty}^{t} e^{S_s(t-\tau)} G_u Y_d(\tau)\,\mathrm{d}\tau \qquad \forall t \in (-\infty, \infty)$$

$$z_{u,d}(t) = -\int_{t}^{\infty} e^{S_u(t-\tau)} G_u Y_d(\tau)\,\mathrm{d}\tau \qquad \forall t \in (-\infty, \infty) \tag{18}$$

This completes the technique. To summarize, the bounded solution (18) is used to find the reference state trajectory as $x_{\mathrm{ref}}(t) = T^{-1}U^{-1}z_d(t)$ and to find the feedforward input $u_{\mathrm{ff}}(\cdot)$ from Eq. (12). This inverse, $[u_{\mathrm{ff}}(\cdot), x_{\mathrm{ref}}(\cdot)]$, is then used in the control scheme shown in Fig. 1 to obtain output tracking.

E. Preactuation Time and Unstable Poles of the Inverse System

The connection between the amount of preactuation time required to apply the inversion-based feedforward input and the unstable poles of the modified inverse is established in the following Lemma.

Lemma:

1) Let the support of $Y_d(\cdot)$ be contained in $[t_0, \infty)$ for some t_0.

2) Let all of the unstable poles of internal dynamics represented by the eigenvalues of S_u lie to the right, in the complex plane, of the line $\mathrm{Re}(s) = \alpha$ for some positive α.

3) Let $\|G_u Y_d(\cdot)\|_\infty < \beta$.

Then there exists M such that $\|u_{\mathrm{ff}}(t)\|_\infty < Me^{\alpha(t-t_0)}$ for all time before the start of the maneuver, $t < t_0$.

Proof: From condition 2 of the Lemma, there exists a positive constant M_{S_u} such that

$$\left\|e^{S_u(t-\tau)}\right\|_\infty < M_{S_u} e^{\alpha(t-\tau)} \qquad \forall t < \tau \tag{19}$$

Then for all $t < t_0$,

$$\|u_{\mathrm{ff}}(t)\|_\infty = \left\|B_y^{-1}\left[y_d^{(r)}(t) - A_\zeta \zeta(t) - A_\eta \eta(t) + v(t)\right]\right\|_\infty$$

from Eq. (12)

$$= \left\|B_y^{-1}[-A_\zeta \zeta - A_\eta \eta(t) + v(t)]\right\|_\infty$$

from condition 1 of Lemma

$$= \left\|\left(\begin{bmatrix} 0 & 0 \\ -B_y^{-1}A_\zeta & -B_y^{-1}A_\eta \end{bmatrix} + F\right)\begin{bmatrix} e_\zeta(t) \\ \eta(t) \end{bmatrix}\right\|_\infty$$

from Eq. (14) and condition 1 of Lemma

$$:= \left\|A_U\begin{bmatrix} e_\zeta(t) \\ \eta(t) \end{bmatrix}\right\|_\infty$$

$$\le \|A_U\|_\infty \left\|\begin{bmatrix} e_\zeta(t) \\ \eta(t) \end{bmatrix}\right\|_\infty$$

$$\le \|A_U\|_\infty \|U^{-1}\|_\infty \left\|\begin{bmatrix} z_s(t) \\ z_u(t) \end{bmatrix}\right\|_\infty \quad \text{from Eq. (17)}$$

$$= \|A_U\|_\infty \|U^{-1}\|_\infty \|z_u(t)\|_\infty$$

because $z_s(t) = \mathbf{0}$ for all $t < t_0$

$$= \|A_U\|_\infty \|U^{-1}\|_\infty \left\|\int_t^\infty e^{S_u(t-\tau)} G_u Y_d(\tau)\,\mathrm{d}\tau\right\|_\infty$$

from Eq. (18)

$$= \|A_U\|_\infty \|U^{-1}\|_\infty \left\|\int_{t_0}^\infty e^{S_u(t-\tau)} G_u Y_d(\tau)\,\mathrm{d}\tau\right\|_\infty$$

from condition 1 of Lemma

$$< \beta M_{S_u} \|A_U\|_\infty \|U^{-1}\|_\infty \int_{t_0}^\infty e^{\alpha(t-\tau)}\,\mathrm{d}\tau$$

from Eq. (19) and condition 3 of the Lemma. Integrating the preceding expression, we get

$$\|u_{\mathrm{ff}}(t)\|_\infty < \left(\beta M_{S_u}/\alpha\right)\|A_U\|_\infty \|U^{-1}\|_\infty e^{\alpha(t-t_0)}$$

$$:= Me^{\alpha(t-t_0)}$$

which concludes the proof. □

The Lemma states that the preactuation input tends to zero exponentially, as we go back in time from the start of the maneuver at t_0. The rate at which the preactuation becomes zero can be increased by moving the unstable poles of the modified inverse away from the imaginary axis at the expense of exact output tracking. The tradeoff between exact tracking of the desired output and reduction of the preactuation time is illustrated in the following example.

III. Example: Helicopter Hover Control

Here, we apply the output-tracking technique to the hover control of a Bell 205 helicopter, which has near nonhyperbolic unstable internal dynamics. We consider one of the cases studied in Ref. 26, wherein the aircraft dynamics was trimmed at a nominal 5-deg pitch attitude, with a midrange weight and a midposition center of gravity and operating in-ground effect at near sea level. The linearized model is given as[26,27]

$$\dot{x} = Ax + Bu \tag{20}$$

where

$$A = \begin{bmatrix} 0 & 0.03 & 0.18 & -0.01 & -0.42 & 0.08 & -9.81 & 0 \\ -0.10 & -0.39 & 0.09 & -0.10 & -0.72 & 0.68 & 0 & 0 \\ 0.01 & -0.01 & -0.19 & 0 & 0.23 & 0.04 & 0 & 0 \\ 0.02 & 0 & -0.41 & -0.05 & -0.27 & 0.27 & 0 & 9.81 \\ 0.03 & -0.02 & -0.88 & -0.04 & -0.57 & 0.14 & 0 & 0 \\ -0.01 & -0.02 & -0.06 & 0.07 & -0.32 & -0.71 & 0 & 0 \\ 0 & 0 & 1 & 0 & 0 & 0 & 0 & 0 \\ 0 & 0 & 0 & 0 & 1 & 0 & 0 & 0 \end{bmatrix} \tag{21}$$

$$B = \begin{bmatrix} 0.08 & 0.13 & 0 & 0 \\ -1.17 & 0.04 & 0 & 0.01 \\ 0 & -0.07 & 0 & 0.01 \\ -0.04 & 0 & 0.11 & 0.19 \\ -0.04 & 0 & 0.22 & 0.17 \\ 0.17 & 0 & 0.03 & -0.47 \\ 0 & 0 & 0 & 0 \\ 0 & 0 & 0 & 0 \end{bmatrix} \tag{22}$$

$$x = \begin{bmatrix} U \\ W \\ Q \\ V \\ P \\ R \\ \theta \\ \phi \end{bmatrix} \tag{23}$$

where U is forward velocity, W vertical velocity, Q pitch rate, V lateral velocity, P roll rate, R yaw rate, θ pitch attitude, and ϕ roll attitude, and

$$u = \begin{bmatrix} \delta_C \\ \delta_B \\ \delta_A \\ \delta_P \end{bmatrix} \tag{24}$$

where δ_C is collective, δ_B longitudinal cyclic, δ_A lateral cyclic, and δ_P tail rotor collective.

It is noted that the helicopter's actual dynamic behavior differs because of modeling errors such as nonlinearities and unmodeled dynamics. In output tracking control schemes that depend on the model, such modeling errors need to be corrected through feedback in the control scheme (see Fig. 1). In particular, modeling errors can be compensated by robust stabilization of the reference state trajectory (see, for example, Ref. 26). The goal is to develop inversion-based feedforward and reference state trajectories for use in the control scheme shown in Fig. 1. In the following, we apply the inversion technique to control the helicopter's forward, lateral, and vertical velocities and its yaw rate. The forward velocity and the yaw rate are to be kept at zero, and the desired profiles of lateral and vertical velocities and accelerations are as shown in Figs. 2 and 3.

A. Internal Dynamics

To find the internal dynamics, we begin with a change in the coordinates. Let ζ be defined as the outputs

$$\zeta(t) := \begin{bmatrix} U(t) \\ W(t) \\ V(t) \\ R(t) \end{bmatrix} \tag{25}$$

and let η be the remaining states

$$\eta(t) := \begin{bmatrix} Q(t) \\ \theta(t) \\ P(t) \\ \phi(t) \end{bmatrix} \tag{26}$$

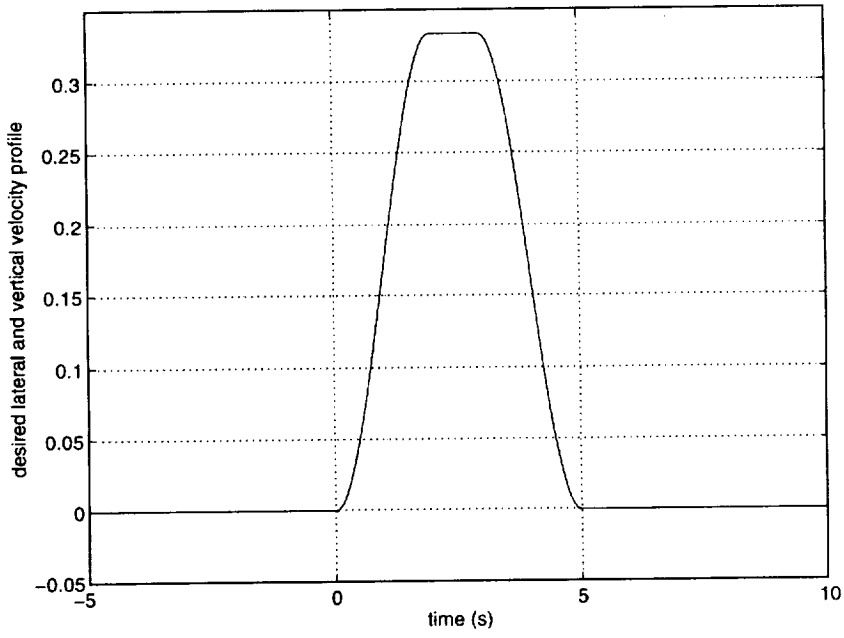

Fig. 2 Desired lateral and vertical velocity profile.

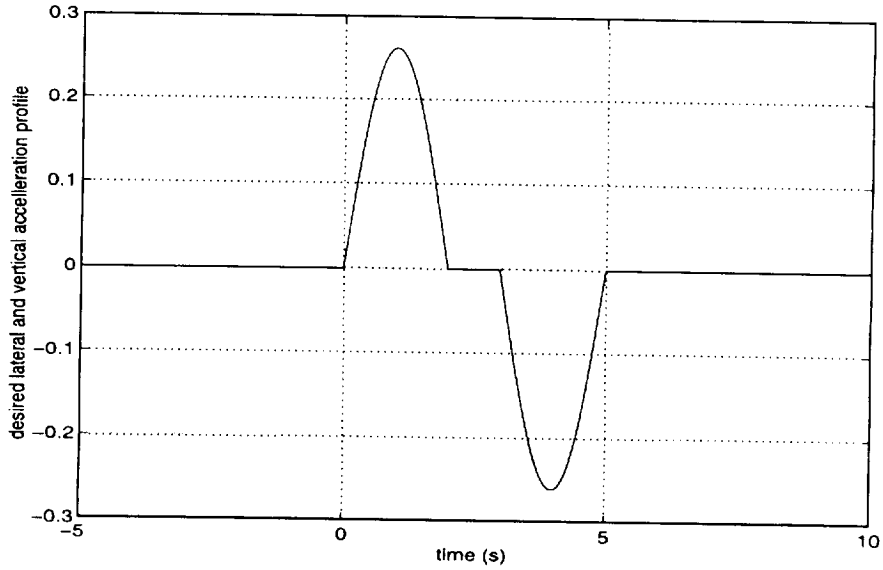

Fig. 3 Desired lateral and vertical acceleration profile.

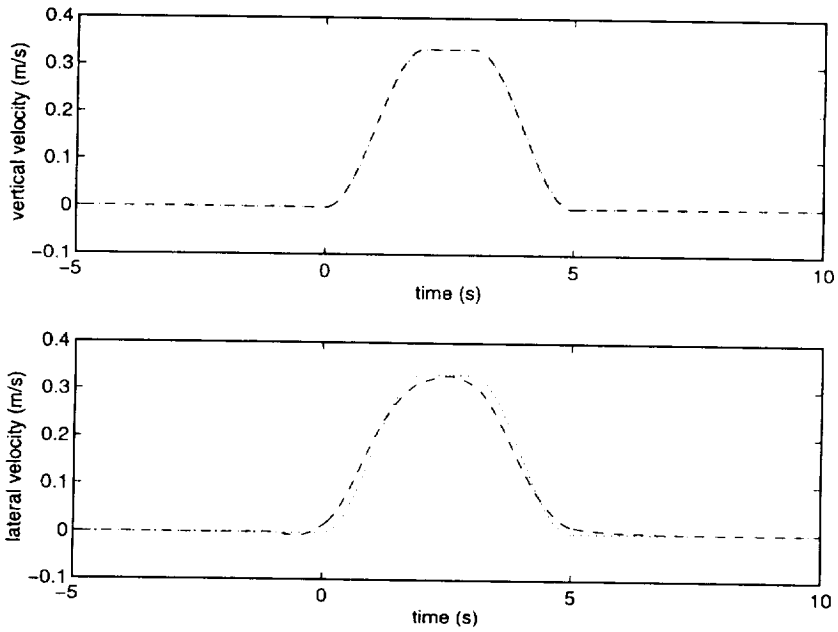

Fig. 4 Lateral and vertical velocity achieved by the inverse reference state trajectory: · · · ·, exact-tracking case without modification of the internal dynamics and – – –, with modification.

In the (ζ, η) coordinate system, given by

$$\begin{bmatrix}\zeta(t)\\ \eta(t)\end{bmatrix} = \begin{bmatrix} 1&0&0&0&0&0&0&0\\ 0&1&0&0&0&0&0&0\\ 0&0&0&1&0&0&0&0\\ 0&0&0&0&0&1&0&0\\ 0&0&1&0&0&0&0&0\\ 0&0&0&0&0&0&1&0\\ 0&0&0&0&1&0&0&0\\ 0&0&0&0&0&0&0&1 \end{bmatrix} x(t)$$

$$:= Tx(t) \tag{27}$$

the system equations can be rewritten as

$$\begin{bmatrix}\dot\zeta(t)\\ \dot\eta(t)\end{bmatrix} = TAT^{-1}\begin{bmatrix}\zeta(t)\\ \eta(t)\end{bmatrix} + TBu(t)$$

$$:= \begin{bmatrix}A_1 & A_2\\ A_3 & A_4\end{bmatrix}\begin{bmatrix}\zeta(t)\\ \eta(t)\end{bmatrix} + \begin{bmatrix}B_1\\ B_2\end{bmatrix}u(t) \tag{28}$$

Given a desired output trajectory and the desired output's time derivatives, $[\zeta_d(\cdot), \dot\zeta_d(\cdot)]$, the exact output tracking control law (see Sec. II.D) is found from Eq. (28) as

$$u_{\text{ff}}(t) = B_1^{-1}[\dot\zeta_d(t) - A_1\zeta_d(t) - A_2\eta(t)] \tag{29}$$

With this control law, the inverse system becomes [from Eq. (28)]

$$\dot\zeta(t) = \dot\zeta_d(t) \tag{30}$$

$$\begin{aligned}\dot\eta(t) &= A_4\eta(t) + A_3\zeta(t) + B_2u(t)\\ &= \left[A_4 - B_2B_1^{-1}A_2\right]\eta(t) + B_2B_1^{-1}[\dot\zeta_d(t) - A_1\zeta_d(t)]\\ &:= A_\eta\eta(t) + B_2B_1^{-1}[\dot\zeta_d(t) - A_1\zeta_d(t)]\end{aligned} \tag{31}$$

The problem is solved by finding a bounded solution to the internal dynamics (31). However, the bounded solution found through stable inversion is noncausal and could require a large preactuation time if the poles of the internal dynamics are unstable and lie close to the imaginary axis in the complex plane. For this particular example, there are two such complex conjugate poles near the imaginary axis, $0.0425 \pm 4.3055i$. We modify the exact tracking control law (29) to

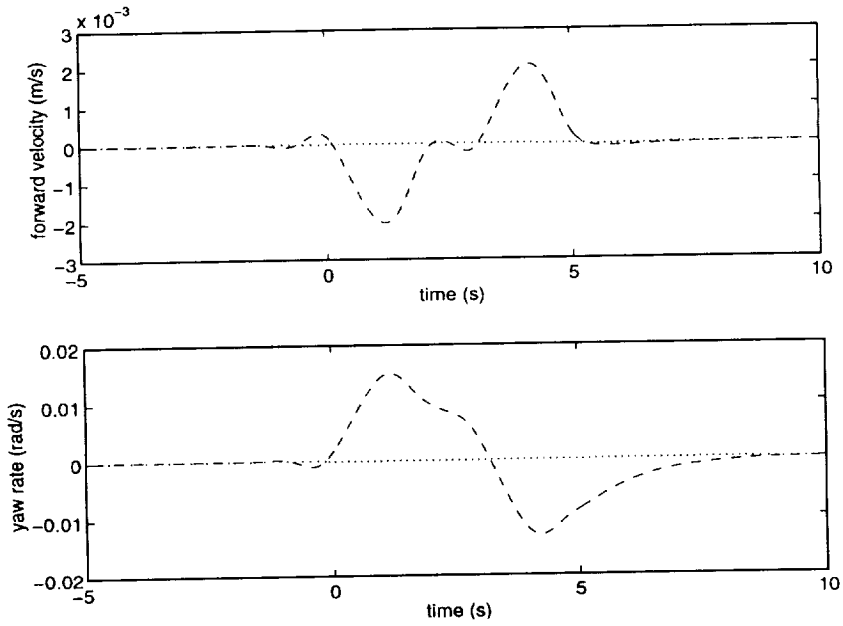

Fig. 5 Forward velocity and yaw rate achieved by the inverse reference state trajectory, the desired value is zero: · · · · ·, exact-tracking case without modification of the internal dynamics and – – –, with modification.

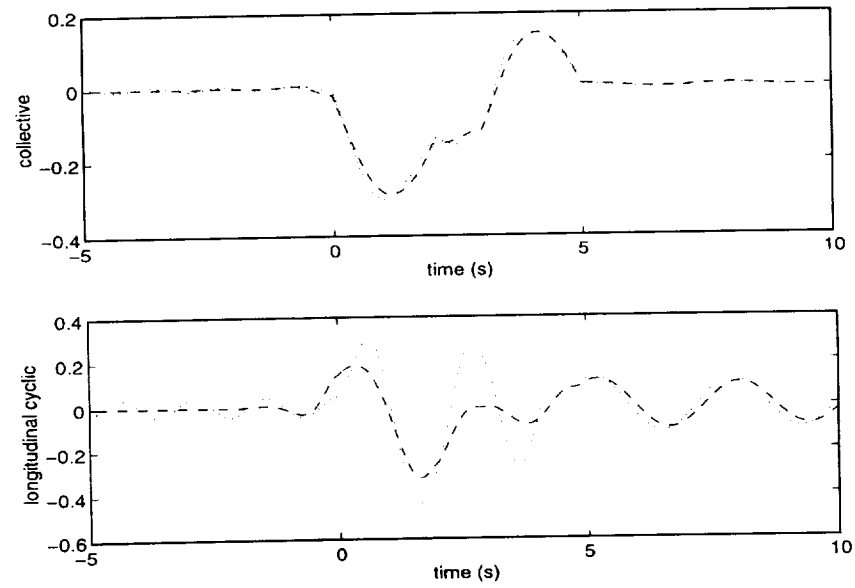

Fig. 6 Feedforward inputs: · · · · ·, without modification of internal dynamics and – – –, with modification.

shift these poles away from the imaginary axis to $2 \pm 4.3055i$. This is described next.

B. Modified Inverse System

Following the approach described in Sec. II.C, we modify the internal dynamics by adding a term $v(t)$ to the control law (29) to obtain

$$u_{\mathrm{ff}}(t) = B_1^{-1}[\dot{\zeta}_d(t) - A_1\zeta(t) - A_2\eta(t) + v(t)] \tag{32}$$

Substituting this control law into Eqs. (30) and (31), the modified inverse system is obtained as

$$\begin{bmatrix} \dot{e}_\zeta(t) \\ \dot{\eta}(t) \end{bmatrix} = \begin{bmatrix} 0 & 0 \\ (A_3 - B_2B_1^{-1}A_1) & A_\eta \end{bmatrix}\begin{bmatrix} e_\zeta(t) \\ \eta(t) \end{bmatrix} + \begin{bmatrix} I \\ B_2B_1^{-1} \end{bmatrix} v(t)$$

$$+ \begin{bmatrix} 0 & 0 \\ (A_3 - B_2B_1^{-1}A_1) & B_2B_1^{-1} \end{bmatrix}\begin{bmatrix} \zeta_d(t) \\ \dot{\zeta}_d(t) \end{bmatrix}$$

$$:= \hat{S}\begin{bmatrix} e_\zeta(t) \\ \eta(t) \end{bmatrix} + G_v v(t) + G_y Y_d(t) \tag{33}$$

where $e_\zeta(t) := \zeta(t) - \zeta_d(t)$. The poles of the inverse system can be moved to any desired location by using the control $v(t)$ because $(\hat{S}, G_v)$ is controllable. However, such modifications, aimed at reducing preactuation time, will also lead to a loss of precision in output tracking. This tradeoff between the reduction of preactuation time and the loss of precision in tracking is illustrated through simulation.

C. Simulation Results and Discussion

Two sets of simulations were performed. First, stable inversion was applied to the original system, which leads to exact output tracking inverse input-state trajectories. Second, simulations were performed when the unstable poles of the inverse system are moved from $0.0425 \pm 4.3055i$ to $2 \pm 4.3055i$ for reducing the amount of preactuation time required. Further, the inverse system also has four poles at the origin, corresponding to four pure integrators for $[e_\zeta(\cdot)]$ dynamics, which were moved to -1, -2, -3, and -4 for stability of the numerical integration scheme.

Figures 2 and 3 show the desired output trajectories for the lateral and vertical motions (corresponding to unit displacements in the two directions), while the forward velocity and yaw rate were to be

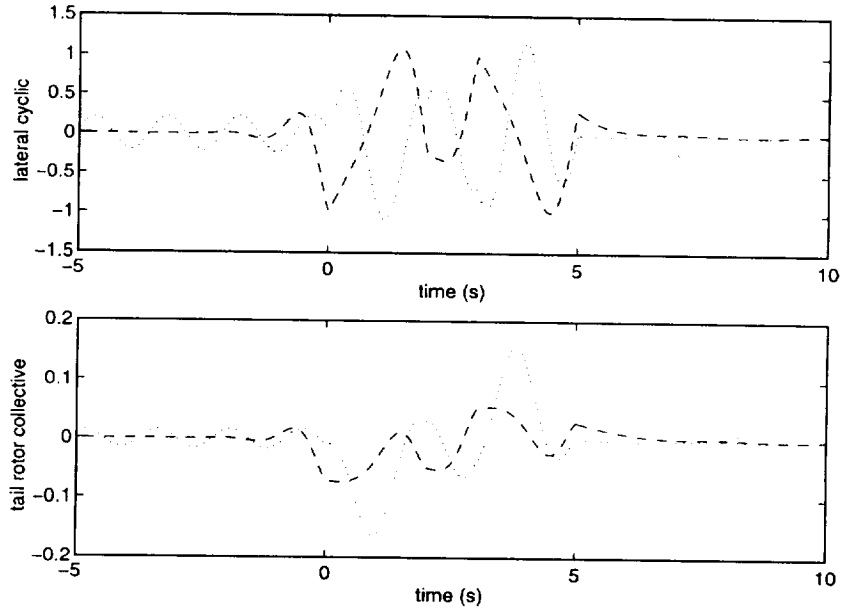

Fig. 7 Feedforward inputs: · · · · ·, without modification of internal dynamics and – – –, with modification.

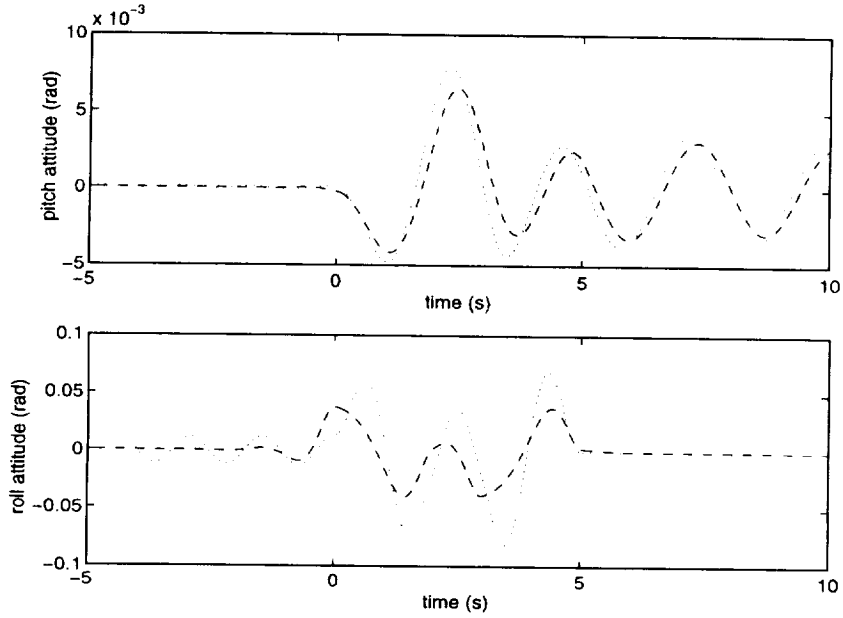

Fig. 8 Internal dynamics: · · · · ·, without modification of internal dynamics and – – –, with modification.

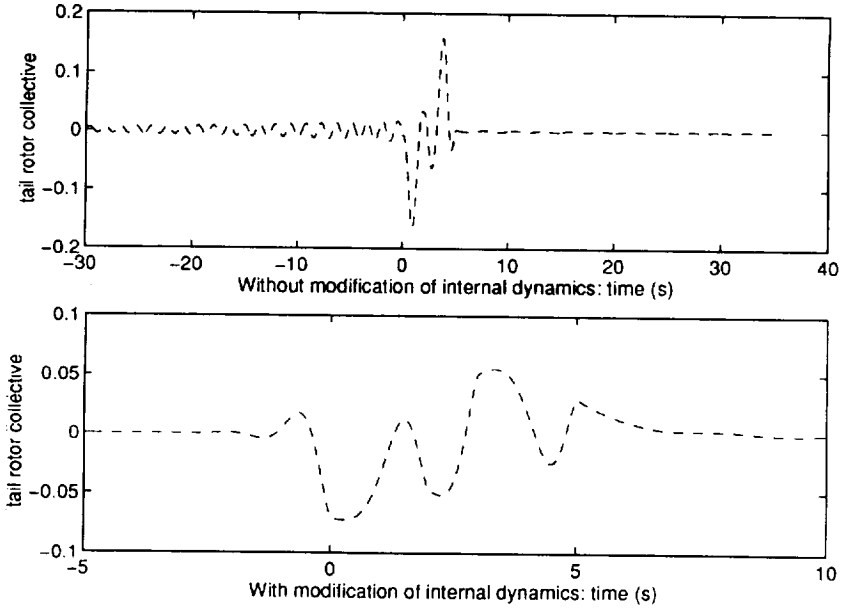

Fig. 9 Comparison of required preactuation in the feedforward.

maintained at zero; the maneuver starts at time $t = 0$. Figures 4 and 5 show the output trajectories achieved by the inverse state trajectory $x_{ref}(\cdot)$, which is to be used as a reference trajectory in the feedback scheme shown in Fig. 1. The corresponding feedforward inputs are shown in Figs. 6 and 7. Note here that the feedforward inputs are nonzero before the start of the maneuver, i.e., time $t < 0$, and hence preactuation is required.

Figures 4 and 5 show that exact output tracking reference state trajectories can be found, even when the internal dynamics is unstable, through the stable inversion approach. The stable inversion technique yields bounded solutions to the unstable internal dynamics, i.e., the pitch and roll motions are bounded, as shown in Fig. 8. However, the feedforward input found through exact inversion requires substantial preactuation time, as shown in Figs. 6 and 7, i.e., the preactuation remains nonzero for a significant time before the start of the maneuver at $t = 0$. Figure 9 shows that about 30 s of preactuation is needed to apply the inverse of the original system for output tracking; in contrast, modification of the internal dynamics reduces the preactuation needed from 30 to 1 s (see Fig. 9). As seen in Figs. 4 and 5, the output trajectories are still tracked well by the modified inverse. Further, this substantial reduction in preactuation time is achieved with similar control efforts and with similar roll and pitch motions (see Figs. 6–8). Thus, the approach presented here allows a tradeoff between precision tracking and the amount of preactuation that is acceptable. Future work will generalize the results to nonlinear nonminimum phase systems with nonhyperbolic internal dynamics.

IV. Conclusions

A technique to achieve output tracking for nonminimum phase linear systems with nonhyperbolic and near nonhyperbolic internal dynamics was presented. This approach is an integration of the stable inversion technique that aims at exact tracking with the approximation approach that modifies the internal dynamics to achieve desirable performance. The method was applied to an example helicopter hover control problem to illustrate the effects of modifying the internal dynamics. It was shown that substantial reduction in preactuation time is possible by giving up some of the precision in tracking, thus making the stable inversion approach viable for practical application.

Acknowledgment

This work was supported by NASA Ames Research Center Grant NAG-2-1042.

References

[1]Qui, L., and Davison, E. J., "Performance Limitations of Non-Minimum Phase Systems in the Servomechanism Problem," *Automatica*, Vol. 29, March 1993, pp. 337–349.

[2]Bayo, E., "A Finite-Element Approach to Control the End-Point Motion of a Single-Link Flexible Robot," *Journal of Robotic Systems*, Vol. 4, No. 1, 1987, pp. 63–75.

[3]Paden, B., and Chen, D., "A State-Space Condition for the Invertibility of Nonlinear Nonminimum-Phase Systems," *Advances in Robust and Nonlinear Control Systems*, ASME Winter Annual Meeting, Dynamic Systems and Control Div., Anaheim, CA, DSC Series, Vol. 43, 1992, pp. 37–41.

[4]Devasia, S., Chen, D., and Paden, B., "Nonlinear Inversion-Based Output Tracking," *IEEE Transactions on Automatic Control*, Vol. 41, No. 7, 1996, pp. 930–943.

[5]Hunt, L. R., Meyer, G., and Su, R., "Noncausal Inverses for Linear Systems," *IEEE Transactions on Automatic Control*, Vol. 41, No. 4, 1996, pp. 608–611.

[6]Francis, B. A., and Wonham, W. M., "The Internal Model Principle of Control Theory," *Automatica*, Vol. 12, No. 5, 1976, pp. 457–465.

[7]Isidori, A., and Byrnes, C. I., "Output Regulation of Nonlinear Systems," *IEEE Transactions on Automatic Control*, Vol. 35, No. 2, 1990, pp. 131–140.

[8]Castillo, B., "Output Regulation of Nonlinear Systems with More Inputs Than Outputs," *International Journal of Control*, Vol. 57, No. 6, 1993, pp. 1343–1356.

[9]Huang, J., "Output Regulation of Nonlinear Systems with Nonhyperbolic Zero Dynamics," *IEEE Transactions on Automatic Control*, Vol. 40, No. 8, 1995, pp. 1497–1500.

[10]Huang, J., and Rugh, W. J., "An Approximation Method for the Nonlinear Servomechanism Problem," *IEEE Transactions on Automatic Control*, Vol. 37, No. 9, 1992, pp. 1395–1398.

[11]Krener, A. J., "The Construction of Optimal Linear and Nonlinear Regulators," *Systems, Models and Feedback: Theory and Application*, edited by A. Isidori and T. J. Tarn, Birhäuser, Boston, 1992, pp. 301–322.

[12]Devasia, S., Paden, B., and Rossi, C., "Exact-Output Tracking Theory for Systems with Parameter Jumps," *International Journal of Control* (to be published).

[13]Silverman, L. M., "Inversion of Multivariable Linear Systems," *IEEE Transactions on Automatic Control*, Vol. 14, No. 3, 1969, pp. 270–276.

[14]Hirschorn, R. M., "Invertibility of Multivariable Nonlinear Control Systems," *IEEE Transactions on Automatic Control*, Vol. 24, No. 6, 1979, pp. 855–865.

[15]Di Benedetto, M. D., and Lucibello, P., "Inversion of Nonlinear Time-Varying Systems," *IEEE Transactions on Automatic Control*, Vol. 38, No. 8, 1993, pp. 1259–1264.

[16]Devasia, S., and Paden, B., "Exact Output Tracking for Nonlinear Time-Varying Systems," *Proceedings of the 33rd IEEE Conference on Decision and Control* (Lake Buena Vista, FL), IEEE Control Systems Society, 1994, pp. 2346–2355.

[17]Paden, B., Chen, D., Ledesma, R., and Bayo, E., "Exponentially Stable Tracking Control for Multi-Joint Flexible Manipulators," *Journal of Dynamic Systems, Measurement and Control*, Vol. 115, No. 1, 1993, pp. 53–59.

[18]Devasia, S., and Bayo, E., "Redundant Actuators to Achieve Minimal Vibration Trajectory Tracking of Flexible Multibodies: Theory and Application," *Journal of Nonlinear Dynamics*, Vol. 6, No. 4, 1994, pp. 419–431.

[19]Martin, P., Devasia, S., and Paden, B., "A Different Look at Output Tracking: Control of a VTOL Aircraft," *Automatica*, Vol. 32, No. 1, 1996, pp. 101–107.

[20]Meyer, G., Hunt, L. R., and Su, R., "Nonlinear System Guidance in the Presence of Transmission Zero Dynamics," NASA TM 4661, Jan. 1995.

[21]Gurumoorthy, R., and Sanders, S. R., "Controlling Non-Minimum Phase Nonlinear Systems—The Inverted Pendulum on a Cart Example," *Proceedings of the 1993 American Control Conference* (San Francisco, CA), American Automatic Control Council, 1993, pp. 680–685.

[22]Xu, Z., and Hauser, J., "Higher Order Approximate Feedback Linearization About a Manifold for Multi-Input Systems," *IEEE Transactions on Automatic Control*, Vol. 40, No. 5, 1995, pp. 833–840.

[23]Gopalswamy, S., and Hedrick, J. K., "Tracking Nonlinear Non-Minimum Phase Systems Using Sliding Control," *International Journal of Control*, Vol. 57, No. 5, 1993, pp. 1141–1158.

[24]Khalil, H. K., *Nonlinear Systems*, Macmillan, New York, 1991, Chap. 3.

[25]Isidori, A., *Nonlinear Control Systems: An Introduction*, Springer–Verlag, Berlin, 1989, Chap. 5.

[26]Pieper, J. K., Baillie, S., and Goheen, K. R., "Linear Quadratic Optimal Model-Following Control of a Helicopter in Hover," *Optimal Control Applications and Methods*, Vol. 17, 1996, pp. 123–140.

[27]Heffley, R. K., Jewell, W. F., Lehman, J. M., and Van Winkel, R. A., "A Compilation of Helicopter Handling Qualities Data," NASA CR 3144, Vol. 1, Grant NAS2-9344, 1979.

Submitted IEEE TAC

Stable Inversion for Nonlinear Systems with Nonhyperbolic Internal Dynamics *

Santosh Devasia †

Dept. of Mechanical Engineering
U. of Utah, SLC, UT 84112, USA

Abstract - A technique to achieve output tracking for nonminimum phase nonlinear systems with nonhyperbolic internal dynamics is presented. The present paper integrates stable inversion techniques (that achieve exact-tracking) with approximation techniques (that modify the internal dynamics) to circumvent the nonhyperbolicity of the internal dynamics – this nonhyperbolicity is an obstruction to applying presently available stable inversion techniques. The theory is developed for nonlinear systems and the method is applied to a two-cart with inverted-pendulum example.

*Work Supported by NASA Ames Research Center Grant NAG-2-1042
†e-mail : santosh@me.utah.edu Tel: (801) 581 4613

1 Introduction

Precision output tracking controllers are needed to meet increasingly stringent performance requirements in applications like flexible structures, aircraft guidance, robotics, and manufacturing systems. While exact tracking of minimum phase systems is relatively easy to achieve through approaches like input-output linearization [1], output tracking of nonminimum phase systems tends to be more challenging due to fundamental performance limitations on transient tracking performance [2]. This *poor* transient performance has been mitigated by using pre-actuation in the stable-inversion based approaches [3, 4]. However, the preactuation time (during which *most* of the preactuation control effort is required) depends on the unstable poles of the linearized internal dynamics – the preactuation time increases as the unstable poles approach the imaginary axis. In the limiting case, with the poles on the imaginary axis (nonhyperbolic internal dynamics), presently available inversion-based techniques fail because the preactuation time needed tends to become infinite. The present work extends previous results for linear systems in [5] to output tracking of nonlinear nonminimum phase systems, which have nonhyperbolic internal dynamics.

Output tracking has a long history marked by the development of regulator theory for linear systems by Francis and Wonham [6] and the generalization to the nonlinear case by Byrnes and Isidori [7]. These approaches asymptotically track an output from a class of exosystem-generated outputs. Further, extensions to the Byrnes-Isidori regulator have been described in [8]. The main problem with the application of these techniques to the output tracking of nonlinear systems is computational. While the linear regulator is designed by solving a manageable set of linear equations, the nonlinear regulator design requires the nontrivial solution of a first order partial differential algebraic equation [9, 10]. In contrast, inversion-based approaches avoid this computational difficulty and trade it to solve the exact tracking problem for a single desired output trajectory rather than solve the asymptotic tracking for a class of outputs. Another problem with the regulator approach is that the exosystem states are often switched to describe the desired output – this leads to transient tracking-errors after the switching instants. Such switching caused transient errors can be avoided by using inversion-based approaches to output tracking [3, 11]. Thus, it is advantageous to use inversion-based output tracking when precision tracking of a particular output trajectory is required.

Inversion, which is key to our approach, was restricted to causal inverses of minimum phase systems in the early works by Silverman and by Hirschorn (e.g., [12, 13]) because these approaches lead to unbounded inverses in the nonminimum phase case. Di Benedetto and Lucibello [14] considered the inversion of time varying nonminimum phase systems with a choice of the system's initial conditions. Rather than choose initial conditions, preactuation was used by noncausal stable inversion techniques developed in [3, 4, 15]. Such noncausal inverses, which require preactuation, have been successfully applied to the output tracking of flexible structures [16, 17], and aircraft and air traffic control [4, 18]. There is, however, a fundamental limitation to the presently available inversion techniques – they are only applicable if the internal dynamics is hyperbolic, and inversion-based output tracking has been a challenge for systems with nonhyperbolic internal dynamics.

Although Huang [8] has proposed some sufficient conditions for developing a regulator for systems with non-hyperbolic internal dynamics, the regulator design remains computationally difficult. There are also several approximation based output tracking techniques, where the central philosophy is to replace the internal dynamics with a dynamics that provides satisfactory behavior, and then to develop the controller based on the altered system [19, 20, 21]. The techniques most relevant to this paper are developed by Gurumoorthy and Sanders [19], and by Gopalswamy and Hedrick [21] – output redefinition (or modification) is used in these to approximate the unstable internal dynamics with a stable system. Such approximation based approaches are integrated, in this paper, with stable-inversion based techniques to achieve inversion of linear systems with nonhyperbolic internal dynamics in [5]. However, the present technique does not use output modification to stabilize the internal dynamics, rather output modification is only used to remove the non-hyperbolicity. Additionally, for near nonhyperbolic systems, the present approach allows a tradeoff between the precision-tracking and the amount of *pre-actuation-time* that is needed in the control effort. This tradeoff between stable-inversion and approximation of the unacceptable internal-dynamics has been studied for helicopter-hover control in [5]. The present work extends the results for linear-system in [5] to nonlinear systems.

We begin with a background on the stable-inversion based output tracking technique, and computational issues are presented in Section 3. The technique is applied to an example in Section 4, and conclusions are

in Section 5.

2 The Stable Inversion problem

2.1 Inversion-Based Output Tracking Scheme

Here we describe how the inversion approach is used to develop output tracking controllers. Consider a system described by

$$\begin{aligned} \dot{x}(t) &= f[x(t)] + g[x(t)]\, u(t) \\ y(t) &= h[x(t)] \end{aligned} \tag{1}$$

where $y(t) = [y_1(t), y_2(t), \ldots, y_p(t)]^T$ is the output, with the same number of inputs and outputs, i.e., $u(t), y(t) \in \Re^p$, and $x(t) \in \Re^n$ is the state. The functions $f(\cdot), g(\cdot)$ and $h(\cdot)$ are assumed to be sufficiently smooth with $f(0) = 0$ (i.e., $x = 0$ is an equilibrium point) and $h(0) = 0$.

Let $y_d(\cdot)$ be the desired output trajectory to be tracked. In the inversion-based approach we, first, find a nominal input-state trajectory, $[u_{ff}(\cdot), x_{ref}(\cdot)]$ that satisfies the system equations 1 and yields the desired output exactly, i.e.,

$$\left.\begin{aligned} \dot{x}_{ref}(t) &= f[x_{ref}(t)] + g[x_{ref}(t)]\, u_{ff}(t) \\ y_d(t) &= h[x_{ref}(t)] \end{aligned}\right\} \quad \forall t \in (-\infty, \infty) \tag{2}$$

and, second, we stabilize the exact-output yielding state trajectory, $x_{ref}(\cdot)$, by using state feedback (see Figure 1). Thus $x(t) \to x_{ref}(t)$ and $y(t) \to y_d(t)$ as $t \to \infty$ and output tracking is achieved. It is noted that in this output tracking scheme, the reference state trajectory $x_{ref}(\cdot)$ and the feedforward input $u_{ff}(\cdot)$ are computed off-line.

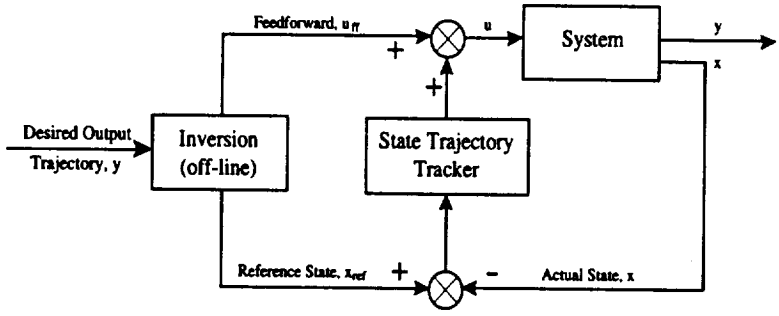

Figure 1. The Control Scheme

While stabilization of the reference state trajectory can be achieved through standard techniques [22] like state feedback of the form $K[x(t) - x_{ref}(t)]$, the main challenge is to find the inverse input-state trajectory $[u_{ff}(\cdot), x_{ref}(\cdot)]$ - especially for systems with nonminimum phase dynamics.

2.2 The Internal Dynamics

In this subsection, it is shown that finding the inverse input-state trajectory is equivalent to finding bounded solutions to the system's internal dynamics.

Assumption 1 *System (1) has a well defined vector relative degree,* $r := [r_1, r_2, \ldots, r_p]$.

The well-defined vector relative degree assumption enables the system equations to be rewritten, through a co-ordinate transformation

$$x(t) = \hat{T}(x(t)) \begin{bmatrix} \zeta(t) \\ \eta(t) \end{bmatrix} = T(\zeta(t), \eta(t)) \begin{bmatrix} \zeta(t) \\ \eta(t) \end{bmatrix}, \tag{3}$$

in the following form [1, 21]

$$\begin{aligned}\dot{\zeta}_1(t) &= A_{\zeta_1}\zeta_1(t) + A_{\zeta_2}\zeta_2(t)\\ \dot{\zeta}_2(t) &= s_1[\zeta(t),\eta(t)] + s_2[\zeta(t),\eta(t)]u(t)\\ \dot{\eta}_2(t) &= s_3[\zeta(t),\eta(t)] + s_4[\zeta(t),\eta(t)]u(t)\end{aligned} \tag{4}$$

where ζ represents the output along with its time derivatives,

$$\zeta := \begin{bmatrix}\zeta_1(t)\\ ----\\ \zeta_2(t)\end{bmatrix} := \begin{bmatrix} y_1 \\ \frac{d^1}{dt^1}y_1 \\ \frac{d^2}{dt^2}y_1 \\ \vdots \\ \frac{d^{r_1-2}}{dt^{r_1-2}}y_1 \\ y_2 \\ \vdots \\ \frac{d^{r_2-2}}{dt^{r_2-2}}y_2 \\ \vdots \\ \frac{d^{r_p-2}}{dt^{r_p-2}}y_p \\ ------ \\ \frac{d^{r_1-1}}{dt^{r_1-1}}y_1 \\ \frac{d^{r_2-1}}{dt^{r_2-1}}y_2 \\ \vdots \\ \frac{d^{r_p-1}}{dt^{r_p-1}}y_p \end{bmatrix} \tag{5}$$

A_{ζ_1} is a block-diagonal matrix

$$A_{\zeta_1} = \text{diag}[A_1, A_2, A_3, \ldots, A_p]$$

with each block consisting of zeros except for ones on the super-diagonal, for example, A_k is a $(r_k-1)\times(r_k-1)$ matrix of the form

$$A_k = \begin{bmatrix} 0 & 1 & 0 & 0 & \ldots & 0 \\ 0 & 0 & 1 & 0 & \ldots & 0 \\ \vdots & \vdots & \vdots & \vdots & \vdots & \vdots \\ 0 & 0 & 0 & 0 & \ldots & 1 \\ 0 & 0 & 0 & 0 & \ldots & 0 \end{bmatrix} \tag{6}$$

(for all $1 \le k \le p$). A_{ζ_2} is a matrix whose elements are zeros except for elements on the $(r_k - 1)$-th row and k-th column, which are ones (for all $1 \le k \le p$). Further from Assumption (1), $s_2(\cdot,\cdot)$ is invertible in a neighborhood of the origin, and since the origin is assumed to be an equilibrium point, we also have $s_1(0,0) = 0$, $s_3(0,0) = 0$.

Note that the desired $\zeta(\cdot)$ is known when the desired output trajectory $y_d(\cdot)$ and its time derivatives are specified. This desired $\zeta(\cdot)$ is defined as $\zeta_d(\cdot)$. If exact output tracking is achieved (i.e., if $\zeta(t) = \zeta_d(t)$) then the control law for maintaining exact tracking can be written as, from equation (4),

$$u(t) = [s_2[\zeta_d(t),\eta(t)]]^{-1}\left[\dot{\zeta}_{2,d}(t) - s_1[\zeta_d(t),\eta(t)]\right] \tag{7}$$

which results in state-equations of the form

$$\dot{\zeta}(t) = \dot{\zeta}_d(t) \tag{8}$$

$$\begin{aligned}\dot{\eta}(t) &= s_3[\zeta(t),\eta(t)] + s_4[\zeta(t),\eta(t)]u(t)\\ &= s_3[\zeta(t),\eta(t)] + s_4[\zeta(t),\eta(t)]\,[s_2(\zeta_d(t),\eta(t))]^{-1}\left[\dot{\zeta}_{2,d}(t) - s_1[\zeta_d(t),\eta(t)]\right]\end{aligned} \tag{9}$$

This is the inverse system and equation (9) is referred to as the internal dynamics. Solving the internal dynamics is key to finding the inverse input state trajectories. If a bounded solution, $\eta_d(\cdot)$, to the internal dynamics (9) can be found then the feedforward input can be found through equation (7) as

$$u_{ff}(t) = [s_2(\zeta_d(t), \eta_d(t))]^{-1} \left[\dot{\zeta}_{2,d}(t) - s_1(\zeta_d(t), \eta_d(t))\right] \tag{10}$$

and the reference trajectory can be found as

$$x_{ref}(t) = T[\zeta_d(t), \eta_d(t)] \begin{bmatrix} \zeta_d(t) \\ \eta_d(t) \end{bmatrix}. \tag{11}$$

Thus, finding a bounded solution, $\eta_d(\cdot)$, to the internal dynamics (Equation 9) is key to finding the inverse (bounded) input-state trajectories (Equations 10 and 11) which is needed to implement the the inversion-based output-tracking scheme shown in Figure 1.

2.3 Modified Internal Dynamics

Standard inversion schemes [12, 13] that integrate (forward in time) the internal dynamics (9) lead to unbounded solutions if the origin of the internal dynamics is unstable (nonminimum phase systems). Noncausal inversion (e.g., [3]) leads to bounded but noncausal solution to the internal dynamics. While significant improvement in output tracking performance is possible, such stable-inversion techniques are not applicable to systems with nonhyperbolic internal dynamics. In this subsection a compromise between stable inversion and approximation based inversion schemes is proposed. The key is to modify the internal dynamics by giving up exact output tracking – enough to remove the nonhyperbolicity, and then to apply stable-inversion. The difference between the proposed technique and other approximate techniques is that the internal dynamics is perturbed only to remove the nonhyperbolicity, and not to stabilize the internal dynamics as in other approximation schemes [19, 21].

To modify the inverse system an extra term, $v(t)$, is added to the control law (7) as follows

$$u(t) = [s_2[\zeta(t), \eta(t)]]^{-1} \left[\dot{\zeta}_{2,d}(t) - s_1[\zeta(t), \eta(t)] + v(t)\right] \tag{12}$$

With this control law the system equation (4) becomes (note that it is not required that exact tracking is achieved, i.e., $\zeta(\cdot) = \zeta_d(\cdot)$ is not required)

$$\begin{aligned} \dot{\zeta}_1(t) &= A_{\zeta_1}\zeta_1(t) + A_{\zeta_2}\zeta_2(t) \\ \dot{\zeta}_2(t) &= \dot{\zeta}_{2,d}(t) + v(t) \\ \dot{\eta}(t) &= s_3[\zeta(t), \eta(t)] + s_4[\zeta(t), \eta(t)]\,[s_2[\zeta(t), \eta(t)]]^{-1} \left[\dot{\zeta}_{2,d}(t) - s_1[\zeta(t), \eta(t)] + v(t)\right] \end{aligned} \tag{13}$$

For ease in notation, we define the tracking error, $e_\zeta(t)$, as

$$e_\zeta(t) := \begin{bmatrix} e_{\zeta_1}(t) \\ e_{\zeta_2}(t) \end{bmatrix} := \begin{bmatrix} \zeta_1(t) - \zeta_{1,d}(t) \\ \zeta_2(t) - \zeta_{2,d}(t) \end{bmatrix}$$

and rewrite Equation (13) as

$$\begin{aligned} \dot{e}_{\zeta_1}(t) &= A_{\zeta_1}e_{\zeta_1}(t) + A_{\zeta_2}e_{\zeta_2}(t) \\ \dot{e}_{\zeta_2}(t) &= v(t) \\ \dot{\eta}(t) &= s_3[e_\zeta(t) + \zeta_d(t), \eta(t)] + \\ &\quad s_4[e_\zeta(t) + \zeta_d(t), \eta(t)]\,[s_2[e_\zeta(t) + \zeta_d(t), \eta(t)]]^{-1} \left[\dot{\zeta}_{2,d}(t) - s_1[e_\zeta(t) + \zeta_d(t), \eta(t)] + v(t)\right] \\ &:= \hat{s}[e_\zeta(t), \eta(t), Y_d(t), v(t)] \end{aligned} \tag{14}$$

where

$$Y_d(t) := \begin{bmatrix} \zeta_d(t) \\ \dot{\zeta}_{2,d}(t) \end{bmatrix}$$

Next, the nonhyperbolicity of the modified internal dynamics (14) is removed by appropriately choosing $v(\cdot)$. We begin with the following assumption.

Assumption 2 *System (1) is controllable in the first approximation [1].*

The above assumption implies that the modified internal dynamics is also controllable in the first approximation since the difference between the original system (1) and the modified internal dynamics (14) is only a co-ordinate transformation and a static state-feedback (see [21] for a similar argument used for output redefinition). Next, a feedback of the form

$$v(t) = F \begin{bmatrix} e_\zeta(t) \\ \eta(t) \end{bmatrix} \tag{15}$$

is chosen such that the modified inverse system is hyperbolic – i.e., all poles on the imaginary axis are moved. Note that this change to an hyperbolic system can be achieved through arbitrarily *small* F since nonhyperbolicity is not a structurally stable property. With this control law Equation (14) becomes

$$\begin{aligned} \dot{e}_{\zeta_1}(t) &= A_{\zeta_1} e_{\zeta_1}(t) + A_{\zeta_2} e_{\zeta_2}(t) \\ \dot{e}_{\zeta_2}(t) &= F \begin{bmatrix} e_\zeta(t) \\ \eta(t) \end{bmatrix} \\ \dot{\eta}(t) &= \hat{s}\left(e_\zeta(t), \eta(t), Y_d(t), F \begin{bmatrix} e_\zeta(t) \\ \eta(t) \end{bmatrix} \right) \end{aligned} \tag{16}$$

which is re-written in a simplified form as

$$\begin{bmatrix} \dot{e}_\zeta(t) \\ \dot{\eta}(t) \end{bmatrix} = s\left(e_\zeta(t), \eta(t), Y_d(t)\right). \tag{17}$$

Next, stable inversion of the modified inverse system (17) is carried out [3].

3 Computation of the Inverse

This section discusses the computation of the inverse for the hyperbolic, modified, inverse-system. First, an iterative algorithm is presented – one of the steps involves finding bounded solutions to a linear (unstable) system. Second, the explicit technique to find bounded solutions is presented, and the amount of preactuation required for implementing the inversion-based controller is discussed. We begin with the algorithm to find bounded solutions to the modified internal dynamics [3].

3.1 Iterative Algorithm to find Inverse

- **Step 1**
  Rewrite the modified inverse (17) as

$$\frac{d}{dt} \begin{bmatrix} e_\zeta(t) \\ \eta(t) \end{bmatrix} = S \begin{bmatrix} e_\zeta(t) \\ \eta(t) \end{bmatrix} + \left\{ s\left(e_\zeta(t), \eta(t), Y_d(t)\right) - S \begin{bmatrix} e_\zeta(t) \\ \eta(t) \end{bmatrix} \right\} \tag{18}$$

  where the first term on the right hand side (r.h.s.) is the linearization of $s(\cdot,\cdot,\cdot)$ with respect to the first two variables, $e_\zeta(\cdot)$ and $\eta(\cdot)$, and the second term on the r.h.s. represents a perturbation. This motivates the following iterative solution of the internal dynamics.

- **Step 2**
  At each iteration in the following scheme, the bounded solution of a linearized system is to be found

$$\frac{d}{dt}\begin{bmatrix} e_\zeta(t) \\ \eta(t) \end{bmatrix}_0 = 0$$

$$\frac{d}{dt}\begin{bmatrix} e_\zeta(t) \\ \eta(t) \end{bmatrix}_{N+1} = S\begin{bmatrix} e_\zeta(t) \\ \eta(t) \end{bmatrix}_{N+1} + \left\{ s\left(e_{(\eta,N)}(t), \eta_N(t), Y_d(t)\right) - S\begin{bmatrix} e_\zeta(t) \\ \eta(t) \end{bmatrix}_N \right\} \tag{19}$$

where

$$\begin{bmatrix} e_\zeta(t) \\ \eta(t) \end{bmatrix}_{N+1} := \begin{bmatrix} e_{\zeta,N+1}(t) \\ \eta_{N+1}(t) \end{bmatrix} \tag{20}$$

and $N = 1, 2, 3 \ldots$.

3.2 Bounded Solution to Unstable Linear System

In the above iterations, solving equation (19) implies finding a bounded solution to a linear, hyperbolic (but potentially unstable) system – this is described next.

We begin by decoupling the linear system (19) into stable (z_s) and unstable (z_u) subsystems. Since the modified internal dynamics is hyperbolic, there exits a decoupling transformation U such that equation (19) can be re-written as

$$\begin{aligned} \dot{z}_{(s,N+1)}(t) &= S_s z_{(s,N+1)}(t) + G_s Y_N(t) \\ \dot{z}_{(u,N+1)}(t) &= S_u z_{(u,N+1)}(t) + G_u Y_N(t) \end{aligned}$$

where

$$z_{N+1}(t) := \begin{bmatrix} z_{(s,N+1)}(t) \\ z_{(u,N+1)}(t) \end{bmatrix} := U\begin{bmatrix} e_{(\eta,N+1)}(t) \\ \eta_{N+1}(t) \end{bmatrix}.$$

and

$$Y_N(t) := \left\{ s\left(e_{(\eta,N)}(t), \eta_N(t), Y_d(t)\right) - S\begin{bmatrix} e_\zeta(t) \\ \eta(t) \end{bmatrix}_N \right\}$$

An approach to find bounded solutions is to enforce the boundary conditions that $z_{(s,N+1)}(-\infty) = 0$ and $z_{(u,N+1)}(\infty) = 0$. This leads to unique bounded solutions by flowing the stable subsystem forward in time and flowing the unstable system backward in time – this yields

$$\begin{aligned} z_{(s,N+1)}(t) &= \int_{-\infty}^{t} e^{S_s(t-\tau)} G_s Y_N(\tau) d\tau \qquad \forall t \in (-\infty, \infty), \\ z_{(u,N+1)}(t) &= \int_{\infty}^{t} e^{-S_u(\tau-t)} G_u Y_N(\tau) d\tau \qquad \forall t \in (-\infty, \infty). \end{aligned} \tag{21}$$

Next, a change of co-ordinates yields the bounded solution to (19) as

$$\begin{bmatrix} e_\zeta(t) \\ \eta(t) \end{bmatrix}_{N+1} = U^{-1}\begin{bmatrix} z_{(s,N+1)}(t) \\ z_{(u,N+1)}(t) \end{bmatrix}_{N+1}. \tag{22}$$

3.3 Convergence of Iterative Algorithm

The following Theorem states that, as $N \to \infty$, the solutions of the above iterative algorithm converge to a bounded solution of the modified internal dynamics (17).

Theorem Let $s(\cdot,\cdot,\cdot)$ and its linearization S satisfy the following Lipshitz like condition

$$\begin{aligned} &\left\| \left\{ s(e_1, \eta_1, Y_1) - S\begin{bmatrix} e_1 \\ \eta_1 \end{bmatrix} \right\} - \left\{ s(e_2, \eta_2, Y_2) - S\begin{bmatrix} e_2 \\ \eta_2 \end{bmatrix} \right\} \right\|_\infty \\ &\leq K_1 \left\| \begin{bmatrix} e_1 \\ \eta_1 \end{bmatrix} - \begin{bmatrix} e_2 \\ \eta_2 \end{bmatrix} \right\|_\infty + K_2 \| Y_1 - Y_2 \|_\infty \end{aligned} \tag{23}$$

Then, provided K_1, K_2 and $\| Y_d(\cdot) \|_\infty$ are small, the iteration scheme converges to a solution to the modified internal dynamics (17), i.e,

$$\begin{bmatrix} e_\zeta \\ \eta \end{bmatrix}_N \to \begin{bmatrix} e_{(\zeta,d)} \\ \eta_d \end{bmatrix}$$

as $N \to \infty$, and $\begin{bmatrix} e_{(\zeta,d)} \\ \eta_d \end{bmatrix}$ satisfies the modified internal dynamics.

Proof
See [3, 4]. □

Thus, stable inversion technique is applied after removing the nonhyperbolicity in the internal dynamics.

This completes the inversion-technique for nonminimum phase systems with nonhyperbolic internal dynamics. To summarize, the reference state trajectory is found as (from Equation 11)

$$x_{ref}(t) \;=\; T[\hat{\zeta}_d(t), \eta_d(t)] \begin{bmatrix} \hat{\zeta}_d(t) \\ \eta_d(t) \end{bmatrix},$$

where

$$\hat{\zeta}_d(t) \;:=\; \zeta_d(t) + e_{(\zeta,d)}(t)$$

and the feedforward input, $u_{ff}(\cdot)$, is found from equation (12) and equation (15) as

$$u_{ff}(t) = \left[s_2[\hat{\zeta}_d(t), \eta_d(t)]\right]^{-1} \left[\dot{\zeta}_{2,d}(t) - s_1[\hat{\zeta}_d(t), \eta(t)] \;+ F \begin{bmatrix} e_{(\zeta,d)}(t) \\ \eta_d(t) \end{bmatrix}\right] \tag{24}$$

This inverse, $[u_{ff}(\cdot), x_{ref}(\cdot)]$, is used in the control scheme shown in Figure 1 to obtain output tracking.

3.4 Preactuation Time

Stable-inversion techniques overcome fundamental limitations on transient tracking performance of nonminimum phase systems [2] by using preactuation. However, the preactuation time (i.e., when *most* of the preactuation effort is required) tends to be unacceptably large if the *unstable* poles of the linearized, modified internal dynamics are close to the imaginary axis – this dependence is established in the following Lemma.

Lemma
Let

- all the unstable poles of linearized, modified internal dynamics (eigenvalues of S_u) lie to the right, in the complex plane, of the line $\text{Real}(s) = \alpha$ for some positive α, and
- the support of $Y_d(\cdot)$ lie in $[t_0, \infty)$ for some t_0.

Then there exists a positive scalar, M, such that the bounded solution to the internal dynamics (defined by the Theorem) satisfies

$$\| \begin{matrix} e_{(\zeta,d)}(t) \\ \eta_d(t) \end{matrix} \|_\infty \;<\; M e^{\frac{\alpha}{2}(t-t_0)}$$

for all time, t, before the start of the maneuver at t_0.

Proof Since the maneuver starts at t_0, any solution to the modified internal dynamics (17) satisfies the autonomous equation,

$$\begin{bmatrix} \dot{e}_\zeta(t) \\ \dot{\eta}(t) \end{bmatrix} \;=\; s\left(e_\zeta(t), \eta(t), 0\right). \tag{25}$$

for all $t < t_0$. Further, any bounded solution to the autonomous equation must lie on the unstable manifold before the start of the maneuver. The rate of convergence to zero as time tends to $-\infty$, of solutions that lie on the unstable manifold of the nonlinear modified inverse system, directly depends on the location of poles of the linearized dynamics. In particular, the rate of convergence depends on the *unstable* poles of

the linearization (which are the eigenvalues of S_u). The existence of a positive scalar M that satisfies the statement of the lemma follows from the saddle-point property (see [23] Theorem 6.1, and [24] Theorem 19.9). ■

The present technique also provides a way to reduce the preactuation time for systems with near non-hyperbolic internal dynamics. The Lemma states that the desired state-trajectory exponentially ends to zero as we go back in time before the start of the maneuver at t_0. Then the continuity of the input with respect to the state (smoothness of f, g and h, and the well defined relative degree assumption) implies that the preactuation input also tends to zero exponentially. The rate at which the preactuation becomes zero can be increased by moving the unstable poles of the linearized, modified internal dynamics (i.e., the eigenvalues of S_u) away from the imaginary axis – by appropriately choosing F in equation (15). This reduction in preactuation-effort is obtained at the expense of exact output tracking (see [5] for a linear example).

4 Example

Here, the inversion-technique is applied to an example two-cart and pendulum system shown in Figure 2. The inverted pendulum on a cart has been well studied in literature (see, for example, [19]), and has nonminimum phase dynamics – the internal dynamics is hyperbolic. An extra cart is added here, which introduces nonhyperbolicity in the internal dynamics. The input to the system is the applied force, $F(t)$, and the output is the position, $x_1(t)$, of the cart carrying the inverted pendulum (see Figure 2). The equation of motion for the system can be obtained as

$$\begin{aligned} (M+m)\ddot{x}_1(t) + ml\cos\theta(t)\,\ddot{\theta}(t) &= F(t) + ml\dot{\theta}^2(t)\sin\theta(t) - K\left(x_1(t) - x_2(t)\right) \\ ml\cos\theta(t)\,\ddot{x}_1(t) + ml^2\,\ddot{\theta}(t) &= mgl\sin\theta(t) \\ M\ddot{x}_2(t) &= -K\left(x_2(t) - x_1(t)\right) \end{aligned} \tag{26}$$

which can be rewritten in state-space form as

$$\begin{aligned} \dot{\zeta}_1(t) &= \zeta_2(t) \\ \dot{\zeta}_2(t) &= \tfrac{1}{\gamma(\eta_1)}\left[F(t)/m + l\eta_2(t)^2\sin\eta_1(t) - K/m\left(\zeta_1(t) - \eta_3(t)\right) - g\cos\eta_1(t)\sin\eta_1(t)\right] \\ \dot{\eta}_1(t) &= \eta_2(t) \\ \dot{\eta}_2(t) &= (K/M)\left(\zeta_1(t) - \eta_1(t)\right) \\ \dot{\eta}_3(t) &= \eta_4(t) \\ \dot{\eta}_4(t) &= \tfrac{1}{\gamma(\eta_3)}\left[-\eta_4(t)^2\sin\eta_3(t)\cos\eta_3(t)\right. \\ &\quad \left. + \tfrac{1}{ml}\left\{(M+m)g\sin\eta_3(t) - F(t)\cos\eta_3(t) + K\left(\zeta_1(t) - \eta_1(t)\right)\cos\eta_3(t)\right\}\right] \end{aligned} \tag{27}$$

where $\zeta_1 := x_1$, $\zeta_2 := \dot{x}_1$, $\eta_1 := x_2$, $\eta_2 := \dot{x}_2$, $\eta_3 := \theta$, and $\eta_4 := \dot{\theta}$,

$$\gamma(\eta_3(t)) := M/m + [\sin\eta_3(t)]^2$$

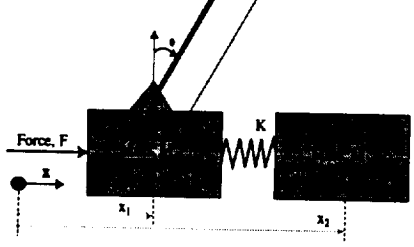

Figure 2. Example: Two Carts and Inverted Pendulum

Given the desired output trajectory profile shown in Figure 3, the input that maintains exact tracking (i.e.,

which maintains $\zeta(t) = \zeta_d(t)$) is obtained from equation (27) as

$$F(t) = m\gamma(\eta_3)\ddot{x}_{1,d}(t) \; - ml[\eta_4(t)]^2 \sin\eta_3(t) \; + K\left[\zeta_1(t) - \eta_1(t)\right] \; + mg[\cos\eta_3(t)]\sin\eta_3(t)$$

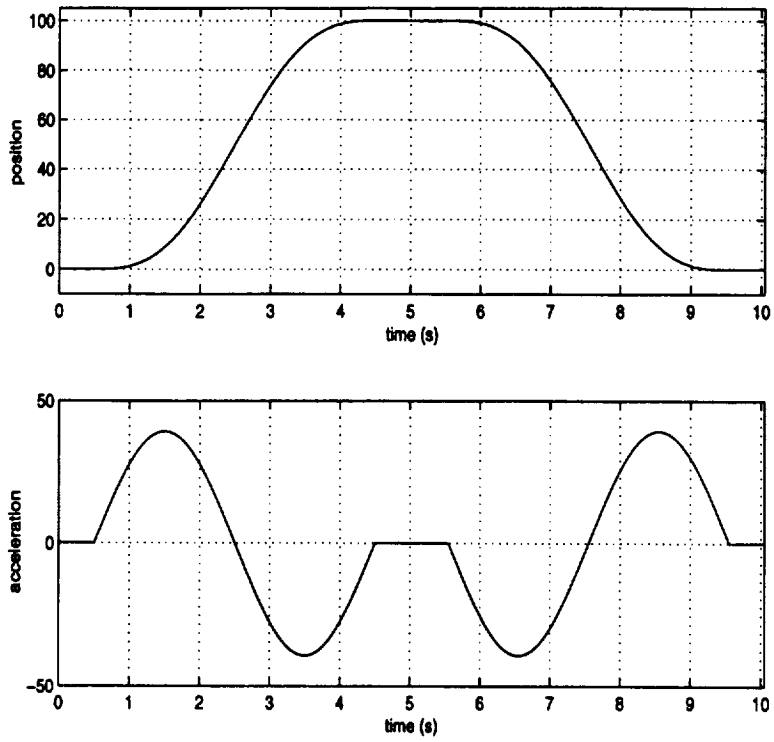

Figure 3. Desired Output Profile for x_1

With this exact tracking control law, the internal dynamics (represented by η), is given by

$$\begin{array}{rcl} \dot{\eta}_1(t) & = & \eta_2(t) \\ \dot{\eta}_2(t) & = & (K/M)\left(x_{1,d}(t) - \eta_1(t)\right) \\ \dot{\eta}_3(t) & = & \eta_4(t) \\ \dot{\eta}_4(t) & = & g/l \sin\eta_3(t) - (1/l)\cos\eta_3(t)\ddot{x}_{1,d}(t) \end{array} \tag{28}$$

The linearization of the internal dynamics (28) is

$$\frac{d}{dt}\begin{bmatrix} \eta_1(t) \\ \eta_2(t) \\ \eta_3(t) \\ \eta_4(t) \end{bmatrix} = \begin{bmatrix} 0 & 1 & 0 & 0 \\ -K/M & 0 & 0 & 0 \\ 0 & 0 & 0 & 1 \\ 0 & 0 & g/l & 0 \end{bmatrix}\begin{bmatrix} \eta_1(t) \\ \eta_2(t) \\ \eta_3(t) \\ \eta_4(t) \end{bmatrix} + \begin{bmatrix} 0 & 0 \\ K/M & 0 \\ 0 & 0 \\ 0 & -1/l \end{bmatrix}\begin{bmatrix} x_{1,d}(t) \\ \ddot{x}_{1,d}(t) \end{bmatrix} \tag{29}$$

Note that the linearization has two poles at $\pm\sqrt{-K/M}$ on the imaginary axis (in the complex plane) which corresponds to the cart dynamics $(x_2, \dot{x}_2)$ with x_1 fixed; this corresponds to a spring-mass system. The other two poles are at $\pm\sqrt{g/l}$ which correspond to the linearization of the inverted pendulum dynamics $(\theta, \dot{\theta})$. The two poles on the imaginary axis lead to nonhyperbolic behavior and stable-inversion techniques fail – this corresponds to the case which requires infinite pre-actuation. In contrast, by modifying the desired trajectory, the internal dynamics can be approximated by a hyperbolic system. This modification is achieved by adding an extra term $v(\cdot)$ to the control as follows

$$\begin{array}{rcl} u_{ff}(t) \; = \; F(t) & = & m\gamma(\eta_3)\left[\ddot{x}_{1,d}(t) + v(t)\right] \; - ml\left[\eta_4(t)\right]^2 \sin\eta_3(t) \\ & & +K\left[\zeta_1(t) - \eta_1(t)\right] \; + mg[\cos\eta_3(t)]\sin\eta_3(t) \end{array} \tag{30}$$

The modified inverse system becomes

$$\begin{aligned}
\dot{e}_{\zeta_1}(t) &= e_{\zeta_2}(t) \\
\dot{e}_{\zeta_2}(t) &= v(t) \\
\dot{\eta}_1(t) &= \eta_2(t) \\
\dot{\eta}_2(t) &= -K/M\eta_1 + K/M\,[x_{1,d}(t) + e_{\zeta_1}(t)] \\
\dot{\eta}_3(t) &= \eta_4(t) \\
\dot{\eta}_4(t) &= g/l \sin\eta_3(t) - 1/l\cos\eta_3(t)\,[\ddot{x}_{1,d}(t) + v(t)]
\end{aligned} \tag{31}$$

where

$$e_\zeta(t) := \begin{bmatrix} e_{\zeta_1}(t) \\ e_{\zeta_2}(t) \end{bmatrix} := \begin{bmatrix} \zeta_1(t) - x_{1,d}(t) \\ \zeta_2(t) - \dot{x}_{1,d}(t) \end{bmatrix}$$

The additional input, v, is chosen ($v = F[e_\zeta^T \;\; \eta^T]^T$) to remove the nonhyperbolicity. This can be achieved, for example, by pole-placement algorithms. Simulation results are presented next. The system parameters were chosen as $K = 10$, $M = 1$, $l = 9.8$, $g = 9.8$ and the F used in simulations is

$$F = [-4.52e-2 \quad -3.04e-1 \quad 5e-4 \quad 1.5e-3 \quad 0 \quad 0].$$

This F removes the nonhyperbolicity of the internal dynamics and stable inversion of the modified inverse system is carried out using the algorithm in Section 3. Simulation results are presented below: Figure 4 shows the desired output trajectory, and the redefined output trajectory. The internal dynamics (x_2, θ) is shown in Figure 5. Note that the nonhyperbolicity is circumvented and stable inversion is achieved with relatively minor modification of the output (see Figure 4).

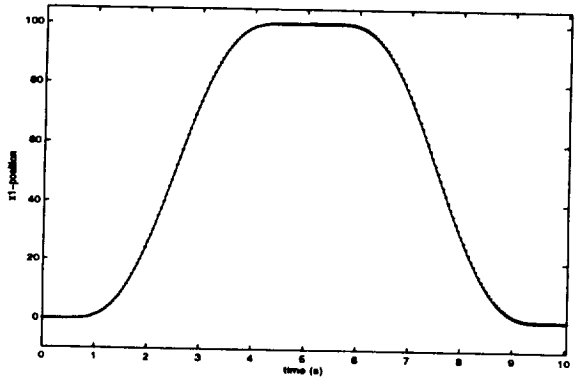

Figure 4. Error in Output Tracking: Solid line is desired output and dotted line is the redefined output.

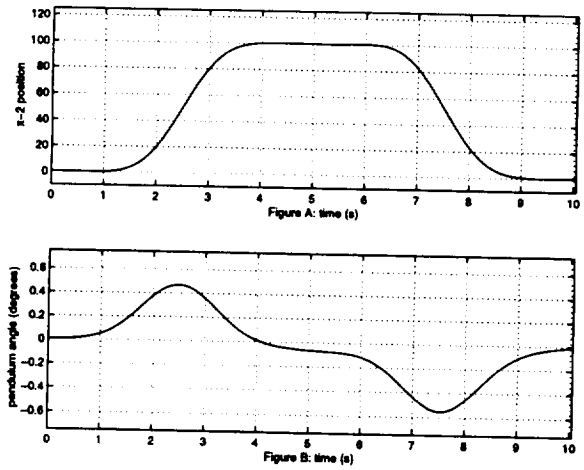

Figure 5. Internal Dynamics

5 Conclusion

A technique to achieve output tracking for nonminimum phase nonlinear systems with nonhyperbolic internal dynamics was presented. The approach integrated stable inversion techniques (that achieve exact tracking) with approximation approaches (that modify the internal dynamics) to remove the nonhyperbolicity of the internal dynamics. It was shown that, by giving up some of the precision in tracking, it is possible to achieve stable inversion of nonlinear nonminimum phase systems with nonhyperbolic internal dynamics.

References

[1] A. Isidori. *Nonlinear Control Systems: An Introduction.* Springler-Verlag, 1989.

[2] L. Qui and E. J. Davison. Performance limitations of non-minimum phase systems in the servomechanism problem. *Automatica*, 29, March:337–349, 1993.

[3] S. Devasia, D. Chen, and B. Paden. Nonlinear inversion-based output tracking. *IEEE Transactions on Automatic Control*, 41(7):930–943, 1996.

[4] G. Meyer, L. R. Hunt, and R. Su. Nonlinear system guidance in the presense of transmission zero dynamics. *NASA Technical Memorandun No. 4661*, January, 1995.

[5] S. Devasia. Output tracking with non-hyperbolic and near non-hyperbolic internal dynamics: Helicopter hover control. *AIAA J. of Guidance, Control, and Dynamics*, 20(3):573–580, 1997.

[6] B.A. Francis and W. M. Wonham. The internal model principle of control theory. *Automatica*, 12(5):457–465, 1976.

[7] A. Isidori and C. I. Byrnes. Output regulation of nonlinear systems. *IEEE Transactions on Automatic Control*, 35(2):131–140, 1990.

[8] J. Huang. Output regulation of nonlinear systems with nonhyperbolic zero dynamics. *IEEE Transactions on Automatic Control*, 40(8):1497–1500, 1995.

[9] J. Huang and W. J. Rugh. An approximation method for the nonlinear servomechanism problem. *IEEE Transactions on Automatic Control*, Sept,37(9):1395–1398, 1992.

[10] A. J. Krener. *The Construction of Optimal Linear and Nonlinear Regulators. In Systems, Models and Feedback: Theory and Application. A. Isidori and T.J. Tarn (editors).* Birkhauser, Boston, 1992.

[11] S. Devasia, B. Paden, and C. Rossi. Exact-output tracking theory for systems with parameter jumps. *International Journal of Control*, 67(1):117–131, 1997.

[12] L. M. Silverman. Inversion of multivariable linear systems. *IEEE Transactions on Automatic Control*, 14(3):270–276, 1969.

[13] R. M. Hirschorn. Invertibility of multivariable nonlinear control system. *IEEE Transactions on Automatic Control*, 24(6):855–865, 1979.

[14] M. D. Di Benedetto and P. Lucibello. Inversion of nonlinear time-varying systems. *IEEE Trans. Automatic Control*, 38(8):1259–1264, 1993.

[15] S. Devasia and B. Paden. Exact output tracking for nonlinear time-varying systems. *Proceedings of the 33rd CDC, Lake Buena Vista, Florida*, pages 2346–2355, 1994.

[16] B. Paden, D. Chen, R. Ledesma, and E. Bayo. Exponentially stable tracking control for multi-joint flexible manipulators. *ASME Journal of Dynamic Systems, Measurement and Control*, 115(1):53–59, 1993.

[17] S. Devasia and E. Bayo. Redundant actuators to achieve minimal vibration trajectory tracking of flexible multibodies: Theory and application. *Journal of Nonlinear Dynamics*, 6(4):419–431, 1994.

[18] P. Martin, S. Devasia, and B. Paden. A different look at output tracking: Control of a vtol aircraft. *Automatica*, 32(1):101–107, 1996.

[19] R. Gurumoorthy and S. R. Sanders. Controling non-minimum phase nonlinear systems - the inverted pendulum on a cart example. *Proceedings of the American Control Conference, San Francisco, CA*, pages 680–685, 1993.

[20] Z. Xu and J. Hauser. Higher order approximate feedback linearization about a manifold for multi-input systems. *IEEE Transactions on Automatic Control*, 40(5):833–840, 1995.

[21] S. Gopalswamy and J.K. Hedrick. Tracking nonlinear non-minimum phase systems using sliding control. *International Journal of Control*, 57(5):1141–1158, 1993.

[22] Hassan K. Khalil. *Nonlinear Systems*. Macmillan, 1991.

[23] Jack K. Hale. *Ordinary Differential Equations*. Wiley-Interscience, 1969.

[24] Herbert Amann. *Ordinary Differential Equations – An introduction to Nonlinear Analysis*. Walter de Gruyter, New York, 1990.

Submitted
AIAA J. of Guidance, Control and Dynamics

Recovery Guidance Maneuvers for Linear Systems with Input and State Constraints *

Santosh Devasia †
Tel: 801 581 4613
E-mail: santosh@me.utah.edu
U. of Utah, Mech. Eng. Dept.
50 S, Campus Center Drive, Room 2202
Salt Lake City, UT 84112-9208

George Meyer
Tel: 415 604 5750
E-mail: gmeyer@mail.arc.nasa.gov
NASA Ames Research Center
MS 262-2, Moffett Field, CA 94035-1000

*Work supported in part by NASA Ames Research Center Grant NAG-2-1042
†Work, by first author, was done when visiting NASA Ames Research Center under IPA Agreement NCC2-8018

Abstract

When a fixed regulator is used to stabilize a desired state trajectory (guidance law), large initial tracking errors can lead to input saturation, which can result in performance deterioration. A method to modify the guidance law for recovering state-trajectory tracking (without violating input and state constraints) is presented. Although it may be feasible to find such a satisfactory recovery guidance maneuver for a given initial tracking error, online development of recovery guidance maneuvers may not be computationally tractable. A technique is developed to use precomputed recovery guidance maneuvers (for a finite set of initial tracking errors) to generate recovery guidance maneuvers for other initial errors. The technique is applied to an illustrative example with input-magnitude-limits and input-rate-limits, and simulation results are presented.

1 Introduction

Inversion of system dynamics can be used for precision output tracking control, for example, in aircraft control [1, 2], and in air traffic control (ATC) [3]. For example, in automated flight management systems, tracking of an accepted clearance (flight plan cleared by the ATC) can be achieved by the following. First, the clearance is converted to an executable reference flight path (desired output trajectory [4]). Second, this flight path is converted into a guidance law (exact output-tracking input-state trajectory) found, for example, by using an inversion based approach [5, 6]. Third, flight path tracking is achieved by stabilizing the guidance trajectory by using a trajectory regulator (see Figure 1). However, relatively large tracking-errors (or a large external disturbance, that can be modeled as a tracking error) can lead to saturation of the inputs and can lead to the violation of state-constraints. This work addresses the issue of modifying the guidance law to recover output-tracking without violating input and state constraints. The recovery guidance problem is addressed in the framework of general linear systems and an example is provided to illustrate the technique.

The Guidance Scheme: The guidance scheme, studied in this paper, is shown in Figure 1, where the state-trajectory regulator, K, is assumed to be

given. The guidance problem, for a prescribed output trajectory, $y_d(\cdot)$, is to find a reference state trajectory, $x_{\text{ref}}(\cdot)$, and a feedforward input trajectory, $u_{\text{ff}}(\cdot)$, that achieve exact-output-tracking which can be accomplished by the inversion of the system dynamics (see, for example, [1, 3, 5, 7]). Note that these input-state trajectories may be precomputed for a given set of desired output trajectories.

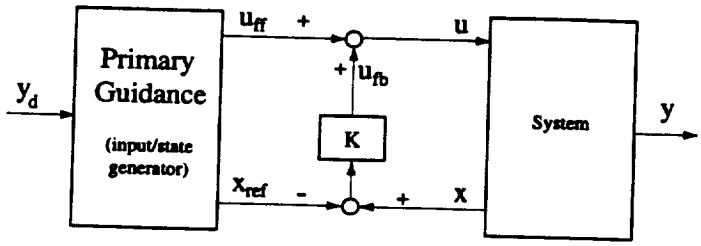

Figure 1. Control Scheme

Violation of Actuator and State Constraints: A significant problem with the approach is that relatively large initial tracking-errors can lead to actuator saturation resulting in performance degradation. Additionally, constraints on the state may also be violated. One approach, to solve such saturation problems, is to re-design the regulator (K in Figure 1) for different magnitudes of the initial errors (see, for example, [8]), or to design appropriate software limits (see, for example, [9] and the references therein). Another approach is to develop a nonlinear feedback that avoids saturation [10]. The present work develops an alternate approach, that doesn't modify the regulator, per se, but effectively bypasses it through recovery guidance maneuvers that modify the primary guidance law. Such an approach, that doesn't modify the regulator, is important to systems where the regulator is not easily accessible to modifications. For example, in the design of flight management systems, modifications of regulator can require extensive testing and re-certification, while the proposed open-loop recovery guidance can be (relatively) easily incorporated into the software. Similar use of less-aggressive reference inputs to avoid saturation can be found using receding horizon strategies [11] (also see references therein). These techniques modify the command signal to avoid actuator constraints. Our approach uses a similar idea to avoid saturation caused by large deviations from a desired trajectory – the desired trajectory is recovered, however, the

recovery maneuvers are chosen to be less aggressive. A key result is the development of a methodology that doesn't require online computation of the recovery guidance maneuvers – rather, in the spirit of the work by Mayne and Schroeder [10], the recovery guidance maneuver is generated as the linear combination of precomputed maneuvers.

We begin with a description of the guidance scheme in Section 2, followed by the development of recovery guidance maneuvers from precomputed maneuvers in Section 3. An optimal approach to develop recovery guidance maneuvers, for a given initial tracking error, is presented in Section 4, followed by an illustrative example and simulation results in Section 5. Our conclusions are in Section 6.

2 Primary Guidance Scheme

Let the system be described by

$$\begin{array}{rcl} \dot{x}(t) & = & A\,x(t) \;\; + B\,u(t) \\ y(t) & = & C\,x(t) \end{array} \tag{1}$$

where $x(t) \in \Re^n$ is the state, $u(t) \in \Re^q$ is the input and $y(t) \in \Re^l$ is the output. Additionally, let a state feedback K be given such that the closed loop system is stable, i.e., $A+BK$ is Hurwitz. In all the following discussions, the feedback, K, is kept constant.

Given a desired output trajectory $y_d(\cdot)$, the primary guidance scheme (see Figure 1) finds a nominal input-state trajectory, $[u_{\rm ff}\,(\cdot), x_{\rm ref}\,(\cdot)]$, that satisfies the system equations (1) and yields the desired output exactly, i.e.,

$$\left.\begin{array}{rcl} \dot{x}_{\rm ref}(t) & = & A\,x_{\rm ref}\,(t) \;\; + B\,u_{\rm ff}\,(t) \\ y_d(t) & = & C\,x_{\rm ref}\,(t) \end{array}\right\} \quad \forall t \in (-\infty, \infty) \tag{2}$$

Next, the exact-output yielding state trajectory, $x_{\rm ref}\,(\cdot)$, is stabilized by using state feedback (see Figure 1). The control law is

$$u(t) \;=\; u_{\rm ff}\,(t) \;+ K\,[x(t) - x_{\rm ref}\,(t)]\;. \tag{3}$$

With this control law, the dynamics of the tracking error,

$$e(t) := x(t) - x_{\rm ref}\,(t),$$

is obtained from equations (1) and (2) as

$$\dot{e}(t) \;=\; (A + BK)\, e(t)\,. \tag{4}$$

Since $A + BK$ is Hurwitz, $x(t) \to x_{\text{ref}}(t)$ and $y(t) \to y_d(t)$ as $t \to \infty$ and therefore, output tracking is achieved. It is noted that in this output tracking scheme, the reference state trajectory $x_{\text{ref}}(\cdot)$ and the feedforward input $u_{\text{ff}}(\cdot)$ can be computed off-line. It is also typical for the desired output trajectory to be a composition of several pre-determined sub-trajectories and the primary guidance scheme may concatenate several precomputed guidance laws. These primary guidance laws could be found using inversion of the plant dynamics (for systems with same number of inputs as outputs see, e.g., [3, 5, 7, 12], and for actuator-redundant systems see [13]).

Problem with the Guidance Scheme: A critical problem with the above guidance scheme is that large errors between the reference state-trajectory and the actual system state, at the beginning of a maneuver, can lead to actuator saturation and to substantially deteriorated performance. Note that the input-saturation problem is accentuated if a relatively *high gain* regulator, K, is used – which may be necessary to achieve high performance for relatively small tracking errors. The goal of the recovery-guidance maneuver is to modify the primary guidance law (reference-state trajectory) such that the system states can be brought close to the reference state trajectory (i.e., output-tracking is recovered) without saturating the actuators and without violating state constraints. Recovery guidance from large external perturbations can also be studied under this framework provided the perturbation is modeled as an initial tracking-error, that triggers the recovery guidance generator.

3 Trajectory Recovery Guidance Scheme

The recovery guidance scheme aims to maneuver the system without violating input and state constraints. The approach is to modify the reference state trajectory to avoid saturation of the actuators (see Figure 2). This modification, $x_{\text{mod}}(\cdot)$, is essentially open-loop, however, it is assumed that the recovery guidance trajectory generator has access to the initial tracking-error (when the recovery guidance is initiated).

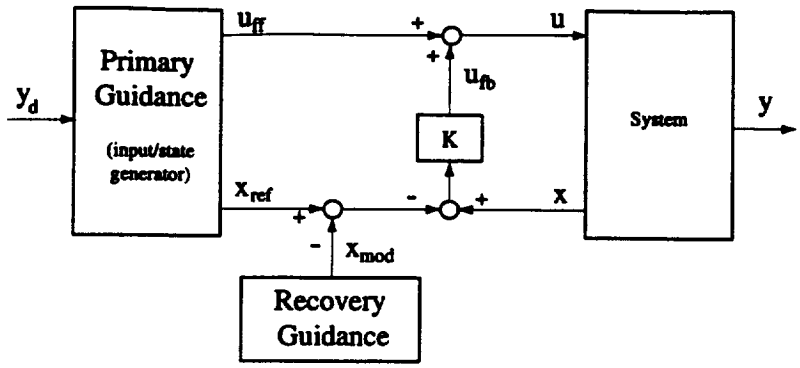

Figure 2. The Recovery Guidance Scheme

With the modified state-trajectory the control law given by equation (3) becomes (see Figure 2)

$$\begin{aligned} u(t) &= u_{\text{ff}}(t) + u_{\text{fb}}(t) \\ &= u_{\text{ff}}(t) + K(x(t) - x_{\text{ref}}(t)) + Kx_{\text{mod}}(t) \\ &= u_{\text{ff}}(t) + K\,e(t) + Kx_{\text{mod}}(t) \end{aligned} \tag{5}$$

where

$$u_{\text{fb}}(t)(t) = K\,e(t) + Kx_{\text{mod}}(t) \tag{6}$$

and the error equation (4) becomes

$$\dot{e}(t) = (A + BK)\,e(t) + BKx_{\text{mod}}(t)\,. \tag{7}$$

3.1 Use of Convexity to Generate Recovery-Maneuvers

The key idea is to pre-compute the trajectory modification for a set of initial conditions (from a set X), and then use these pre-computed modifications for other initial-conditions. This is summarized in the following proposition that uses the convexity argument due to Mayne and Schroeder [10]. The proposition states that if satisfactory recovery guidance is known for a set of initial conditions, X, then satisfactory recovery guidance maneuvers can be obtained for any initial conditions in the convex hull of X, provided the following assumption holds.

Assumption 1 *The region of acceptable states in $\Re^n$ and the region of acceptable inputs in $\Re^q$ are both convex regions that contain the origin.*

Given a positive integer p let

$$\Lambda_p \;:=\; \left\{ \lambda \in \Re^p \mid \lambda_m \geq 0 \quad \forall m \in (1,2 \ldots p), \text{ and } \sum_{m=1}^{p} \lambda_m = 1 \right\} . \qquad (8)$$

where the subscript indicates the component of a vector.

Proposition 1 *For each initial condition, $x^m(0) \in X$, let $x^m_{\text{mod}}(\cdot)$ be a trajectory-modification, that enables guidance-recovery while satisfying the state and input constraints. Let $x(0)$ be an initial condition in the convex hull of X and $\lambda_{x(0)} \in \Lambda_p$ for some p, such that*

$$x(0) \;=\; \sum_{m=1}^{p} \lambda_{[x(0),m]}\, x^m(0)$$

where the superscript denotes elements of a sequence. Then, the trajectory modification,

$$x_{\text{mod}}(t) \;:=\; \sum_{m=1}^{p} \lambda_{[x(0),m]}\, x^m_{\text{mod}}(t)\,,$$

is a valid recovery guidance law, i.e., input constraints and state constraints are satisfied.

Proof The error dynamics (equation (7)) is linear in the initial condition, $e(0)$ and in the input $x_{\text{mod}}(\cdot)$. Since $e(0)$ and $x_{\text{mod}}(\cdot)$ are linear combinations of $e^m(0)$ and $x^m_{\text{mod}}(\cdot)$ with the same weights for each $m \in (1,2,\ldots p)$, the linearity of the error dynamics yields

$$e(t) = \sum_{m=1}^{p} \lambda_{[x(0),m]}\;\; e^m(t)\,.$$

Here, $e^m(\cdot)$ is the solution to the error dynamics corresponding to the trajectory modification $x^m_{\text{mod}}(\cdot)$ and initial condition $e^m(0)$.

Let $x^m(\cdot)$ is the solution to the modified state equation with initial condition $x^m(0)$ and the guidance modification $x^m_{\text{mod}}(\cdot)$. Then, the definition of the error yields $x^m(\cdot) \;=\; x_{\text{ref}}(\cdot) \;+ e(\cdot)$. This and $\sum_{m=1}^{p} \lambda_{[x(0),m]} \;=\; 1$,

imply that

$$\begin{aligned} x(t) &:= x_{\text{ref}}(t) + e(t) \\ &= \textstyle\sum_{m=1}^{p} \lambda_{[x(0),m]}\ x_{\text{ref}}(t) + \sum_{m=1}^{p} \lambda_{[x(0),m]}\ e^m(t) \\ &= \textstyle\sum_{m=1}^{p} \lambda_{[x(0),m]}\ x^m(t) \end{aligned} \tag{9}$$

Thus, the convex hull of $x^m(t)$ forms a tube (as time varies) – Assumption 1 implies that the tube is in the acceptable region of the state space and hence $x(\cdot)$, which lies in this tube, is also acceptable.

Similarly, linearity of the modified input in $e(\cdot)$ and $x_{\text{mod}}(\cdot)$ (see equation (5)) yields

$$\begin{aligned} u(t) &:= u_{\text{ff}}(t) + Ke(t) + Kx_{\text{mod}}(t) \\ &= \textstyle\sum_{m=1}^{p} \lambda_{[x(0),m]}\ u_{\text{ff}}(t) + \sum_{m=1}^{p} \lambda_{[x(0),m]}\ e^m(t) + K \sum_{m=1}^{p} \lambda_{[x(0),m]}\ x^m_{\text{mod}}(t) \\ &= \textstyle\sum_{m=1}^{p} \lambda_{[x(0),m]}\ u^m(t) \end{aligned} \tag{10}$$

where $u^m_{\text{ff}}(\cdot)$ is the modified input for the initial condition $x^m(0)$. Thus the convex hull of $u^m_{\text{ff}}(t)$ also forms a tube (as time varies) – Assumption 1 implies that the tube is in the acceptable region of the input space and hence $u_{\text{ff}}(\cdot)$ which lies in this tube is also acceptable.

□

Remark 1 *The above proposition is also valid for time-varying systems.*

3.2 Decoupling Guidance Recovery from Primary Guidance

In the above approach, the guidance modification, $x_{\text{mod}}(\cdot)$, might depend on the particular maneuver being considered – thus, for each maneuver, the $x_{\text{mod}}(\cdot)$ to be stored is different even if the initial tracking-error $e^m(0)$ remains the same. We propose a method to trade-off the storage requirements with performance – to remove the dependence of guidance modification, $x_{\text{mod}}(\cdot)$, from the primary guidance maneuver, $[u_{\text{ff}}(\cdot),\ x_{\text{ref}}(\cdot)]$.

Note that bounds on the input-components can be decoupled into bounds on the feedforward and feedback by using the triangle inequality

$$\begin{aligned} |u_i(t)| &\leq \left|u_{(ff,i)}(t)\right| + \left|K\left(e_i(t) + x_{(mod,i)}(t)\right)\right| \\ &:= \left|u_{(ff,i)}(t)\right| + \left|u_{(fb,i)}(t)\right| \quad \forall i \in (1,2,\ldots q). \end{aligned} \tag{11}$$

The primary guidance can be designed to ensure that the feedforward input components, $|u_{(ff,i)}(t)|$, are within bounds and the recovery guidance design can be aimed at limiting the feedback components, $|u_{(fb,i)}(t)|$. This distribution of control authority allows the bounds on feedback-input to be independent of the feedforward input, which could depend on the particular maneuver.

Similarly, bounds on the state-components can also be decoupled into bounds on the components of the error, $|e_i(t)|$, and bounds on maneuver-dependent reference state trajectory components, $|x_{(ref,i)}(t)|$

$$\begin{aligned} |x_i(t)| &\leq \left|x_{(ref,i)}(t)\right| + \left|\left(x_i(t) - x_{(ref,i)}(t)\right)\right| \\ &:= \left|x_{(ref,i)}(t)\right| + |e_i(t)| \quad \forall i \in (1,2,\ldots n). \end{aligned} \tag{12}$$

Again, the primary guidance can be designed to ensure that $|x_{(ref,i)}(t)|$ is within bounds and the recovery guidance design can be aimed at limiting $|e_i(t)|$. This decoupling is formalized by the following proposition.

Assumption 2 *The region of acceptable errors in $\Re^n$, and the region of acceptable feedback inputs in $\Re^q$ are convex regions that contain the origin.*

Proposition 2 *For any initial error, $e^m(0) \in E$, let $x^m_{\text{mod}}(\cdot)$ be a trajectory-modification, that enables guidance-recovery and satisfies the error and feedback-input constraints. Then, given an initial condition, $e(0)$, in the convex hull of E and $\lambda_{e(0)} \in \Lambda_p$ for some p, such that*

$$e(0) = \sum_{m=1}^{p} \lambda_{[e(0),m]}\, e^m(0)\,,$$

the trajectory modification

$$x_{\text{mod}}(t) = \sum_{m=1}^{p} \lambda_{[e(0),m]}\, x^m_{\text{mod}}(t)\,,$$

is a valid recovery guidance law i.e., the input and state constraints are satisfied.

Proof This follows from arguments similar to those for the proof of Proposition 1 and inequalities (11) and (12). □

Note that the proposition allows the design of the trajectory modifications that are only dependent on the initial error. Thus, x_{mod} need not depend on the particular primary guidance law – note that this decoupling trades off performance for reduced-storage.

4 Recovery Guidance Generation

Recovery for a single initial condition: Given a specific initial condition, any algorithm may be used to find a particular recovery guidance maneuver. To illustrate the method, in the following, an optimal control formulation is used to design the recovery maneuvers.

The tradeoff between the need to bound the error and the need to bound the feedback input can be posed as an optimization problem – as the minimization of (over all inputs, $x_{\text{mod}}(\cdot)$, to the error-dynamics (7))

$$\begin{aligned} J &:= \int_0^\infty \left\{ e^T(t)\, Q_e\, e(t) \;+ u_{\text{fb}}^T(t)\, R\, u_{\text{fb}}(t) \;+ x_{\text{mod}}^T(t)\, Q_{mod}\, x_{\text{mod}}(t) \right\} \text{dt} \\ &= \int_0^\infty \left\{ x_{\text{mod}}^T(t) \left(K^T R K + Q_{mod} \right) x_{\text{mod}}(t) + 2e^T(t) \left(K^T R K \right) x_{\text{mod}}(t) \right. \\ &\qquad \left. + e^T(t) \left(K^T R K + Q_e \right) e(t) \right\} \text{dt} \\ &:= \int_0^\infty \left\{ x_{\text{mod}}^T(t)\, \hat{R}\, x_{\text{mod}}(t) \;+ 2e^T(t)\, \hat{S}\, x_{\text{mod}}(t) \;+ e^T(t)\, \hat{Q}\, e(t) \right\} \text{dt} \,. \end{aligned} \tag{13}$$

where Q_e is the weighting factor on the error, and R is the weighting factor on the feedback input. This is the standard optimal control problem for the modified error dynamics equation (7), with $x_{\text{mod}}(\cdot)$ as the input

$$\dot{e}(t) = (A + BK)\, e(t) \;+ BK x_{\text{mod}}(t)$$

The optimal trajectory modification law is then obtained as (see, for example,

[14] for the development of the standard optimal control law and conditions on the weighting matrices)

$$x_{\text{mod}}(t) = \hat{K}e(t) \tag{14}$$

where

$$\hat{K} = -\hat{R}^{-1}\left((BK)^T P + \hat{S}\right)$$

and P is the solution to the algebraic Riccati equation

$$P(A+BK) + (A+BK)^T P - (P(BK)+\hat{S})\,\hat{R}^{-1}\,((BK)^T P + \hat{S}^T) + \hat{Q} = 0$$

Substituting the modification law into the error dynamics equation (7) and solving the resulting equation yields an open-loop trajectory modification that depends only on the initial error

$$\begin{aligned} x_{\text{mod}}(t) &= \exp\left[(A + BK + BK\hat{K})(t)\right]e(0) \\ &:= \exp[(A + BK_e)(t)]e(0) \end{aligned} \tag{15}$$

For each initial error, $e(0)$, the weightings (Q_e, R, Q_{mod}) used in the above optimization cost-criterion can be different, however, only the resulting K_e in equation (15) needs to be stored for each of the initial conditions.

Note, again, that other algorithms may be used to obtain suitable recovery guidance laws for prespecified initial conditions in E. Alternate approaches to finding such guidance modification, $x_{\text{mod}}(\cdot)$, include the following.

- The weighting factors in the above cost function Q_e, R, Q_{mod} can be time-varying [14].
- The optimization problem can also be posed in the frequency domain and the weighting factors can also be made frequency-dependent to account for band-width limitation of the individual actuators [15].
- Another approach is to achieve zero tracking-error in finite time [14].

Next, we discuss using these precomputed recovery guidance laws to generate recovery guidance for other initial conditions.

Recovery Guidance for initial error in Convex Hull of E : In general, given an initial error and a set initial-errors, E, for which the recovery guidance maneuvers are known, an initial error in the convex hull of E may be written as the convex combination of elements of E

$$e(0) = \sum_m \lambda_m \, e^m(0) \tag{16}$$

where $e^m(0) \in E$. This representation may not be unique, however, each representation leads to an acceptable recovery guidance maneuver (by Proposition 2).

Remark 2 *The particular choice of the convex combination $e^m(0)$ can be optimized by using additional criterion – for example, to maximize the convergence rate of the error dynamics. Note that the resulting error dynamics, $e(\cdot)$, will converge atleast as fast as the slowest $e^m(\cdot)$ that have nonzero coefficients in equation (16) – which gives a lower bound to the convergence-rate. Therefore the coefficients, λ_m, of the convex combination in equation (16) may be chosen such that lower-bound of the convergence-rate is maximized.*

We present one technique to find a recovery guidance law by appropriately defining the set of initial errors, E, for which the recovery guidance maneuver is precomputed. Let the set of acceptable errors, $V_{(\alpha,\beta)}$, be defined by upper and lower bounds on the components of the error vector, i.e., let $\alpha \in \Re^n$ and $\beta \in \Re^n$ be given such that

$$\alpha_i \;<\; \beta_i \;, \quad \forall i \in (1,2,\ldots n) \tag{17}$$

and any acceptable initial-error, $e(0) \in V_{(\alpha,\beta)}$, satisfies

$$\alpha_i \;\leq\; e_i \;\leq\; \beta_i \;, \quad \forall i \in (1,2,\ldots n)\,. \tag{18}$$

We define the corner points of the set of acceptable errors, $V_{(\alpha,\beta)}$, as the set of initial errors, E, for which the recovery guidance maneuvers are precomputed, where

$$E \;:=\; \{e \mid e_i = \alpha_i \;\text{ or }\; e_i = \beta_i \,, \quad \forall i \in (1,2,\ldots n)\}\,.$$

Let $\{e^m\}_{m=1}^{m=2^n}$ be an enumeration of E. Then any initial error $e(0) \in E$ can be written as

$$e(0) = \sum_{m=1}^{2^n} \lambda_m \, e^m \tag{19}$$

where

$$\lambda_m = \prod_{i=1}^{n} \gamma_i(e_i,\ e_i^m) \tag{20}$$

with

$$\begin{aligned} \gamma_i(e_i,\ e_i^m) \ &:= \ \tfrac{\beta_i - e_i}{\beta_i - \alpha_i} \ \text{ if } e_i^m \ = \ \alpha_i \\ &:= \ \tfrac{e_i - \alpha_i}{\beta_i - \alpha_i} \ \text{ if } e_i^m \ = \ \beta_i \end{aligned} \tag{21}$$

The weighting, λ_m, in equation (19) is used to generate the recovery guidance maneuver as discussed in the Proposition 2.

Remark 3 *The performance of the recovery guidance maneuvers can be improved by decomposing the set of initial errors into smaller sets,* $V_{(\alpha^j,\,\beta^j)}$, $j \in (1, 2, \ldots J)$, *and developing recovery guidance maneuvers for each of the smaller sets. This can lead to increased performance, however, it also requires an increase in storage (to store precomputed recovery maneuvers for the corner points of each of the smaller sets).*

5 Example

System: Consider the motion of a point mass (for example, the linearized single-axis dynamics of an aircraft, see Meyer and Smith [6])

$$\begin{aligned} \dot{x}_1(t) \ &= \ x_2(t) \\ \dot{x}_2(t) \ &= \ \hat{u}(t) \\ \\ y(t) \ &= \ x_1(t) \end{aligned} \tag{22}$$

where $y, \dot{y}, \ddot{y}$ (i.e., $x_1, x_2, \dot{x}_2$) represent the generalized position, velocity and acceleration, respectively. Additionally (as is typical in aircraft control) we consider the case when the generalized force $\hat{u}(t)$ is not directly accessible. We assume that the servo-actuator, that generates the input, $\hat{u}$, is represented by a second order system of the form [6]

$$\frac{\hat{u}(s)}{u^*(s)} \ = \ \frac{k\omega^2}{s^2 \ + 2\zeta\omega s \ + \omega^2} \tag{23}$$

and consider the case when the magnitude of the servo-input, u^*, is limited by saturation. Further, we consider rate-boundedness of the servo-input by adding an integrator in the actuator-model, as follows (see Figure 3)

$$\frac{u^*(s)}{u(s)} = \frac{1}{s}, \tag{24}$$

and by adding a constraint on the servo-input-rate, u. If saturation is avoided, then the state space model of the entire system can be described as

$$\begin{array}{rcl} \dot{x}_1(t) &=& x_2(t) \\ \dot{x}_2(t) &=& x_3(t) \\ \dot{x}_3(t) &=& x_4(t) \\ \dot{x}_4(t) &=& -\omega^2 x_3(t) \quad - 2\zeta\omega x_4(t) \quad + k\omega^2 x_5(t) \\ \dot{x}_5(t) &=& u(t) \end{array} \tag{25}$$

where the constants are chosen as $k = 1, \omega = 1$ and $\zeta = 0.7$ in the simulations. Further, a feedback law, K, is also assumed to be given such that the closed loop system is stable. For all simulations, K is fixed as

$$K = [-10 \quad -20.5 \quad -17.3 \quad -3.75]$$

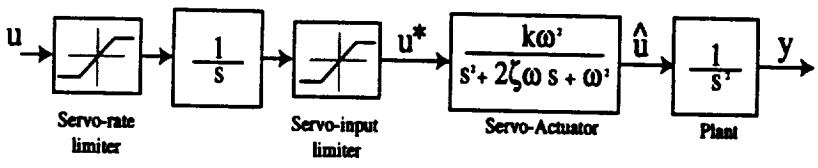

Figure 3. Example System

Constraints: The servo-input is to be limited as (see Figure 3)

$$u^*(t) = x_5(t) \in [-1, 1],$$

which also limits the input to the system, $\hat{u}(t)$. This input, $\hat{u}(t)$, represents the generalized acceleration, $\ddot{y}(t) = x_3(t)$. Further, the servo-input-rate, $u(t)$, is limited to

$$u(t) \in [-1, 1] \ .$$

In the following, the control authority is split 50-50 between the primary guidance and the recovery guidance as follows: the primary guidance generator is to ensure that the servo-input and the servo-input-rate are less than half the maximum limits, i.e.,

$$\begin{aligned} |u_{\text{ff}}(t)| &\leq 0.5 \\ |x_{5_{\text{ref}}}(t)| &\leq 0.5 \end{aligned} \tag{26}$$

and the recovery guidance generator should ensure that the servo-input and the servo-input-rate do not saturate – by limiting them also to half the acceptable bounds, i.e.,

$$\begin{aligned} |u_{\text{fb}}(t)| &\leq 0.5 \\ |e_5(t)| := |x_5(t) - x_{5_{\text{ref}}}(t)| &\leq 0.5 \ . \end{aligned} \tag{27}$$

Design of the Primary Guidance Generator: Let a desired output profile, $y_d(\cdot)$, and its time derivatives (upto the fifth time derivative) be given. Then, the exact-output tracking input-state trajectory can be found from equation (25) as (note that the existence of the time derivatives is a necessary condition for exact-tracking [7])

$$\begin{bmatrix} x_{1_{\text{ref}}} \\ x_{2_{\text{ref}}} \\ x_{3_{\text{ref}}} \\ x_{4_{\text{ref}}} \\ x_{5_{\text{ref}}} \end{bmatrix}(t) = \begin{bmatrix} y_d(t) \\ y_d^{(1)}(t) \\ y_d^{(2)}(t) \\ y_d^{(3)}(t) \\ \frac{1}{k\omega^2}\left[y_d^{(4)}(t) + 2\zeta y_d^{(3)}(t) + \omega^2 y_d^{(2)}(t)\right] \end{bmatrix} \tag{28}$$

where the bracketed superscript stands for time-derivative. The exact-tracking input-trajectory is obtained by differentiating, with respect to time, $x_{5_{\text{ref}}}$ in equation (28), to get

$$u_{\text{ff}}(t) = \dot{x}_{5_{\text{ref}}}(t) = \frac{1}{k\omega^2}\left[y_d^{(5)}(t) + 2\zeta y_d^{(4)}(t) + \omega^2 y_d^{(3)}(t)\right] . \tag{29}$$

Note that the restrictions on the primary guidance, equation (26), may imply that some of the desired trajectory profiles may not be feasible – thus requiring the redesign of the desired output trajectory profiles (see [16] for an

optimal approach to output-trajectory redesign for invertible systems). Figure 4 shows a primary guidance trajectory for changing the the generalized position, y, from 0 to 10. Figure 5 shows the system response, when the input is allowed to saturate – note the rapid degradation of tracking-performance. The initial error was a 10% error in the position (compared to the maximum change in position of 10) and all other state-components has zero error. . Next we discuss the generation of the recovery guidance maneuvers for such *large* errors that lead to performance deterioration. Note that if the initial errors were relatively much smaller, then recovery guidance is not needed.

Development of Recovery Guidance: To reduce the number of simulations, in the following discussion, it is assumed that the initial conditions of the actuator states, x_3, x_4, x_5, are zero, i.e. initial errors have the form

$$[e_1 \;\; e_2 \;\; 0 \;\; 0 \;\; 0]^T$$

If the initial tracking errors in the actuator states are non-zero, then the only change is that the number of initial errors (corner points of the error-set) for which the recovery guidance needs to be precomputed increases from 2^2 to 2^5 (and 28 more simulations needs to be presented).
In the simulations, the non-zero initial tracking errors of the generalized position and velocity are also assumed to be in the following range (see Figure 6) $|e_1| \leq 5$ and $|e_2| \leq 0.5$. This corresponds to a 50% error in the initial-position when compared to the maximum change in position in the primary guidance law (see Figure 4), and approximately 50% error in the initial-velocity when compared to the maximum velocities in the primary guidance law (see Figure 4).

For this particular example, we compute recovery guidance laws for four extreme initial errors (e^1, e^2, e^3, e^4, which are corner points of the set of acceptable initial errors in Figure 6), and the results of the recovery guidance maneuvers are shown in Figures 7-10. Even with substantially large initial tracking errors the resulting recovery guidance maneuvers lead to recovery of trajectory-tracking without violating input or state constraints (compare Figures 7-10 with the case without recovery-guidance in Figure 5). However the design of such recovery guidance requires the manipulation of the weighting matrices in the cost-criterion and requires repeated simulations to check performance. This design is not computationally-feasible, on-line, for

an arbitrary initial condition. The idea is to generate recovery guidance laws that satisfies the system and input constraints for a few initial conditions and then use these to generate, on-line, recovery guidance laws for other initial conditions.

For the present problem, the other acceptable initial conditions are in the square, defined by the four extreme (corner) points in Figure 6. An acceptable initial error, $e(0)$ can then be written as a convex combination of the corner points $(e^1,\ e^2,\ e^3,\ e^4)$ as

$$e(0) \ = \ \sum_{m=1}^{4} \lambda_m \ e^m$$

with $\lambda_m \ := \ \gamma_1^m \ \gamma_2^m$ where

$$\begin{array}{rcll} \gamma_1^m & := & (1/10)\,(e_1(0) \ + 5) & \text{if } m \in \{1,\ 2\} \\ & := & (1/10)\,(5 \ - e_1(0)) & \text{if } m \in \{3,\ 4\} \\ \gamma_2^m & := & (e_2(0) \ + 0.5) & \text{if } m \in \{1,\ 4\} \\ & := & (0.5 \ - e_2(0)) & \text{if } m \in \{2,\ 3\}\ . \end{array} \qquad (30)$$

The recovery guidance law can also be written as as a convex combination of the precomputed recovery guidance laws (for the corner points) as in Proposition 2. Simulation results are presented in Figure 11, which shows the results of the recovery guidance maneuver – output-tracking is achieved without violating the constraints. Note that this is the same initial error that lead to input saturation and lead to loss of tracking when recovery-guidance was not used (compare Figures 5 and 11). In contrast, the recovery guidance maneuver is guaranteed to satisfy state and input constraints. A second initial-error is also chosen that represents a larger 25% initial-error in position. As seen in Figure 12, output-tracking is still recovered by the guidance generator without saturating the servo-input or the servo-input-rate.

6 Conclusions

A method to modify guidance laws to recover trajectory-tracking without violating input and state constraints was presented. The technique uses recovery guidance laws that are precomputed for a few initial conditions to generate satisfactory recovery guidance maneuvers for other initial conditions. The technique was applied to an illustrative example and simulation

results showed that guidance modifications can successfully achieve recovery of trajectory tracking even with relatively large initial tracking errors, which could otherwise lead to actuator saturation and eventual loss of tracking.

References

[1] P. Martin, S. Devasia, and B. Paden. A different look at output tracking: Control of a vtol aircraft. *Automatica*, 32(1):101–107, 1996.

[2] C. Tomlin, J. Lygeros, and S. Sastri. Output tracking for a nonminimum phase dynamic ctol aircraft model. *Controls and Decision Conference*, pages 1867–1872, 1995.

[3] G. Meyer, L. R. Hunt, and R. Su. Nonlinear system guidance in the presense of transmission zero dynamics. *NASA Technical Memorandun No. 4661*, January, 1995.

[4] Rhonda Slattery and Yiyuan Zhao. Trajectory synthesis for air traffic automation. *AIAA Journal of Guidance, Control, and Dynamics*, 20(2):232–238, March-April 1997.

[5] S. Devasia, D. Chen, and B. Paden. Nonlinear inversion-based output tracking. *IEEE Transactions on Automatic Control*, 41(7):930–943, 1996.

[6] G. Meyer and G. Allan Smith. Dynamic forms part ii: Applications to aircraft guidance. *NASA Technical Paper*, 1997.

[7] A. Isidori. *Nonlinear Control Systems: An Introduction.* Springler-Verlag, 1989.

[8] E. C. Gilbert and K. C. Tan. Linear systems with state and control constraints: the theory and application of maximal output admissible sets. *IEEE Transactions on Automatic Control*, 36:1008–1020, 1991.

[9] R. A. Hess and S. A. Snell. Flight control system design with rate saturating actuators. *AIAA Journal of Guidance, Control, and Dynamics*, 20(1):90–96, Jan-Feb 1997.

[10] D. Q. Mayne and W. R. Schroeder. Nonlinear control of constrained linear systems. *International Journal of Control*, 60(5):1035–1043, 1994.

[11] R. B. Miller and M. Pachter. Maneuvering flight control with actuator constraints. *AIAA Journal of Guidance, Control, and Dynamics*, 20(4):729–734, July-August 1997.

[12] L. M. Silverman. Inversion of multivariable linear systems. *IEEE Transactions on Automatic Control*, 14(3):270–276, 1969.

[13] S. Devasia and E. Bayo. Redundant actuators to achieve minimal vibration trajectory tracking of flexible multibodies: Theory and application. *Journal of Nonlinear Dynamics*, 6(4):419–431, 1994.

[14] B. D. O. Anderson and J. B. Moore. *Optimal Control - Linear Quadratic Methods*. Prentice Hall, 1990.

[15] N. K. Gupta. Frequency shaped cost functionals: Extension of linear-quadratic-gaussian design methods. *Journal of Guidance and Control*, 3(6):529–535, November, 1980.

[16] S. Devasia. Optimal output-trajectory redesign for invertible systems. *AIAA J. of Guidance, Control, and Dynamics*, 19(5):1189–1191, 1996.

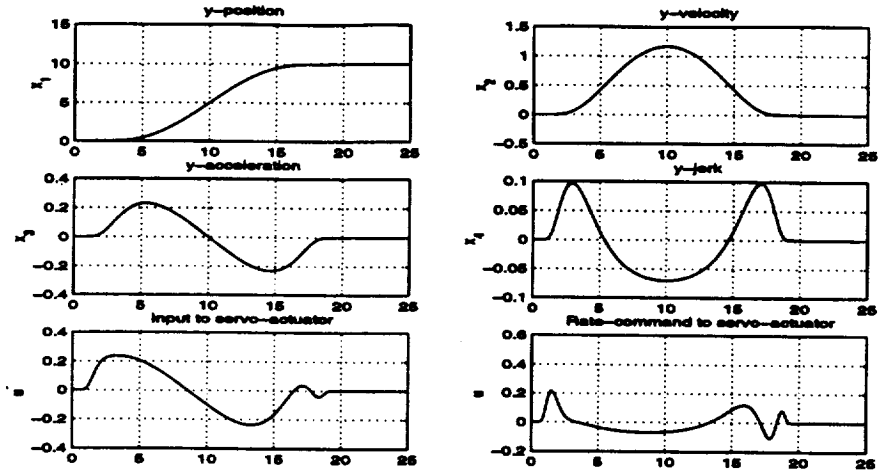

Figure 4. The Primary Guidance Law (x-axis represents time).

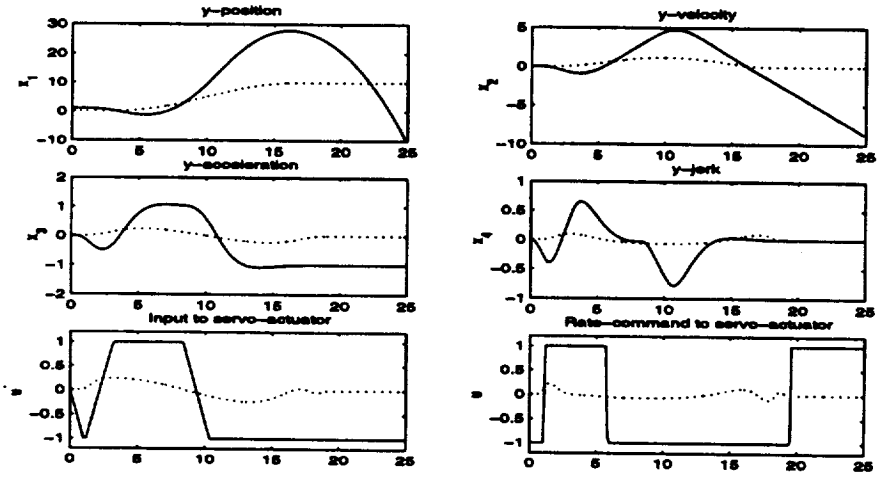

Figure 5. Results with Input-Saturation. Initial Position Error = 1, Initial Velocity Error = 0. Dotted line represents primary guidance. x-axis represents time.

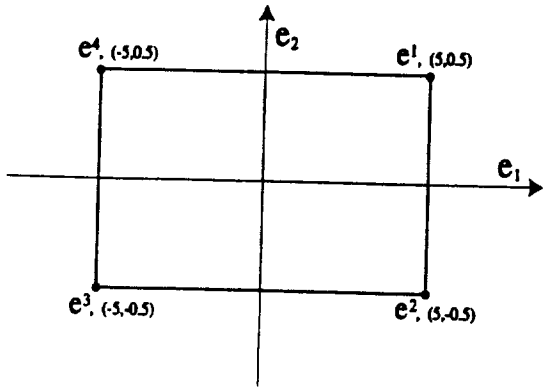

Figure 6. Convex Set of Initial Errors

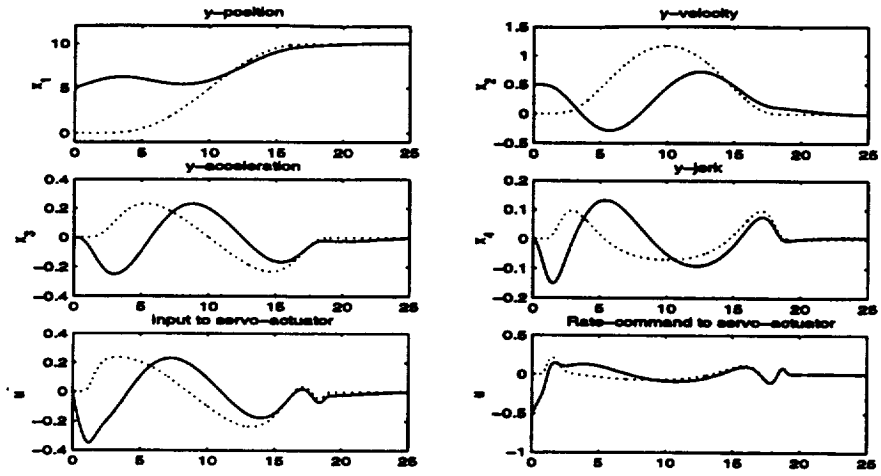

Figure 7. Precomputed Maneuver: Initial Position Error = 5, Initial Velocity Error = 0.5. Dotted line represents primary guidance. Solid line represents modified maneuver. x-axis represents time.

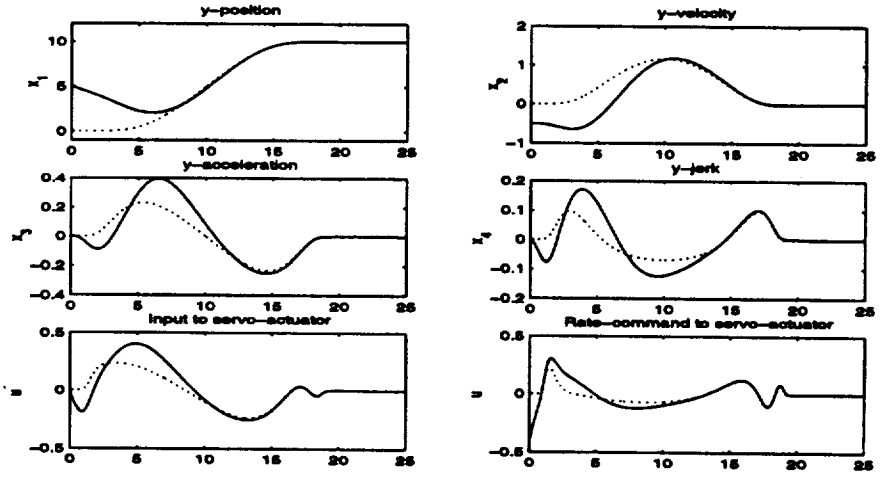

Figure 8. Precomputed Maneuver: Initial Position Error = 5, Initial Velocity Error = −0.5. Dotted line represents primary guidance. Solid line represents modified maneuver. x-axis represents time.

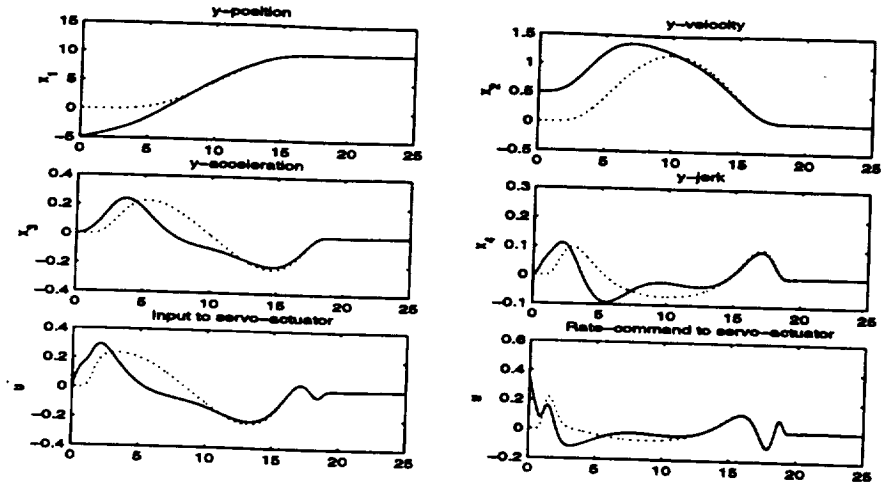

Figure 9. Precomputed Maneuver: Initial Position Error = -5, Initial Velocity Error = 0.5. Dotted line represents primary guidance. Solid line represents modified maneuver. x-axis represents time.

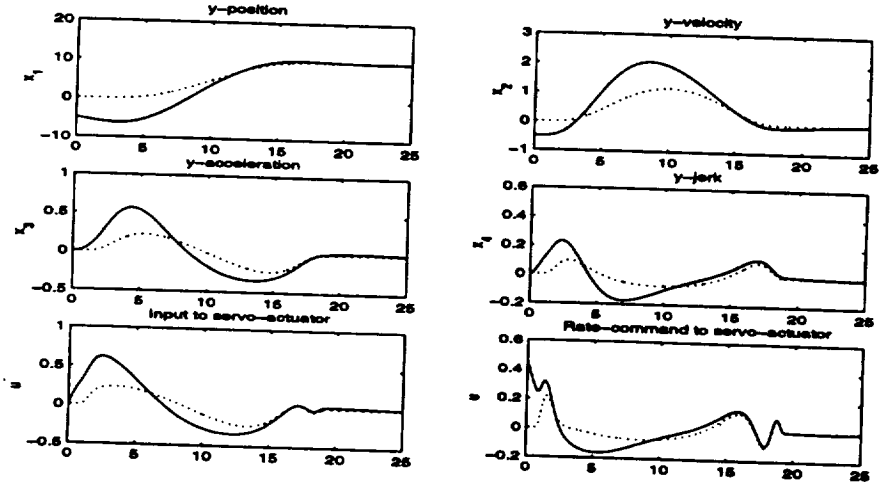

Figure 10. Precomputed Maneuver: Initial Position Error = -5, Initial Velocity Error = -0.5. Dotted line represents primary guidance. Solid line represents modified maneuver. x-axis represents time.

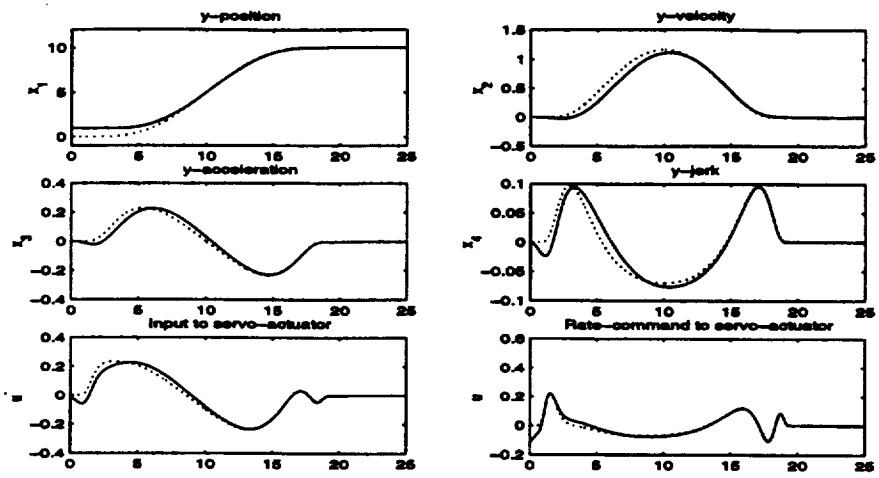

Figure 11. Results of Recovery Guidance Using Precomputed Trajectories Initial Position Error = 1, Initial Velocity Error = 0. Dotted line represents primary guidance. Solid line represents modified maneuver. x-axis represents time.

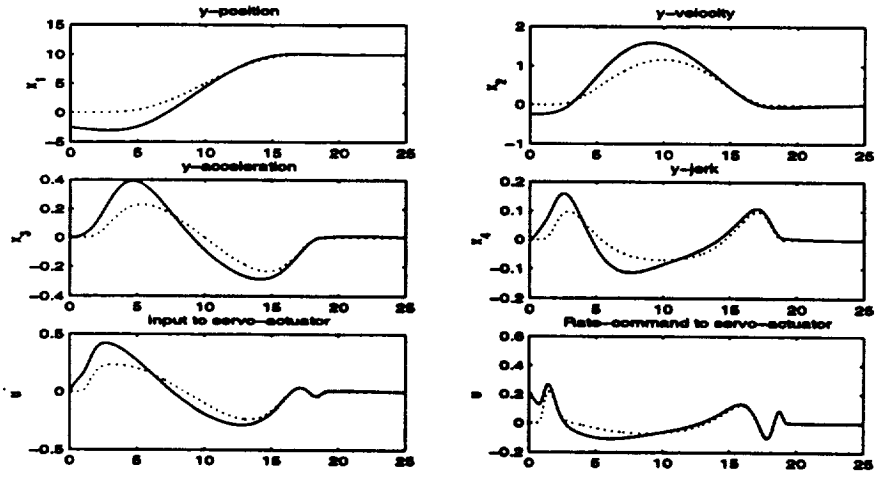

Figure 12. Results of Recovery Guidance Using Precomputed Trajectories Initial Position Error = −2.5, Initial Velocity Error = −0.25. Dotted line represents primary guidance. Solid line represents modified maneuver. x-axis represents time.

Accepted IEEE TAC

Stable Inversion for Nonlinear Nonminimum-Phase Time-Varying Systems

S. Devasia *
Mechanical Engineering Department, U. of Utah, SLC, UT 84112
B. Paden†
Mechanical Engineering Department, UC Santa Barbara, CA 93106

Abstract

In this paper, we extend stable inversion to nonlinear time-varying systems and study computational issues - - the technique is applicable to minimum-phase as well as nonminimum-phase systems. The inversion technique is new, even in the linear time-varying case, and relies on partitioning (the dichotomic split of) the linearized system dynamics into time-varying, stable and unstable, submanifolds. This dichotomic split is used to build time-varying filters which are, in turn, the basis of a contraction used to find a bounded inverse input-state trajectory. Finding the inverse input-state trajectory allows the development of exact-output tracking controllers. The method is local to the time-varying trajectory and requires that the internal dynamics vary slowly, however, the method represents a significant advance relative to presently available tracking controllers. Present techniques are restricted to time-invariant nonlinear systems and, in the general case, track only asymptotically.

*email:santosh@me.utah.edu
†email:paden@engineering.ucsb.edu

1 Introduction

In this paper, the stable inversion problem for nonlinear time-varying systems is solved. The approach is quite novel in that it applies to nonminimum phase systems - - even the linear version of our approach is new in the time-varying context. The basic idea is to compute the inverse dynamics, through a contraction, to find an input-state trajectory that achieves a desired output trajectory. To develop output tracking controllers, the input trajectory (found through inversion) can be used as a feedforward input signal in conjunction with any conventional feedback control law that stabilizes the inverse state-trajectory [1]. The present work completes a line of research which was motivated by the inversion of time-invariant articulated flexible structure dynamics [2], and extends our work on inversion of general affine-in-control time-invariant nonlinear systems [3].

System inversion is key to recent results in exact-output tracking for autonomous systems [1, 3, 4, 5] - this paper extends these results to exact-output tracking of time-varying systems. The output tracking problem has a long history marked by the solution of the linear time-invariant regulator problem by Francis [6] and the nonlinear time-invariant generalization made by Isidori and Byrnes [7]. The linear regulator is designed by solving a manageable set of linear matrix equations, whereas the nonlinear regulator requires the nontrivial solution of a first order partial differential algebraic equation. These approaches asymptotically track any member in a given family of output signals. More recently, there have been refinements of these approaches. Huang and Rugh [8] used a formal Taylor series expansion of the Isidori-Byrnes PDE and gave a sufficient condition for solvability. Krener [9] extended this work by providing necessary and sufficient conditions for the term-by-term solvability of the Taylor series. Robustness issues are studied by Huang and Rugh [10] and Huang and Lin [11]. Other methods that result in approximate tracking can be found in ([12], [13] and [14]).

The Francis and Isidori-Byrnes regulators apply to time-invariant systems and have the property that they track any one of a family of signals asymptotically. Our approach trades the requirement of solving the partial differential algebraic equation encountered in the Isidori-Byrnes regulator with the requirement of tracking a specific trajectory (rather than any one of a family). Moreover, no exosystem is required, and the specification of trajectories is simplified. We do, however, introduce boundedness and integrability requirements on the output trajectory. The key to our approach is finding a bounded inverse, even for nonminimum phase nonlinear systems, for use in generating feedforward inputs. Since inversion is key to our method, the works of Hirschorn [15], and Di Benedetto and Lucibello ([16] and [17]) on inversion are most relevant to this paper. The early work of Hirschorn is restricted to causal inverses of time-invariant systems and agrees with our inverse in this restricted case. Di Benedetto and Lucibello consider the (nonlinear time-varying) system's initial condition as an input and use inversion in this context – the difference is that we, in effect, use noncausal input to set up the desired initial condition, and provide the framework for constructing the noncausal input.

Noncausal feedforward can be used if trajectory preview is possible, or truncated to a causal signal at the cost of introducing transient tracking errors [3]. Such noncausal character is seen in the linear quadratic setting, but the use of exact inverses in nonlinear tracking control is new. The noncausal inverses used here have been applied to the control of flexible-link robots in [18]. A recent work by Meyer, Hunt and Su [4] makes extensions in the context of air-traffic control.

More concretely, consider a nonlinear system described in the following normal form [19]

$$\begin{aligned} y^{(r)}(t) &= \alpha[\zeta(t),\eta(t),t] + \beta[\zeta(t),\eta(t),t]u(t), \\ \dot{\eta}(t) &= s_1[\zeta(t),\eta(t),t] + s_2[\zeta(t),\eta(t),t]u(t), \end{aligned} \tag{1.1}$$

where $t \in \Re^1$ represents time, $r = (r_1, r_2, \ldots, r_p)^t$ is a vector of positive integers, $y(t) = [y_1(t), y_2(t), \ldots, y_p(t)]^T$ is the output, ζ represents the output, y, along with the output's time derivatives, and

$$y^{(r)}(t) \triangleq \left[\frac{d^{r_1}y_1}{dt^{r_1}}(t), \frac{d^{r_2}y_2}{dt^{r_2}}(t), \quad \cdots \quad , \frac{d^{r_p}y_p}{dt^{r_p}}(t)\right]^T.$$

Further, $\alpha(\cdot,\cdot,\cdot)$ and $\beta(\cdot,\cdot,\cdot)$ are smooth in their arguments with $\alpha(0,0,t) = 0$ and $s_1(0,0,t) = 0$ for all t. Let $Y_d(\cdot)$, describe a desired output trajectory – this includes information of the time-derivatives of the desired output, i.e., the desired $\zeta(\cdot)$ represented by $\zeta_d(\cdot)$, and the desired $y^{(r)}(\cdot)$ represented by $y_d^{(r)}(\cdot)$. For this desired output, the input trajectory that maintains exact tracking is given by

$$u(t) \triangleq [\beta[\zeta_d(t),\eta(t),t]]^{-1}\left[y_d^{(r)}(t) - \alpha[\zeta_d(t),\eta(t),t]\right]. \tag{1.2}$$

where it is assumed, for invertibility [1], that the absolute value of $\det[\beta]$ is greater than a positive scalar, ϵ_β. Then, the system's internal dynamics is given by

$$\begin{aligned} \dot{\eta}(t) &= s_1[\zeta_d(t),\eta(t),t] + s_2[\zeta_d(t),\eta(t),t][\beta[\zeta_d(t),\eta(t),t]]^{-1}\left[y_d^{(r)}(t) - \alpha[\zeta_d(t),\eta(t),t]\right] \\ &\triangleq s[\eta(t), Y_d(t), t]. \end{aligned} \tag{1.3}$$

Note that, if a bounded solution, $\eta_d(\cdot)$, to the internal dynamics [equation (1.3)] is found, then a bounded input trajectory (that maintains exact-tracking) can also be found using equation (1.2) as

$$u_d(t) = [\beta[\zeta_d(t),\eta_d(t),t]]^{-1}\left[y_d^{(r)}(t) - \alpha[\zeta_d(t),\eta_d(t),t]\right]. \tag{1.4}$$

The main difficulty is that the internal dynamics could have an unstable equilibrium at $\eta = 0$. Then, typical solutions to the unstable internal dynamics equation (1.3) are unbounded, and consequently the inputs found through equation (1.2) are also unbounded. A technique to find bounded solutions to nonlinear unstable internal dynamics has been developed in [1] with extensions made in [4]. Such stable inverse input-state trajectories have been used to develop output-tracking controllers in [3]. In this paper we extend the theory to the case when the internal dynamics is time-varying, and study computational issues.

2 A Nonlinear I/O Operator

In this Section we develop a nonlinear input/output (I/O) operator denoted $\mathcal{N}$, which is central to the inversion of nonlinear nonminimum phase systems. This operator maps bounded inputs into bounded Caratheodory solutions [20] of equation (1.3),

$$\dot{\eta}(t) = s(\eta(t), Y_d(t), t)\,; \quad \eta(\pm\infty) = 0.$$

Note that the input to the operator is $Y_d(\cdot)$, which consists of the desired output trajectory and its time derivatives. The basic idea is to construct a contraction whose fixed point is a solution to (1.3). The contraction is motivated in the following way. Since it is not known whether or not $\dot{\eta}(t) = s[\eta(t), Y_d(t), t]$ with $\eta(\pm\infty) = 0$ has a solution, we expand $s(\cdot,\cdot,\cdot)$ into linear and perturbation terms

$$\dot{\eta}(t) \;=\; A(t)\eta(t) \;+ [s[\eta(t), Y_d(t), t] - A(t)\eta(t)]\,, \tag{2.1}$$

where the term in the large square brackets represents the perturbation term. If we know the perturbation term, then we can establish conditions for the existence of a bounded solution to this forced linear system. Our approach is to take a guess at the perturbation term and iterate – we start with

$$\eta_1(\cdot) = 0,$$

and at each iteration ($n \geq 1$) solve for a bounded solution to the linear (but potentially unstable) equation

$$\dot{\eta}_{n+1}(t) = A(t)\eta_{n+1}(t) \;+ [s[\eta_n(t), Y_d(t), t] - A(t)\eta_n(t)]\,.$$

We then prove that this iteration converges to, $\eta_d(\cdot) \triangleq \mathcal{N}[Y_d(\cdot)]$, a bounded solution of the differential equation (1.3). We begin with the linear counterpart of $\mathcal{N}$, denoted $\mathcal{A}$ which finds bounded solutions to the above (unstable) linear equation, i.e.,

$$\eta_{n+1}(t) \;\triangleq\; \mathcal{A}\,[\,s[\eta_n(\cdot), Y_d(\cdot), \cdot] - A(\cdot)\eta_n(\cdot)\,]\,(t),$$

2.1 Linear operator $\mathcal{A}$

For a system of the form $\dot{\eta}(t) = \hat{A}\eta(t) + \hat{B}u(t)$, with $\hat{A}$ having no $j\omega$-axis eigenvalues, various input-output operators may be defined. The most common operator used in control theory imposes an initial condition of the form $\eta(t_0) = \eta_0$ on the state trajectory. In this Subsection, we define an operator $\mathcal{A}$, which imposes an alternative boundary condition, $\eta(\pm\infty) = 0$, on the state trajectory: so that the resulting state trajectories are necessarily bounded.

Consider a linear time-varying system of the form

$$\dot{\eta}(t) \;=\; A(t)\eta(t) + v(t) \tag{2.2}$$

where $\eta(t) \in \Re^{n_\eta}$ and $A(t) \in \Re^{n_\eta \times n_\eta}$. The key idea is to make a state transformation splitting the system (2.2) into two decoupled subsystems; one of which is exponentially stable and the other is exponentially unstable. By integrating the stable subsystem forward in time, and the unstable subsystem backward in time, a bounded solution to the differential equation is obtained (see [3] for a similar approach in the time-invariant case). Although the decoupling of time-invariant linear systems is easily done by using a state-transformation constructed with the eigenvectors of the A matrix, this approach does not lead to the necessary decoupling in the time-varying case [21].

In the following, we use results by Coppel [21], to establish the dichotomic split that enables extension of the stable-inversion theory to the time-varying case.

Definition 1 Kinematic Similarity [21]

The homogeneous equation

$$\dot{\eta}(t) \;=\; A(t)\eta(t) \tag{2.3}$$

with $A(\cdot)$ continuous for all $t \in \Re^1$, is defined to be *kinematically similar* to

$$\dot{w}(t) \;=\; B(t)w(t). \tag{2.4}$$

provided: there exists a transformation $S(\cdot)$ such that for any given solution $w(\cdot)$ to equation (2.4)

$$\eta(t) \;=\; S(t)w(t) \tag{2.5}$$

is a solution to equation (2.3), $S(t)$ is a continuously-differentiable invertible matrix, and both $S(t)$ and $S^{-1}(t)$ are uniformly bounded for $t \in \Re^1$. □

By substituting equation (2.5) into equation (2.3) we see that $S(t)$ necessarily satisfies

$$\dot{S}(t) \;=\; A(t)S(t) - S(t)B(t).$$

The key is to find a Kinematic similarity that achieves the dichotomic split of the linear system (2.2) into stable and unstable subsystems. This dichotomic split is possible provided $A(t)$: (a) is slowly varying in t; (b) is uniformly bounded in t; and (c) is hyperbolic. These conditions are formalized next, and the dichotomic split is established in the following Theorem.

Condition I $A(t) \in \Re^{n_\eta \times n_\eta}$ satisfies condition I, if there exists positive M, α, β such that for every $t \in \Re^1$

1. $\| A(t) \|_{1+\infty} \leq M$. See Nomenclature for the definition of $\| \cdot \|_{1+\infty}$
2. $A(t)$ has k eigenvalues with real part less than or equal to $-\alpha < 0$ and $n_\eta - k$ eigenvalues with real part greater than or equal to $\beta > 0$, where $0 < k < n_\eta$. □

Theorem 1

Let $A(t)$ satisfy condition I. Then for any positive scalar $\epsilon < min(\alpha, \beta)$ there exists a positive scalar $\delta = \delta(M, \alpha + \beta, \epsilon)$ such that, if $\| \frac{d}{dt} A(t) \|_{1+\infty} \leq \delta$ for every $t \in \Re^1$, then

1. Equation (2.3) is *kinematically similar* to

$$\frac{d}{dt}\begin{bmatrix} w_s(t) \\ w_u(t) \end{bmatrix} \;=\; \begin{bmatrix} B_s(t) & 0 \\ 0 & B_u(t) \end{bmatrix}\begin{bmatrix} w_s(t) \\ w_u(t) \end{bmatrix}, \tag{2.6}$$

   where $w_s(t) \in \Re^k$, $w_u(t) \in \Re^{(n_\eta - k)}$.

2. Further, $\dot{w}_s(t) = B_s(t)w_s(t)$ is exponentially stable and $\dot{w}_u(t) = B_u(t)w_u(t)$ is exponentially unstable. That is, the respective fundamental matrix solutions (see [20], pg.80) W_s and W_u satisfy

$$\begin{aligned} \| W_s(t)W_s^{-1}(s) \|_{1+\infty} &\leq Ke^{-(\alpha-\epsilon)(t-s)} \quad \textit{for } t \geq s \\ \| W_u(t)W_u^{-1}(s) \|_{1+\infty} &\leq Ke^{-(\beta-\epsilon)(s-t)} \quad \textit{for } s \geq t. \end{aligned} \tag{2.7}$$

3. The associated transformation S satisfies

$$\| S(t) \|_{1+\infty} \leq N_1(M, \alpha+\beta, \epsilon) \tag{2.8}$$
$$\| S^{-1}(t) \|_{1+\infty} \leq N_2(M, \alpha+\beta, \epsilon). \tag{2.9}$$

Proof: This follows from Coppel's work [21] (in particular, see Lemma 2 and Theorem 3). □

Remark 1 Note that an important condition in the above Theorem is that $A(\cdot)$ is slowly varying in time. □

The above dichotomic split of the system into stable (w_s) and unstable (w_u) subsystems leads to the following bounded solution to linear system (2.2). Given $A(\cdot)$ satisfying the conditions of Theorem 1, a linear operator $\mathcal{A}$ that finds bounded solutions to system (2.2) is given by

Definition 2 .
For $v(\cdot) \in L_1 \cap L_\infty$,

$$\mathcal{A}(v)(t) \triangleq S(t) \begin{bmatrix} \int_{-\infty}^{t} W_s(t) W_s^{-1}(\tau) S_s(\tau) v(\tau) d\tau \\ -\int_{t}^{\infty} W_u(t) W_u^{-1}(\tau) S_u(\tau) v(\tau) d\tau \end{bmatrix},$$

where

$$S_s(t) \triangleq \left[I^{k\times k} \;\; 0^{k\times(n_\eta-k)} \right] S^{-1}(t)$$
$$S_u(t) \triangleq \left[0^{(n_\eta-k)\times k} \;\; I^{(n_\eta-k)\times(n_\eta-k)} \right] S^{-1}(t),$$

W_s, W_u, S are as in Theorem 1, and without loss of generality $W_s(0) = I^{k\times k}$, $W_u(0) = I^{(n_\eta-k)\times(n_\eta-k)}$. □

Corollary 1.1 Given an operator $\mathcal{A}$ as in Definition 2,

1. $\| \mathcal{A}[v(\cdot)](\cdot) \|_{1+\infty} \leq G_{\mathcal{A}} \| v(\cdot) \|_{1+\infty}$ for some $G_{\mathcal{A}}$ (finite gain property)
2. $\mathcal{A} : L_1 \cap L_\infty \to L_1 \cap L_\infty \cap C^0$
3. $\lim_{t\to-\infty} \mathcal{A}(v)(t) = \lim_{t\to+\infty} \mathcal{A}(v)(t) = 0$

Proof: See [1]. □
This linear operator, $\mathcal{A}$, finds a bounded solution to an unstable linear system. This operator is extended to a nonlinear operator (that finds bounded solutions to the nonlinear internal dynamics) in the next Subsection.

2.2 Generalizing $\mathcal{A}$ to Nonlinear Case; the Operator $\mathcal{N}$

The following Condition requires that, the perturbation term in equation (2.1) satisfies a locally Lipschitz-like condition in both η and Y.

Condition II The pair $[s(\cdot,\cdot,\cdot), A(\cdot)]$ satisfies condition II if, for any $Y_1(\cdot), Y_2(\cdot) \in \mathcal{B}_r^{n_Y}$ and $\eta_1(\cdot), \eta_2(\cdot) \in \mathcal{B}_r^{n_\eta}$, the perturbation term $s[\eta(\cdot), Y(\cdot), \cdot] - A(\cdot)\eta(\cdot)$ satisfies the following Lipschitz-like condition (uniformly in t),

$$\| \{s[\eta_1(t), Y_1(t), t] - A(t)\eta_1(t)\} - \{s[\eta_2(t), Y_2(t), t] - A(t)\eta_2(t)\} \|_{1+\infty}$$

$$\leq K_1 \| \eta_1(t) - \eta_2(t) \|_{1+\infty} + K_2 \| Y_1(t) - Y_2(t) \|_{1+\infty} \tag{2.10}$$

where $s : \Re^{n_\eta} \times \Re^{n_Y} \times \Re \to \Re^{n_\eta}$, $A \in \Re^{(n_\eta \times n_\eta)}$, and $\mathcal{B}_r$ denotes a ball of radius r in the appropriate space (see nomenclature) . □

Remark 2 Condition II is applicable even when $s(\cdot,\cdot,\cdot)$ is not differentiable. For example, $s[\eta(t), Y(t), t] = \eta(t) + 0.1|\eta(t)| + Y(t)$, which is not differentiable at $\eta = 0$, satisfies the above condition with $A(t) = 1$. However, a $s[\eta(\cdot), Y(\cdot), \cdot]$ with a step discontinuity in the first variable at $\eta = 0$ does not satisfy this Lipschitz-like Condition II for any $A(\cdot)$. □

Next, the linear operator $\mathcal{A}$ is used to define a contraction, $\mathcal{P}_Y(\cdot)$. In particular, Theorem 2 will show that $\mathcal{P}_Y(\cdot)$ is a contraction and Theorem 3 will show that the fixed point of $\mathcal{P}_{Y_d}(\cdot)$ is a bounded solution to the nonlinear internal dynamics (1.3). Note that, for ease in notation, $Y(\cdot)$ and $Y_d(\cdot)$ are represented as Y and Y_d respectively.

Definition 3

$$\mathcal{P}_Y(\eta)(t) \triangleq \mathcal{A}\,[\,s[\eta(\cdot), Y(\cdot), \cdot] - A(\cdot)\eta(\cdot)\,](t), \tag{2.11}$$

where $Y(\cdot) \in \mathcal{B}_r^{n_Y}$, $\eta(\cdot) \in \mathcal{B}_r^{n_\eta}$, $A(\cdot)$ satisfies Condition I and the conditions of Theorem 1, and $[s(\cdot,\cdot,\cdot), A(\cdot)]$ satisfies condition II. Note that, for ease in notation, $\eta(\cdot)$ is represented by η whenever the meaning is clear. □

Theorem 2 Let the conditions in Definition 3 be satisfied, and the Lipschitz constants, (K_1, K_2), in Condition II satisfy $K_1 G_{\mathcal{A}} < 1$, and $K_2 G_{\mathcal{A}} < 1 - K_1 G_{\mathcal{A}}$, where $G_{\mathcal{A}}$ is the bound on the gain of the linear operator $\mathcal{A}$ (see Corollary 1.1). Then, there exists a unique $\eta_Y^*(\cdot) \in \mathcal{B}_r^{n_Y}$, such that $\eta_Y^*(t) = \mathcal{P}_Y[\eta_Y^*(\cdot)](t)$.

Proof: From Corollary 1.1 for any $Y(\cdot) \in \mathcal{B}_r^{n_Y}$ we have

$$\begin{aligned} \| \mathcal{P}_Y(\eta)(\cdot) \|_{1+\infty} &\leq G_{\mathcal{A}} \| s[\eta(\cdot), Y(\cdot), \cdot] - A(\cdot)\eta(\cdot) \|_{1+\infty} \\ &\leq G_{\mathcal{A}} \left(K_1 \| \eta(\cdot) \|_{1+\infty} + K_2 \| Y(\cdot) \|_{1+\infty} \right). \end{aligned} \tag{2.12}$$

Since $Y(\cdot) \in \mathcal{B}_r^{n_Y}$ implies $\| Y(\cdot) \|_{1+\infty} < r$, we have from $K_2 G_{\mathcal{A}} < 1 - K_1 G_{\mathcal{A}}$, that $\mathcal{P}_Y(\cdot) : \mathcal{B}_r^{n_\eta} \to \mathcal{B}_r^{n_\eta}$. Next, from the definition of $\mathcal{P}_Y$, linearity of $\mathcal{A}$, Corollary 1.1 and condition II, we obtain

$$\| \mathcal{P}_Y(\eta_1)(\cdot) - \mathcal{P}_Y(\eta_2)(\cdot) \|_{1+\infty} \leq G_{\mathcal{A}} K_1 \| \eta_1(\cdot) - \eta_2(\cdot) \|_{1+\infty}. \tag{2.13}$$

$G_{\mathcal{A}} K_1 < 1$, implies that $\mathcal{P}_Y(\cdot)$ is a contraction, and the Theorem follows from the Contraction Mapping Theorem. □

Remark 3 Equation (2.13) implies that $\mathcal{P}_Y[\eta(\cdot)](\cdot)$ is Lipschitz in $\eta(\cdot)$. □

Theorem 3 Let the conditions of Theorem 2 be satisfied, $Y(\cdot) \in \mathcal{B}_r^{n_Y}$ and $\mathcal{N}(Y) \triangleq \eta_Y^*(\cdot)$. Then (see [3] for an analogous result)

1. $\mathcal{N}(\cdot) : \mathcal{B}_r^{n_Y} \to \mathcal{B}_r^{n_\eta} \cap C_0$ and $\frac{d}{dt}[\mathcal{N}(Y)](t) = s[[\mathcal{N}(Y)](t), Y(t), t]$ a.e. in $t \in \Re$.
2. $\lim_{t\to-\infty}[\mathcal{N}(Y)](t) = \lim_{t\to+\infty}[\mathcal{N}(Y)](t) = 0$

Proof: Theorem 2 and the Contraction Mapping Theorem implies the existence of a unique fixed point $\eta_Y^*(\cdot) \in \mathcal{B}_r^{n_\eta}$ such that

$$\eta_Y^*(t) = \mathcal{P}_Y(\eta_Y^*)(t) = \mathcal{A}\,[s[\eta_Y^*(\cdot), Y(\cdot), \cdot] - A(\cdot)\eta_Y^*(\cdot)](t)$$

$$\| \eta_Y^*(\cdot) \|_{1+\infty} \leq \frac{K_2 G_{\mathcal{A}}}{1 - K_1 G_{\mathcal{A}}} \| Y(\cdot) \|_{1+\infty} \tag{2.14}$$

hence $\eta_Y^*(\cdot) \in L_1 \cap L_\infty \cap C^0$ from which the first assertion of the Theorem follows. Next, consider the sequence

$$\begin{aligned} \eta_Y^0(\cdot) &= 0 \\ \eta_Y^{n+1}(t) &= \mathcal{P}_Y(\eta_Y^n)(t), \end{aligned} \tag{2.15}$$

which converges to $\eta_Y^*(\cdot)$ uniformly in t. The uniform convergence of this sequence, and the fact that

$$\lim_{t\to-\infty} \eta_Y^n(t) = \lim_{t\to+\infty} \eta_Y^n(t) = 0$$

for all $n > 0$ (by Corollary 1.1), implies the second assertion of the Theorem. □
In particular, the last Theorem shows that $\eta_d(\cdot) \triangleq [\mathcal{N}(Y_d)](\cdot) = \eta_{Y_d}^*(\cdot)$ is a bounded solution to the internal dynamics (1.3), i.e., $\dot{\eta}_d(t) = s[\eta_d(t), Y_d(t), t]$.

3 Computational Issues

Computation of the inverse input-trajectory, $u_d(\cdot)$ requires: (a) iterative integrations over an infinite time window to find $[\mathcal{N}(Y_d)](\cdot)$ (Section 2); and (b) computation of a transformation S that achieves the dichotomic split (Definition 1), which is also an iterative process (see [21], Theorem 2 and Theorem 3). In this Section we show that it is possible to compute with a single iterative process, an *approximate* inverse input-trajectory, $\hat{u}_d(\cdot)$, and establish bounds on the error, $\| \hat{u}_d(\cdot) - u_d(\cdot) \|_{1+\infty}$.

3.1 Errors due to truncations and finite iterations

In the last Section, we found a bounded solution to the internal dynamics (1.3) by iteratively finding the fixed point of the contraction $\mathcal{P}_{Y_d}(\cdot)$. Each step in the iterative procedure required computations over the whole real line. Here we truncate $\mathcal{P}_{Y_d}(\cdot)$, to the compact interval $[-T, T]$ and thus define a new operator $\mathcal{P}_{Y_d,T}(\cdot)$. In the following, we begin with a general output trajectory $Y(\cdot)$.

Definition 4 Let the conditions in Definition 3 be satisfied, $v(\cdot) \in L_1 \cap L_\infty$, $Y(\cdot) \in \mathcal{B}_r^{n_Y}$, and $T \in \Re$. Then

$$\begin{aligned} \mathcal{A}_T(v)(t) &\triangleq S(t) \begin{bmatrix} \int_{-T}^{t} W_s(t) W_s^{-1}(\tau) S_s(\tau) v(\tau) d\tau \\ -\int_{t}^{T} W_u(t) W_u^{-1}(\tau) S_u(\tau) v(\tau) d\tau \end{bmatrix}, \\ &\qquad \text{for all } t \in [-T, T] \\ &\triangleq 0 \quad \text{otherwise,} \end{aligned}$$

$$\mathcal{P}_{Y,T}(\eta)(t) \triangleq \mathcal{A}_T \left[s[\eta(\cdot), Y(\cdot), \cdot] - A(\cdot)\eta(\cdot) \right](t)$$

with S, S_s, S_u, W_s, W_u as in Definition 2 . □

The following Theorem will establish that the above truncated map, $\mathcal{P}_{Y,T}(\cdot)$, is also a contraction. The goal is to show that, for a given $Y(\cdot)$, the fixed point of the truncated map is *close* to the fixed point of the original map, $\mathcal{P}_Y(\cdot)$.

Theorem 4 If $G_{\mathcal{A}}$, the bound on the gain of the linear operator $\mathcal{A}$ K_1 and K_2 are sufficiently small then there exists $\eta_{Y,T}^*(\cdot)$, a unique fixed point of $\mathcal{P}_{Y,T}(\cdot)$. Further, the sequence $\{\eta_{Y,T,m}(\cdot)\}_{m=0}^{\infty}$, defined by

$$\begin{aligned} \eta_{Y,T,0}(\cdot) &\triangleq 0 \\ \eta_{Y,T,m+1}(t) &\triangleq \mathcal{P}_{Y,T}(\eta_{Y,T,m})(t) \end{aligned} \tag{3.1}$$

converges to $\eta_{Y,T}^*(\cdot)$ in the $\| \cdot \|_{1+\infty}$ sense (as m increases).

Proof: This follows from arguments similar to those in the proof of Theorem 3. □

The following lemma establishes that $\mathcal{P}_Y(\eta)(\cdot) = \lim_{T \to \infty} \mathcal{P}_{Y,T}(\eta)(\cdot)$, in the $\| \cdot \|_{1+\infty}$ sense.

Lemma 1 Let $\eta(\cdot) \in \mathcal{B}_r^{n_\eta}$. Then $\lim_{T \to \infty} \| \mathcal{P}_Y(\eta)(\cdot) - \mathcal{P}_{Y,T}(\eta)(\cdot) \|_{1+\infty} = 0$

Proof: We first show that

$$\lim_{T \to \infty} \| \mathcal{P}_Y(\eta)(\cdot) - \mathcal{P}_{Y,T}(\eta)(\cdot) \|_1 = 0.$$

For ease in terminology we will use the following notations

$$\begin{aligned} \gamma(t) &\triangleq s[\eta(t), Y(t), t] - A(t)\eta(t) \\ \gamma_s(t, \tau) &\triangleq W_s(t) W_s^{-1}(\tau) S_s(\tau) \gamma(\tau) \\ \gamma_u(t, \tau) &\triangleq W_u(t) W_u^{-1}(\tau) S_u(\tau) \gamma(\tau). \end{aligned}$$

Then from Definitions 2,3 and 4, we obtain

$$\begin{aligned} \| \mathcal{P}_Y(\eta)(\cdot) - \mathcal{P}_{Y,T}(\eta)(\cdot) \|_1 &= \int_{-\infty}^{-T} \| \mathcal{A}(\gamma)(t) - \mathcal{A}_T(\gamma)(t) \|_1 dt \\ &+ \int_{-T}^{T} \| \mathcal{A}(\gamma)(t) - \mathcal{A}_T(\gamma)(t) \|_1 dt \\ &+ \int_{T}^{\infty} \| \mathcal{A}(\gamma)(t) - \mathcal{A}_T(\gamma)(t) \|_1 dt \end{aligned}$$

We illustrate the proof technique for only one of the terms. The rest of the proof follows from similar algebraic manipulations. From Definition 2 and Definition 4,

$$\begin{aligned} \int_{-\infty}^{-T} \| \mathcal{A}(\gamma)(t) - \mathcal{A}_T(\gamma)(t) \|_1 (dt) &\leq \int_{-\infty}^{-T} \| S(t) \|_1 \int_{-\infty}^{t} \| \gamma_s(t,\tau) \|_1 d\tau dt \\ &+ \int_{-\infty}^{-T} \| S(t) \|_1 \int_{T}^{+\infty} \| \gamma_u(t,\tau) \|_1 d\tau dt \end{aligned}$$

For the first term on the r.h.s. apply inequalities, (2.7), (2.8) and (2.9) to obtain

$$\begin{aligned} \int_{-\infty}^{-T} \| S(t) \|_1 \int_{-\infty}^{t} \| \gamma_s(t,\tau) \|_1 d\tau dt &\leq N_1 N_2 K \int_{-\infty}^{-T} \int_{-\infty}^{t} e^{-(\alpha-\epsilon)(t-\tau)} \| \gamma(\tau) \|_1 d\tau dt \\ &\leq N_1 N_2 K \int_{-\infty}^{-T} \int_{\tau}^{-T} e^{-(\alpha-\epsilon)(t-\tau)} \| \gamma(\tau) \|_1 dt d\tau \\ &= \frac{N_1 N_2 K}{\alpha - \epsilon} \int_{-\infty}^{-T} \left[1 - e^{(\alpha-\epsilon)(T+\tau)} \right] \| \gamma(\tau) \|_1 d\tau \, . \end{aligned}$$

Since $\tau \leq -T$, and $\alpha - \epsilon > 0$, we have $0 < e^{(\alpha-\epsilon)(T+\tau)} \leq 1$ and hence

$$\int_{-\infty}^{-T} \| S(t) \|_1 \int_{-\infty}^{t} \| \gamma_s(t,\tau) \|_1 d\tau dt \leq \frac{N_1 N_2 K}{\alpha - \epsilon} \int_{-\infty}^{-T} \| \gamma(\tau) \|_1 d\tau \, .$$

This tends to 0 as $T \to \infty$ if $\gamma(\cdot) \in L_1$, which follows from the definition of $\gamma(\cdot)$, Condition II, $\eta(\cdot) \in L_1 \cap L_\infty$ and $Y(\cdot) \in L_1 \cap L_\infty$. Similarly, the other terms also tend to zero as $T \to \infty$. The key is to rewrite them, either as integrals from $-\infty$ to $-T$, or as integrals from T to ∞ and then show that the integrals go to zero as T tends to infinity.

Next we show that $\lim_{T\to\infty} \| \mathcal{P}_Y(\eta)(t) - \mathcal{P}_{Y,T}(\eta)(t) \|_\infty = 0$, uniformly in t. We split the proof into three parts: (a) $t \leq -T$; (b) $-T \leq t \leq T$; and (c) $T \leq t$. We illustrate the proof technique for case $t \leq -T$ only. For $t \leq -T$

$$\begin{aligned} \| \mathcal{P}_Y(\eta)(t) - \mathcal{P}_{Y,T}(\eta)(t) \|_\infty &\leq \| \mathcal{P}_Y(\eta)(t) - \mathcal{P}_{Y,T}(\eta)(t) \|_1 \\ &= \| \mathcal{A}(\gamma)(t) - \mathcal{A}_T(\gamma)(t) \|_1 \\ &\leq \| S(t) \|_{1+\infty} \left(\int_{-\infty}^{t} \| \gamma_s(t,\tau) d\tau \|_1 + \int_{T}^{\infty} \| \gamma_u(t,\tau) d\tau \|_1 \right) \end{aligned}$$

$$\leq N_1 N_2 K \left(\int_{-\infty}^{t} e^{-(\alpha-\epsilon)(t-\tau)} \| \gamma(\tau) d\tau \|_1 + \int_{T}^{\infty} e^{-(\beta-\epsilon)(\tau-t)} \| \gamma(\tau) d\tau \|_1 \right)$$
$$\leq N_1 N_2 K \left(\int_{-\infty}^{-T} \| \gamma(\tau) d\tau \|_1 + \int_{T}^{\infty} \| \gamma(\tau) d\tau \|_1 \right)$$

$\gamma \in L_1$ implies that the *r.h.s* tends to 0 as $T \to \infty$ independent of t, and hence *l.h.s* tends to zero uniformly in t. The other two cases, when $t \geq -T$, can be proved by similar arguments.

Thus, the limit is established in the $\| \cdot \|_1$ and in the $\| \cdot \|_\infty$ norms, which completes the proof. □

The next Lemma states that $\eta^*_{Y,T}(\cdot)$, the fixed point of the truncated operator $\mathcal{P}_{Y,T}(\cdot)$, tends to $\eta^*_Y(\cdot)$, the fixed point of the operator $\mathcal{P}_Y(\cdot)$, as $T \to \infty$
(see [20], page 7, for a related Theorem).

Lemma 2 For all $\epsilon_1 > 0$ there exists $T_1(\epsilon_1)$ such that $T > T_1(\epsilon_1)$ implies that $\| \eta^*_{Y,T}(\cdot) - \eta^*_Y(\cdot) \|_{1+\infty} \leq \epsilon_1$.

Proof:

$$\| \eta^*_{Y,T}(\cdot) - \eta^*_Y(\cdot) \|_{1+\infty} = \| \mathcal{P}_{Y,T}\left(\eta^*_{Y,T}\right)(\cdot) - \mathcal{P}_Y\left(\eta^*_Y\right)(\cdot) \|_{1+\infty}$$
$$\leq \| \mathcal{P}_Y\left(\eta^*_{Y,T}\right)(\cdot) - \mathcal{P}_Y\left(\eta^*_Y\right)(\cdot) \|_{1+\infty} + \| \mathcal{P}_Y\left(\eta^*_{Y,T}\right)(\cdot) - \mathcal{P}_{Y,T}\left(\eta^*_{Y,T}\right)(\cdot) \|_{1+\infty}$$

using the triangle inequality. Next, using the Lipschitz property of $\mathcal{P}_Y(\cdot)$ we obtain (see Remark 3)

$$\| \eta^*_{Y,T}(\cdot) - \eta^*_Y(\cdot) \|_{1+\infty} \leq K_1 G_{\mathcal{A}} \| \eta^*_{Y,T}(\cdot) - \eta^*_Y(\cdot) \|_{1+\infty} + \| \mathcal{P}_Y\left(\eta^*_{Y,T}\right)(\cdot) - \mathcal{P}_{Y,T}\left(\eta^*_{Y,T}\right)(\cdot) \|_{1+\infty}$$
$$\Longrightarrow \quad \| \eta^*_{Y,T}(\cdot) - \eta^*_Y(\cdot) \|_{1+\infty} \leq \frac{1}{1 - K_1 G_{\mathcal{A}}} \| \mathcal{P}_Y\left(\eta^*_{Y,T}\right)(\cdot) - \mathcal{P}_{Y,T}\left(\eta^*_{Y,T}\right)(\cdot) \|_{1+\infty}.$$

Note, from Lemma 1, we have $\mathcal{P}_Y(\eta^*_{Y,T}) = \lim_{T\to\infty} \mathcal{P}_{Y,T}(\eta^*_{Y,T})$, and hence the right hand side can be made arbitrarily small by choosing T large enough. □

The next Theorem gives the main result that, the inverse trajectory can be approximated (arbitrarily closely) by choosing a large enough time window for computations in each iteration and by using a sufficiently large number of iterations.

Theorem 5 Given $\epsilon > 0$ there exists M, T^* such that $m > M$, $T > T^*$ implies that $\| \hat{u}_d(\cdot) - u_d(\cdot) \|_{1+\infty} \leq \epsilon$, where u_d is defined by equation (1.4) and the approximate inverse-input $\hat{u}_d(\cdot)$ is defined as

$$\hat{u}_d(t) \triangleq [\beta[\zeta_d(t), \eta_{Y_d,T,m}(t), t]]^{-1} \left[y_d^{(r)}(t) - \alpha[Y_d(t), \eta_{Y_d,T,m}(t), t] \right]. \qquad (3.2)$$

Proof: Lemma 2 and the convergence of sequence $\eta_{Y_d,T,m}(\cdot)$ (see equation (3.1)) imply that $\| \eta_{Y_d,T,m}(\cdot) - \eta^*_{Y_d}(\cdot) \|_{1+\infty}$ can be made arbitrarily small by choosing T and m large enough. The Theorem follows from the continuity of $\hat{u}(t)$ in $\eta(t)$. □

Summarizing, given an $\epsilon > 0$, $\hat{u}_d(\cdot)$ can be computed through a finite number (m) of iterative integrations performed over a closed time interval $[-T^*, T^*]$, such that $\| \hat{u}_d(\cdot) - u_d(\cdot) \|_{1+\infty} < \epsilon$. This bound, ϵ, can be made arbitrarily small by increasing T^* and m.

3.2 Computation of $S(\cdot)$

Given a nonlinear time-varying internal dynamics, $\dot{\eta}(t) = s[\eta(t), Y(t), t]$, the key is to find a pair $(A(\cdot), S(\cdot))$ such that: (a) $s[\eta(t), Y(t), t] - A\eta(t)$ satisfies the Lipschitz-like Condition II; and (b) the change of variables $\eta(t) = S(t)w(t)$ achieves the dichotomic split of the linear equation $\dot{\eta}(t) = A(t)\eta(t)$. The existence of the block-diagonalizing transformation $S(t)$ has been studied in [21], however, the computation of the transformation is iterative. Below, we present a modified algorithm that circumvents the iteration.

Algorithm for $S(\cdot)$ [Coppel]

1. Choose $\hat{A}(\cdot)$ (not necessarily $= \frac{d}{d\eta}s$) such that; (a) $\| \hat{A}(t) \|_{1+\infty}$ is bounded, and slowly varying; and (b) $s[\eta(t), Y(t), t] - \hat{A}\eta(t)$ satisfies the Lipschitz-like Condition II.

2. Compute the projection operator (onto the stable subspace of $\hat{A}(t)$)

$$P(t) \triangleq \frac{1}{2\pi i} \int_\gamma [\lambda I - \hat{A}(t)]^{-1} d\lambda,$$

   where γ is the simple closed curve in the left half plane formed by the imaginary axis and part of the circle $|\lambda| > \| \hat{A} \|$ (see [21], page 511)

3. solve the first order linear ordinary differential equation ([21], page 513)

$$\dot{U}(t) = [\dot{P}(t)P(t) - P(t)\dot{P}(t)]U(t); \quad U(0) = I,$$

4. and compute $S(t) \triangleq U(t)R^{-1}(t)$ with

$$R(t) \triangleq [P(0)U^*(t)U(t)P(0) + \{I - P(0)\}U^*(t)U(t)\{I - P(0)\}]^{1/2}.$$

   This $S(t)$ cannot be used to decouple $\hat{A}(t)$, although such a decoupling transformation can be found using the iterative algorithm in ([21], see Theorem 2). Instead, we choose an alternate $A(\cdot)$ matrix.

5. Choose $A(t) \triangleq \hat{A}(t) + \dot{S}(t)S^{-1}(t)$ □

It follows from Coppel ([21] Theorem 3) that: (a) $S(\cdot)$ decomposes $A(\cdot)$ as in Theorem 1; and (b) $\| \dot{S}(t)S^{-1}(t) \|_{1+\infty}$ is proportional to the $\| \hat{A}(\cdot) \|_{1+\infty}$. This proportional dependence implies that $A(\cdot)$ also satisfies the Lipschitz-like Condition II. (if it is satisfied by a slowly-varying $\hat{A}(\cdot)$). This concludes the algorithm to compute the dichotomic split of the linearized internal dynamics.

4 Conclusions

In this paper we have defined a new method for inverting nonlinear nonminimum-phase time-varying systems, and have presented a constructive algorithm for computing inverse trajectories. The inverse trajectories form the basis of a new exact output tracking controller. Since the noncausal inverses decay to zero exponentially in negative time, truncation is attractive and was analyzed - all the desirable continuity properties of the truncation were shown to hold.

Acknowledgment

The authors would like to thank Petar Kokotovic for his encouragement in pursuing this line of research and observing the utility of Coppel's results. Support through National Science Foundation grant MSS-9216690, NASA Ames Research Center Grant NAG-2-1042, and the Astro Aerospace Corporation are gratefully acknowledged.

Nomenclature

If $x(\cdot)$ (also denoted by x) is a vector valued function with $x(t) = [x_1(t)\, x_2(t)\, x_3(t) \ldots\, x_n(t)]^T$ i.e., $x(t) \in \Re^n$, then $\| x(t) \|_1 \triangleq \sum_{i=1}^{i=n} |x_i(t)|$ is the standard 1-norm in $\Re^n$, $\| x(t) \|_\infty \triangleq \max_i |x_i(t)|$ is the standard ∞-norm in $\Re^n$, and $\| x(t) \|_{1+\infty} \triangleq \| x(t) \|_1 + \| x(t) \|_\infty$.

If $z(t) \in \Re^{n \times n}$ is a matrix then $\| z(t) \|_1$ is the induced 1-norm,
$\| z(t) \|_1 \triangleq \sup_{y \neq 0,\, y \in \Re^n} \| z(t)\, y \|_1 / \| y \|_1$,
$\| z(t) \|_\infty$ is the induced ∞-norm, $\| z(t) \|_\infty \triangleq \sup_{y \neq 0,\, y \in \Re^n} \| z(t)\, y \|_\infty / \| y \|_\infty$,
and $\| z(t) \|_{1+\infty} \triangleq \| z(t) \|_1 + \| z(t) \|_\infty$

If $x(\cdot)$ (also denoted by x) is a vector valued measurable function, then
$\| x \|_1 \triangleq \| x(\cdot) \|_1 \triangleq \int_{-\infty}^{\infty} \| x(t) \|_1 dt$,
$\| x \|_\infty \triangleq \| x(\cdot) \|_\infty \triangleq \text{ess sup}_{t \in \Re} \| x(t) \|_\infty$, and
$\| x(\cdot) \|_{1+\infty} \triangleq \| x(\cdot) \|_1 + \| x(\cdot) \|_\infty$.

$Y(\cdot) \in \mathcal{B}_r^{n_Y}$ implies $Y(t) \in \Re^{n_Y}$ and $\| Y(\cdot) \|_{1+\infty} < r$.

$\eta(\cdot) \in \mathcal{B}_r^{n_\eta}$ implies $\eta(t) \in \Re^{n_\eta}$ and $\| \eta(\cdot) \|_{1+\infty} < r$.

References

[1] S. Devasia and B. Paden. Exact output tracking for nonlinear time-varying systems. *Proceedings of the 33rd CDC, Lake Buena Vista, Florida*, pages 2346–2355, 1994.

[2] E. Bayo. A finite-element approach to control the end-point motion of a single-link flexible robot. *J. of Robotic Systems*, 4(1):63–75, 1987.

[3] S. Devasia, D. Chen, and B. Paden. Nonlinear inversion-based output tracking. *IEEE Transactions on Automatic Control*, 41(7):930–943, 1996.

[4] G. Meyer, L. R. Hunt, and R. Su. Nonlinear system guidance in the presense of transmission zero dynamics. *NASA Technical Memorandun No. 4661*, January, 1995.

[5] P. Martin, S. Devasia, and B. Paden. A different look at output tracking: Control of a vtol aircraft. *Proceedings of the 33rd Conference on Decision and Control, Lake Buena Vista, Florida*, pages 2376–2381, 1994.

[6] B.A.Francis. The linear multivariable regulator problem. *SIAM94 J. Control and Optimization*, 15:486–505, 1977.

[7] A. Isidori and C. I. Byrnes. Output regulation of nonlinear systems. *IEEE Transactions on Automatic Control*, 35(2):131–140, 1990.

[8] J. Huang and W. J. Rugh. An approximation method for the nonlinear servomechanism problem. *IEEE Transactions on Automatic Control*, Sept,37(9):1395–1398, 1992.

[9] A. J. Krener. *The Construction of Optimal Linear and Nonlinear Regulators. In Systems, Models and Feedback: Theory and Application. A. Isidori and T.J. Tarn (editors).* Birkhauser, Boston, 1992.

[10] J. Huang and W. J. Rugh. On a nonlinear multivariable servomechanism problem. *Automatica*, 26(6):963–972, 1990.

[11] J. Huang and C. F. Lin. Internal model principle and robust control of nonlinear systems. *Proc. of the 32nd CDC, San Antonio, Texas*, pages 1501–1506, 1993.

[12] J. Hauser, S. Sastri, and G. Meyer. Nonlinear control design for slightly nonminimum phase systems: Application to v/stol aircraft. *Automatica*, 28(4):665–679, 1992.

[13] R. Gurumoorthy and S. R. Sanders. Controling non-minimum phase nonlinear systems - the inverted pendulum on a cart example. *Proceedings of the American Control Conference, San Francisco, CA*, pages 680–685, 1993.

[14] S. Gopalswamy and J.K. Hedrick. Tracking nonlinear non-minimum phase systems using sliding control. *International Journal of Control*, 57(5):1141–1158, 1993.

[15] R. M. Hirschorn. Invertibility of nonlinear control systems. *SIAM J. Control and Optimization*, 17(2):289–297, 1979.

[16] M. D. Di Benedetto and P. Lucibello. Inversion of nonlinear time-varying systems. *IEEE Trans. Automatic Control*, 38(8):1259–1264, 1993.

[17] P. Lucibello and M. D. Di Benedetto. Output tracking for a nonlinear flexible arm. *ASME Dynamical Systems*, 115(1):78–85, 1993.

[18] B. Paden, D. Chen, R. Ledesma, and E. Bayo. Exponentially stable tracking control for multi-joint flexible manipulators. *ASME Journal of Dynamic Systems, Measurement and Control*, 115(1):53–59, 1993.

[19] A. Isidori. *Nonlinear Control Systems: An Introduction.* Springler-Verlag, 1989.

[20] Jack K. Hale. *Ordinary Differential Equations.* Wiley-Interscience, 1969.

[21] W. A. Coppel. Dichotomies and reducibility. *Journal of Differential Equations*, 3(4):500–521, 1967.

Optimal Output Trajectory Redesign for Invertible Systems

S. Devasia

Reprinted from

Journal of Guidance, Control, and Dynamics

Volume 19, Number 5, Pages 1189–1191

AIAA

A publication of the
American Institute of Aeronautics and Astronautics, Inc.
1801 Alexander Bell Drive, Suite 500
Reston, VA 22091

Optimal Output Trajectory Redesign for Invertible Systems

S. Devasia*
University of Utah, Salt Lake City, Utah 84112

I. Introduction

GIVEN a desired output trajectory, inversion-based techniques find input-state trajectories required to exactly track the output.[1,2] These inversion-based techniques have been successfully applied to the endpoint tracking control of multijoint flexible manipulators in Ref. 3 and to aircraft control in Ref. 4. The specified output trajectory uniquely determines the required input and state trajectories that are found through inversion. These input-state trajectories exactly track the desired output; however, they might not meet acceptable performance requirements. For example, during slewing maneuvers of flexible structures, the structural deformations, which depend on the required state trajectories, may be unacceptably large. Further, the required inputs might cause actuator saturation during an exact tracking maneuver, for example, in the flight control of conventional takeoff and landing aircraft.[5] In such situations, a compromise is desired between the tracking requirement and other goals such as reduction of internal vibrations and prevention of actuator saturation; the desired output trajectory needs to be redesigned.

Here, we pose the trajectory redesign problem as an optimization of a general quadratic cost function and solve it in the context of linear systems. The solution is obtained as an off-line prefilter of the desired output trajectory. An advantage of our technique is that the prefilter is independent of the particular trajectory. The prefilter can therefore be precomputed, which is a major advantage over other optimization approaches (see Ref. 6 for further references).

Previous works have addressed the issue of preshaping inputs to minimize residual and in-maneuver vibrations for flexible structures; see, for example, Refs. 6 and 7. Since the command preshaping is computed offline, in Ref. 8, the use of noncausal prefilters has been suggested—such noncausality is allowable since the command preshaping is computed off-line. Further, minimization of optimal quadratic cost functions has also been previously used to preshape command inputs for disturbance rejection in Ref. 9. All of these approaches are applicable when the inputs to the systems are known a priori. Typically, outputs (not inputs) are specified in tracking problems, and hence the input trajectories have to be computed. The inputs to the system are, however, difficult to determine for nonminimum phase systems like flexible structures. One approach to solve this problem is to 1) choose a tracking controller (the desired output trajectory is now an input to the closed-loop system) and 2) redesign this input to the closed-loop system. Thus, we effectively perform output redesign.[6] These redesigns are, however, dependent on the choice of the tracking controllers.[10] Thus, the controller optimization and trajectory redesign problems become coupled; this coupled optimization is still an open problem. In contrast, we decouple the trajectory redesign problem from the choice of feedback-based tracking controller. It is noted that our approach remains valid when a particular tracking controller is chosen. In addition, the formulation of our problem not only allows for the minimization of residual vibrations as in available techniques[6] but also allows for the optimal reduction of vibrations during the maneuver, e.g., the altitude control of flexible spacecraft.[9] We begin by formulating the optimal output trajectory redesign problem and then solve it in the context of general linear systems. This theory is then applied to an example flexible structure, and simulation results are provided.

Received April 22, 1996; revision received May 30, 1996; accepted for publication May 30, 1996.

*Assistant Professor, Department of Mechanical Engineering. Member AIAA.

II. Problem Formulation

System Inversion for Exact Tracking

Consider a square system described by

$$\dot{x} = Ax + Bu; \qquad y = Cx$$

where $x \in \Re^n$, $u \in \Re^p$, and $y \in \Re^p$. The inversion approach[2] finds a bounded input-state trajectory that satisfies the preceding system equations and yields the exact desired output, i.e.,

$$\dot{x}_{\text{ref}} = Ax_{\text{ref}} + Bu_{ff}; \qquad y_d = Cx_{\text{ref}}$$

The inverse input-state trajectories can be described in terms of Fourier transforms as[1,11]

$$\begin{aligned} u_{ff}(j\omega) &= [C(j\omega I - A)^{-1}B]^{-1}y_d(j\omega) = G_y^{-1}(j\omega)y_d(j\omega) \\ x_{\text{ref}}(j\omega) &= [(j\omega I - A)^{-1}B]u_{ff}(j\omega) = G_x(j\omega)u_{ff}(j\omega) \end{aligned} \tag{1}$$

This Fourier-based inversion approach has been extended to nonlinear time-varying nonminimum phase systems in Ref. 2; however, we restrict our discussion to linear time-invariant systems.

Remark. We note two results. One, an inverse exists if the output and a certain number of its time derivatives are bounded. The number of time derivatives of the output that needs to be specified for an inverse to exist is well defined and depends on the relative degree of the system.[2,12] Second, for linear hyperbolic systems, if the inverse exists, then it is unique.[1,2]

Performance Criterion

Trajectory redesign seeks a compromise between the goal of tracking the desired trajectory and other goals such as reducing the magnitude of input and vibrations. We formulate this redesign problem as the minimization of a quadratic cost function of the type

$$\int_{-\infty}^{\infty} \left\{ u(t)^T Ru(t) + x(t)^T Q_x x(t) + [y(t) - y_d(t)]^T Q_y [y(t) - y_d(t)] \right\} dt$$

where R, Q_x, and Q_y represent the weight on control input, states, and the error in output tracking, respectively.

Using Parseval's theorem, we rewrite our optimization problem in frequency domain as the minimization of the cost function

$$J = \int_{-\infty}^{\infty} \left\{ u(j\omega)^* Ru(j\omega) + x(j\omega)^* Q_x x(j\omega) + [y(j\omega) - y_d(j\omega)]^* Q_y [y(j\omega) - y_d(j\omega)] \right\} d\omega \tag{2}$$

where the superscript $*$ denotes complex conjugate transpose.

Optimal Redesign of the Output

Our main result is given by the following lemma, which shows that the optimal output trajectory redesign can be described as a prefilter, which maps desired output trajectories y_d to the redesigned output trajectory y_{opt}. This prefilter G_f does not depend on the particular choice of desired trajectory and hence can be precomputed.

Lemma. The modified output trajectory y_{opt} is given by $y_{\text{opt}}(j\omega) = G_f(j\omega)y_d(j\omega)$, where

$$G_f(j\omega) = 1 - G_y\left[R + G_x^* Q_x G_x + G_y^* Q_y G_y\right]^{-1} \times \left[R + G_x^* Q_x G_x\right] G_y^{-1}$$

The modified input trajectory u_{opt} is given by $u_{\text{opt}}(j\omega) = u_{ff}(j\omega) + v_{\text{opt}}(j\omega)$, where $v_{\text{opt}}(j\omega) = G_v(j\omega)y_d(j\omega)$ and

$$G_v(j\omega) = -\left(R + G_x^* Q_x G_x + G_y^* Q_y G_y\right)^{-1} \times \left(R + G_x^* Q_x G_x\right) G_y^{-1} \tag{3}$$

Note that the dependence on $j\omega$ is not explicitly written for compactness.

Proof. Without loss of generality, we rewrite the input u as the sum of the feedforward input, $G_y^{-1}y_d$, found from inversion of the desired trajectory, and an arbitrary v:

$$u(j\omega) = u_{ff}(j\omega) + v(j\omega) = G_y^{-1}(j\omega)y_d(j\omega) + v(j\omega) \tag{4}$$

Substituting $x(j\omega) = G_x(j\omega)u(j\omega)$ and $y(j\omega) = G_y(j\omega)u(j\omega)$ along with the preceding Eq. (4) for u into the cost function given by Eq. (2), we obtain

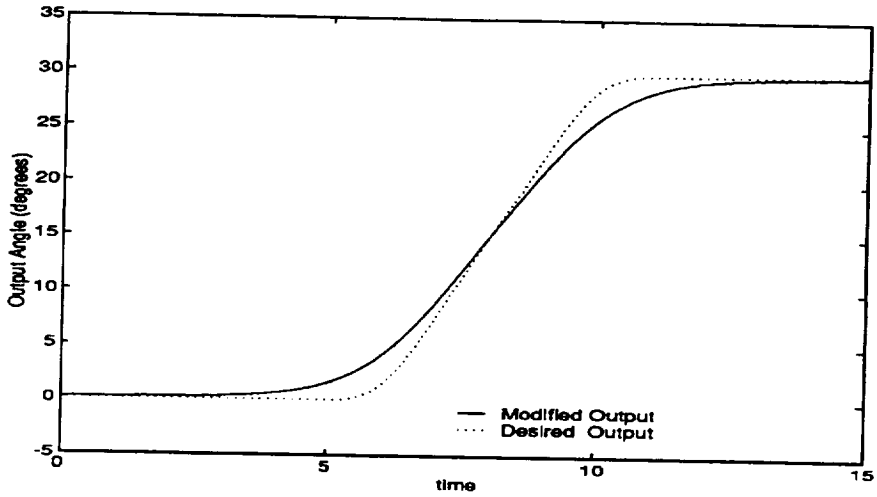

Fig. 1 Output redesign.

$$J = \int_{-\infty}^{\infty} \{[v + (R + G_x^* Q_x G_x + G_y^* Q_y G_y)^{-1} \times (R + G_x^* Q_x G_x) G_y^{-1} y_d]^* * (R + G_x^* Q_x G_x + G_y^* Q_y G_y) \times [v + (R + G_x^* Q_x G_x + G_y^* Q_y G_y)^{-1} \times (R + G_x^* Q_x G_x) G_y^{-1} y_d] + (G_y^{-1} y_d)^* [(R + G_x^* Q_x G_x) + (R + G_x^* Q_x G_x)^* * (R + G_x^* Q_x G_x + G_y^* Q_y G_y)^{-1} \times (R + G_x^* Q_x G_x)](G_y^{-1} y_d)\} \, dw$$

Note that the cost function is quadratic in v. Therefore, the cost function is minimized by setting this quadratic term to zero, i.e., choosing $v(j\omega) = v_{opt}(j\omega) = G_v(j\omega) y_d(j\omega)$, where G_v is defined by Eq. (3) in the lemma. The choice of $v = v_{opt}$ defines the optimal input u_{opt} through Eq. (4) as

$$u_{opt}(j\omega) = [G_y^{-1}(j\omega) + G_v(j\omega)] y_d(j\omega) \tag{5}$$

The result follows from $y_{opt}(j\omega) = G_y(j\omega) u_{opt}(j\omega) = [1 + G_y(j\omega) G_v(j\omega)] y_d(j\omega)$. □

III. Example

Consider a flexible structure consisting of two freely rotating disks connected by a thin shaft. A motor is attached between the connecting shaft and one of the disks. Input to the system is torque τ provided by a dc motor, and the outputs are the angular rotations of the two disks θ_1 and θ_2. These angular rotations are measured using potentiometers. The transfer function of an experimental system, which includes the rigid-body mode and one flexible mode, was obtained using a HP3562A Dynamic Signal Analyzer as

$$\frac{\theta_1}{\tau} = \frac{1.8139s^2 + 0.3077s + 6.1041}{s^4 + 0.2765s^3 + 6.1041s^2}$$
$$\frac{\theta_2}{\tau} = \frac{0.27s^2 - 0.1187s + 6.1041}{s^4 + 0.2765s^3 + 6.1041s^2} \tag{6}$$

With the state vector x chosen as $x = [\theta_1 \ \theta_2 \ \dot{\theta}_1 \ \dot{\theta}_2]^T$, the system equations can be represented in state–space form as $\dot{x} = Ax + Bu$, i.e.,

$$\frac{d}{dt}\begin{bmatrix} \theta_1 \\ \theta_2 \\ \dot{\theta}_1 \\ \dot{\theta}_2 \end{bmatrix} = \begin{bmatrix} 0 & 1 & 0 & 0 \\ -3.1555 & -0.1640 & 3.1555 & 0.3845 \\ 0 & 0 & 0 & 1 \\ 2.8956 & -0.0899 & -2.8956 & -0.1124 \end{bmatrix} \times \begin{bmatrix} \theta_1 \\ \theta_2 \\ \dot{\theta}_1 \\ \dot{\theta}_2 \end{bmatrix} + \begin{bmatrix} 0 \\ 1.8139 \\ 0 \\ 0.27 \end{bmatrix} \tau$$

with $y = \theta_2 = [0 \ 1 \ 0 \ 0]x$. The control objective is to track the angular rotation θ_2 of the disk that is farthest away from the motor (see Fig. 1 for the desired output trajectory).

The relative degree of a single-input/single-output linear system is the number of zeros at infinity.[12] For our system, with the torque as input and θ_2 as output, the transfer function has four poles and two finite zeros [see Eq. (6)]. Thus, the number of zeros at infinity are two, and hence the relative degree is two. This implies that the second derivative of the desired output, i.e., the desired angular acceleration profile of the output, uniquely determines the required input-state trajectory and the resulting structural vibration, $\theta_1 - \theta_2$.[2] If the internal vibrations are to be reduced, then we have to relax the exact tracking requirement. Similarly, to reduce the required input amplitudes we have to compromise exact tracking. This tradeoff can be represented as the minimization of a general quadratic cost function (Sec. II) of the form

$$\int_{-\infty}^{\infty} \{u(t)^T R u(t) + x(t)^T Q_x x(t) + [y(t) - y_d(t)]^T Q_y [y(t) - y_d(t)]\} \, dt$$

where $R = r$, $Q_y = q_y$, and

$$Q_x = q_x \begin{bmatrix} 1 & -1 & 0 & 0 \\ -1 & 1 & 0 & 0 \\ 0 & 0 & 0 & 0 \\ 0 & 0 & 0 & 0 \end{bmatrix}$$

The scalars r, q_x, and q_y represent the relative weight on the reduction of inputs, structural vibrations, and tracking errors, respectively. To reduce the vibrations and control inputs, we choose $r = 1$, $q_x = 5000$, and $q_y = 1$ in our simulations. Figure 1 shows the modification for a desired trajectory— about 10% of the final slew angle. The maximum magnitude of the required input, however, is reduced by 60%, and the corresponding structural vibration, $\theta_1 - \theta_2$, is reduced by 20% (compared with results from exact tracking of the initial desired trajectory).

IV. Conclusion

We formulated and solved the trajectory redesign problem in the context of linear invertible systems, including nonminimum phase systems. Thus, we provide a systematic approach to an optimal tradeoff between tracking desired trajectory and other goals such as vibration reduction and reduction of required inputs. The approach was applied to an example flexible structure, and simulation results were presented. Future work will address trajectory redesign for nonlinear systems.

Acknowledgment

This work was funded through NASA Ames Research Center Grant NAG 2-1042.

References

[1]Bayo, E., "A Finite-Element Approach to Control the End-Point Motion of Single-Link Flexible Robot," *Journal of Robotic Systems*, Vol. 4, No. 1, 1987, pp. 63–75.

[2]Devasia, S., and Paden, B., "Exact Output Tracking for Nonlinear Time-Varying Systems," *Proceedings of the 33rd IEEE Conference on Decision and Control* (Lake Buena Vista, FL), IEEE Control Systems Society, New York, 1994, pp. 2346–2355.

[3]Paden, B., Chen, D., Ledesma, R., and Bayo, E., "Exponentially Stable Tracking Control for Multi-Joint Flexible Manipulators," *Journal of Dynamic Systems, Measurement and Control*, Vol. 115, March 1993, pp. 53–59.

[4]Martin, P., Devasia, S., and Paden, B., "A Different Look at Output Tracking: Control of a VTOL Aircraft," *Proceedings of the 33rd IEEE Conference on Decision and Control* (Lake Buena Vista, FL), IEEE Control Systems Society, New York, 1994, pp. 2376–2381.

[5]Tomlin, C., Lygeros, J., and Shastri, S., "Output Tracking for a Nonminimum Phase Dynamic CTOL Aircraft Model," *Proceedings of the 34th IEEE Conference on Decision and Control* (New Orleans, LA), IEEE Control Systems Society, New York, 1995, pp. 1867–1872.

[6]Singer, N. C., and Seering, W. P., "Preshaping Command Inputs to Reduce System Vibration," *Journal of Dynamic Systems, Measurement and Control*, Vol. 112, March 1990, pp. 76–82.

[7]Smith, O. J. M., *Feedback Control Systems*, McGraw–Hill, New York, 1958.

[8]Singer, N. C., and Seering, W. P., "Using Acausal Shaping Techniques to Reduce Robot Vibration," *Proceedings of the IEEE International Conference on Robotics and Automation*, Vol. 3, IEEE Control Systems Society, New York, 1988, pp. 1434–1439.

[9]Chun, H. M., Turner, J. D., and Juang, J., "Disturbance-Accommodating Tracking Maneuvers of Flexible Spacecraft," *Journal of the Astronautical Sciences*, Vol. 33, No. 2, 1985, pp. 197–216.

[10]Cook, G., "Discussion: Preshaping Command Inputs to Reduce System Vibration," *Journal of Dynamic Systems, Measurement and Control*, Vol. 115, June 1993, pp. 309, 310.

[11]Kwon, D., and Book, W. J., "An Inverse Dynamic Method Yielding Flexible Manipulator State Trajectories," *Proceedings of the American Control Conference*, American Automatic Control Council, New York, 1990, pp. 186–193.

[12]Isidori, A., *Nonlinear Control Systems: An Introduction*, Springer–Verlag, New York, 1989.

INT. J. CONTROL, 1997, VOL. 67, NO. 1, 117–131

Exact-output tracking theory for systems with parameter jumps

SANTOSH DEVASIA†, BRAD PADEN‡ and CARLO ROSSI§

We consider the exact output tracking problem for systems with parameter jumps. Necessary and sufficient conditions are derived for the elimination of switching-introduced output transient. Previous works have studied this problem by developing a regulator that maintains exact tracking through parameter jumps (switches). Such techniques are, however, only applicable to minimum-phase systems. In contrast, our approach is applicable to non-minimum-phase systems and it obtains bounded but possibly non-causal solutions. If the reference trajectories are generated by an exosystem, then we develop an exact-tracking controller in a feedback form. As in standard regulator theory, we obtain a linear map from the states of the exosystem to the desired system state which is defined via a matrix differential equation. The constant solution of this differential equation provides asymptotic tracking, and coincides with the feedback law used in standard regulator theory. The obtained results are applied to a simple flexible manipulator with jumps in the pay-load mass.

1. Introduction

We study the exact-output tracking of systems that are described by

$$\left.\begin{aligned} \dot{x}(t) &= A[k(t)]x(t) + B[k(t)]u(t) \\ y(t) &= C[k(t)]x(t) \end{aligned}\right\} \tag{1}$$

where $x \in \mathbb{R}^n$, with the same number of inputs as outputs $u(t)$, $y(t) \in \mathbb{R}^p$. The system matrices $A(k)$, $B(k)$ and $C(k)$ are constant over the time intervals I_k, where k belongs to a finite index set $\mathscr{K} \triangleq [0, \ldots, N]$, and the parameter change (switch) occurs at times $t = t_1, t_2, \ldots, t_N$ (see Fig. 1). Here, the switching times are known, in contrast to systems where the switches may be signal-driven.

For constant linear systems, asymptotic output-tracking problems have received much attention in the past. In particular, the regulator theory (Francis 1977, Basile and Marro 1992, Wonham 1985) provides a general framework in which the asymptotic output tracking can be solved when the reference trajectory is generated through a linear exosystem. In the presence of switches in the system, one technique for achieving output regulation is to switch the regulator. Note that regulation can be recovered between two consecutive switches (due to asymptotic properties), especially if the switching occurs far apart in time. However, this technique also tends to induce transients in the output during the switches.

Received 10 February 1996. Revised 21 July 1996. Communicated by Professor D. Q. Mayne.

† Department of Mechanical Engineering, University of Utah, Salt Lake City, UT 84112, U.S.A. Tel: +1 (801) 581 4613; e-mail: santosh@me.utah.edu.

‡ Department of Mechanical Engineering, University of California at Santa Barbara, CA 93106, U.S.A.

§ DEIS—Universitá di Bologna, Viale Risorgimento 2, 401362 Bologna, Italy.

0020-7179/97 $12.00 © 1997 Taylor & Francis Ltd.

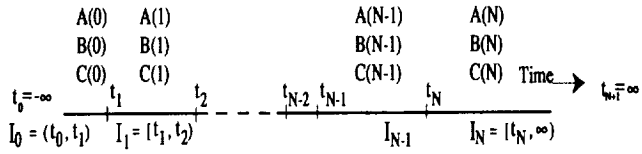

Figure 1. The switching times.

In order to eliminate these switching-caused transients, a regulation scheme that maintains exact trajectory tracking across system switches must be used. This fairly new problem has been studied by Marro and Piazzi (1993) for minimum-phase systems. In this work, a feedforward action is used in conjunction with the feedback defined by the regulator to cancel the output transients across the switches.

We propose an alternative approach for exact output-tracking of switched systems, which is also applicable to non-minimum-phase systems. In the non-minimum-phase case, a bounded non-causal solution is obtained (Devasia *et al.* 1996) that requires preknowledge of the reference trajectory and of all the switching times. Such exact tracking schemes based on non-causal schemes is useful in problems like aircraft guidance (Meyer *et al.* 1995, Hunt *et al.* 1996).

We present necessary and sufficient conditions for the solvability of the inversion problem for linear systems with switches; the inverse is used to track the desired output. We consider two kinds of desired output trajectory: a single pre-specified trajectory, or one belonging to a class of outputs generated by a given linear exosystem, that could undergo parameter changes as well. In this latter case, we obtain the solution in a time-varying feedback form, where the feedback matrix satisfies a matrix ordinary differential equation. The equilibrium solution of this differential equation solves the asymptotic output tracking problem, and coincides with the feedback matrix resulting from the standard regulator. This establishes an interesting connection between our approach and the traditional regulator theory.

The paper is organized as follows: in § 2 the exact tracking of a single prescribed output trajectory is considered, and necessary and sufficient conditions are presented. A geometric version of the obtained conditions is also provided. In § 3 the case of reference trajectory obtained through a linear exosystem will be treated. The conditions of the previous section when rearranged establish a close relationship with the traditional theory of output regulation. Section 4 focuses on the additional problem of stability of the closed loop system. Finally, § 5 presents the application of the developed theory to a simple non-minimum-phase switched system, given by a flexible beam subjected to step variation of the pay-load mass. Conclusions end the paper.

2. Tracking a prescribed output trajectory

Below we formulate the exact tracking problem for a prescribed output trajectory, and establish necessary and sufficient conditions for its solvability. Geometric interpretations of these conditions are also provided.

2.1. *The inversion problem*

Given a desired output trajectory y_d, find a pair of state and input trajectories x_d and u_d such that:

(*a*) x_d and u_d satisfy the system (1):

$$\dot{x}(t) = A[k(t)]x_d(t) + B[k(t)]u_d(t), \quad \forall t \in (-\infty, \infty) \tag{2}$$

(*b*) exact output tracking is achieved (even across switches):

$$y_d(t) = C[k(t)]x_d(t), \quad \forall t \in (-\infty, \infty)$$

(*c*) and the inputs and state are bounded:

$$\|x_d(\cdot)\|_\infty < \infty$$
$$\|u_d(\cdot)\|_\infty < \infty$$

2.2. *Using the inverse for exact-output tracking*

The existence of an inverse (u_d, x_d) implies that there are input-state trajectories that yield the desired output; exact output tracking is easily achieved by stabilizing the desired state trajectory. For example, use u_d as feedforward and use the error $x - x_d$ for feedback (see Fig. 2). Stabilization is not the central issue in this paper, and any scheme for feedback design can be used. For example, given $(A(k), B(k))$ controllable for all k, the system may be stabilized through pole placement with all the closed-loop poles in the same locations for all k.

Note that typically the initial conditions of the system are different from the initial conditions of the desired state trajectory leading to initial transient errors typical of all tracking controllers. However, once the desired level of tracking has been achieved (due to an exponential reduction in error) our technique will maintain tracking across parameter switches. In contrast, switching standard regulators when the system parameters change will cause transient errors at the switching instants; tracking will not be maintained across switches.

2.3. *Exact-tracking maintaining input*

We will assume the following.

Assumption 1: *The system $A(k)$, $B(k)$ and $C(k)$ has a well defined vector relative degree (Isidori 1989) for each $k \in \mathcal{K}$.*

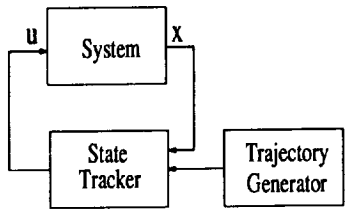

Figure 2. The control scheme.

Then we can find a coordinate transformation $\hat{Q}_k$ such that (Isidori 1989)

$$\begin{bmatrix} Y_k(t) \\ z_k(t) \end{bmatrix} = \hat{Q}_k x(t) = \begin{bmatrix} C_k^* \\ Z_k \end{bmatrix} x(t)$$

where

$$Y_k(t) \left[y_1, \dot{y}_1, \ldots, \frac{\mathrm{d}^{(r_{k,1}-1)}}{\mathrm{d}t^{(r_{k,1}-1)}} y_1, y_2, \dot{y}_2, \ldots, \frac{\mathrm{d}^{(r_{k,2}-1)}}{\mathrm{d}t^{(r_{k,2}-1)}} y_2, \ldots, y_p, \dot{y}_p, \ldots, \frac{\mathrm{d}^{(r_{k,p}-1)}}{\mathrm{d}t^{(r_{k,p}-1)}} y_p \right]'$$

and $r_k = [r_{k,1} \; r_{k,2} \; \ldots \; r_{k,p}]$ is the system's vector relative degree for $t_k \leqslant t \leqslant t_{k+1}$ (where we assume $t_0 = -\infty$). Here C_k^* maps the system states into the outputs and its time derivatives and Z_p maps the states into the internal dynamics z_k.

Note that a necessary condition for exact output tracking in the interval I_k is that the system state at time t_k is such that

$$Y_k(t_k) = Y_{k,\mathrm{d}}(t_k)$$

In addition, to maintain exact tracking we need to ensure that

$$\dot{Y}_k(t) = \dot{Y}_{k,\mathrm{d}}(t), \quad \forall t \in [t_k, t_{k+1})$$

Let

$$y_{\mathrm{d}}^{(r_k)} = \left[\frac{\mathrm{d}^{(r_{k,1})}}{\mathrm{d}t^{(r_{k,1})}} y_{\mathrm{d},1}, \frac{\mathrm{d}^{(r_{k,2})}}{\mathrm{d}t^{(r_{k,2})}} y_{\mathrm{d},2}, \ldots, \frac{\mathrm{d}^{(r_{k,p})}}{\mathrm{d}t^{(r_{k,p})}} y_{\mathrm{d},p} \right]'$$

then we can find the following unique control law (provided that Assumption 1 is satisfied) (Isidori 1989):

$$u_{\mathrm{d}}(t) = F_k x(t) + G_k y_{\mathrm{d}}^{(r_k)}(t) \tag{3}$$

such that the time derivative of the output is the same as that of the desired output trajectory y_{d} (this is also a necessary condition for exact output tracking). This exact-tracking control is completely determined by the state $x(t_k)$, and by the desired output along with its derivatives up to the order r_k.

Substituting the control law (3) into (2) we obtain for $t \in I_k$:

$$\dot{x}(t) = A_y(k)x(t) + B_y(k)y_{\mathrm{d}}^{(r_k)}(t) \tag{4}$$

where $A_y(k) = A(k) + B(k)F_k$, $B_y(k) = B(k)G_k$. In the transformed coordinates the system equations for $t \in I_k$ are of the form

$$\left.\begin{aligned} \dot{Y}_k(t) &= \dot{Y}_{k,\mathrm{d}}(t) \\ \dot{z}_k(t) &= A_z(k)z_k(t) + A_{z,y}(k)Y_k(t) + B_z(k)y_{\mathrm{d}}^{(r_k)}(t) \end{aligned}\right\} \tag{5}$$

Our objective is to define under which conditions it is possible to define a feasible state trajectory $x_{\mathrm{d}}(t)$ such that exact trajectory tracking is preserved through all the time intervals. There are two main hurdles. Firstly, the existence of at least a state trajectory which maintains exact output tracking needs to be determined. This depends on compatibility of the desired output with the given system. Secondly, the state trajectories need to be bounded. In systems with unstable internal dynamics (non-minimum-phase systems) generic solutions tend to be unbounded. In this case, we need to establish additional conditions for the existence of bounded solutions to the internal dynamics.

In this paper we restrict ourselves to the case where: $Y_{k,\mathrm{d}}$, the output along with its time derivatives, has a compact support $[T_i, T_f] \in (-\infty, \infty)$; (*b*) the switching occurs within this compact set; and (*c*) the internal dynamics are hyperbolic before T_i and after T_f. More formally, we have the following assumption.

Assumption 2: *The desired output trajectory* $y_{\mathrm{d}}(\cdot)$ *and its time derivatives are bounded and have compact support* $S(y_{\mathrm{d}}) = [T_i, T_f]$. *The switching in the system parameters are at fixed times* $t_k \in (T_i, T_f)$ *for every* $k \in [1, \ldots, N]$.

Assumption 3: *The system* (1) *has hyperbolic internal dynamics, i.e. the eigenvalues of* $A_z(k)$ *have non-zero real parts (no centres) for* $k = 0$ *and* $k = N$. *This is equivalent to requiring that the original system* (1) *have no zeros which lie on the imaginary axis (Isidori* 1989*) for* $k = 0$ *and* $k = N$.

The last assumption implies the existence of transformations Q_0 and Q_N such that the system state can be partitioned into

$$\begin{bmatrix} Y_k(t) \\ z_{sk}(t) \\ z_{uk}(t) \end{bmatrix} = Q_k x(t) = \begin{bmatrix} C_k^* \\ Z_{sk} \\ Z_{uk} \end{bmatrix} x(t) \tag{6}$$

where z_{sk} and z_{uk} are the coordinates for the stable and the unstable subspaces of the system's internal dynamics.

2.4. *Notations*

Towards establishing conditions for the existence of solutions to the exact tracking problem for a prescribed output, we first study the dynamic evolution of the system for a given initial condition.

Given an initial condition in an interval I_k, the system's evolution for $t_k \leqslant t \leqslant t_{k+1}$ is described by

$$x_{\mathrm{d}}(t) = \exp\left[A_y(k)(t - t_k)\right] x_{\mathrm{d}}(t_k) + \int_{t_k}^{t} \exp\left[A_y(k)(t - \tau)\right] B_y(k) y_{\mathrm{d}}^{(r_k)}(\tau)\, \mathrm{d}\tau$$

In a more compact form

$$x_{\mathrm{d}}(t) = \Phi_k(t, t_k) x_d(t_k) + h_k(t, t_k)$$

where

$$\Phi_k(t, t_k) = \exp\left[A_y(k)(t - t_k)\right]$$

and

$$h_k(t, t_k) = \int_{t_k}^{t} \exp\left[A_y(k)(t - \tau)\right] B_y(k) y_{\mathrm{d}}^{(r_k)}(\tau)\, \mathrm{d}\tau$$

The above equations describe the flow in an interval where the system does not undergo switches. To obtain a representation of the system state in terms of an initial state that does not belong to the same interval, we define flow compositions as follows:

$$\Psi_{k,i}(t, t_i) = \Phi_k(t, t_k) \circ \Phi_{k-1}(t_k, t_{k-1}) \circ \cdots \circ \Phi_i(t_{i+1}, t_i)$$

$$H_{k,i}(t, t_i) = h_k(t, t_k) + \sum_{j=i}^{k-1} \Psi_{k-1,j}(t_{k-1}, t_j) h_j(t_{j+1}, t_j)$$

where

$$\Psi_{i,i}(t, t_i) = \Phi_i(t, t_i)$$

and

$$H_{i,i}(t, t_i) = h_i(t, t_i)$$

The system evolution for an initial condition $x(T_i)$ can be rewritten as

$$x(t) = \Psi_{k,0}(t, T_i)x(T_i) + H_{k,0}(t, T_i) \tag{7}$$

2.5. *Necessary and sufficient conditions*

We first formally state the result.

Lemma 1: *Under Assumptions* 1–3, *the exact output tracking problem is solvable with bounded solution if and only if the system of equations:*

$$Y_{dk}(t_k) = C_k^* Q_k \Psi_{k-1,0}(t_k, T_i) Q_0^{-1} \begin{bmatrix} 0 \\ 0 \\ z_{u,0}(T_i) \end{bmatrix} + C_k^* Q_k H_{k-1,0}(t_k, T_i), \quad \forall k = 1, \ldots, N \tag{8}$$

$$0 = Z_{uN} \left(\Psi_{N,0}(T_f, T_i) Q_0^{-1} \begin{bmatrix} 0 \\ 0 \\ z_{u,0}(T_i) \end{bmatrix} + H_{N,0}(T_f, T_i) \right) \tag{9}$$

admits a solution in $z_{u,0}(T_i)$.

Proof: System trajectories outside $[T_i, T_f]$, the compact support of Y_d, are bounded if and only if z_{uN}, the unstable component of the internal-dynamics, is zero at the end of the motion T_f and similarly the stable component z_{s0} is zero before time T_i. Formally

$$x(T_i) = Q_0^{-1} \begin{bmatrix} 0 \\ 0 \\ z_{u,0}(T_i) \end{bmatrix}$$

$$x(T_f) = Q_N^{-1} \begin{bmatrix} 0 \\ z_{s,N}(T_f) \\ 0 \end{bmatrix}$$

Substitution of the preceding expressions into (7) computed at $t = T_f$

$$x(T_f) = \Psi_{N,0}(T_f, T_i)x(T_i) + H_{N,0}(T_f, T_i)$$

gives (9). In addition, exact tracking in every interval I_k is possible if it is possible to find state trajectories that are continuous and such that $C_k^* x(t_k) = Y_{dk}(t_k)$. By using (7), that gives the state at $t = t_k$ as a function of the initial state and the constraint on $x(T_i)$, (8) easily follows. □

Equation (8) will be referred in the following as compatibility conditions, and (9) will be referred to as stability condition. The compatibility conditions ensure that Y_d does not jump across switches (or else unbounded inputs would be required). The stability condition ensures that the autonomous system dynamics for $t \to \pm\infty$ are bounded.

The algebraic conditions expressed by Lemma 1 can also be interpreted in a geometric coordinate-free framework. To this end, let

$$\mathscr{L}_k = \{x : Y_k = Y_{d,k}(t_k)\}, \quad k \in [0, \ldots, N]$$

represents the set of the admissible system states at time t_k to achieve exact tracking in the time interval $t_k \leqslant t < t_{k+1}$. $\mathscr{L}_k$ is in general a linear variety in the state space that reduces to a linear subspace (the system internal dynamics) for $k = 0$.

A necessary condition for achieving exact tracking when $t < T_i$ is $x_d(T_i) \in \mathscr{L}_0$. Furthermore, to maintain a bounded solution for all $t < T_i$ it is necessary that the initial state belong to the unstable subspace of the system internal dynamics $x_d(T_i) \in \mathscr{L}_{u,0}$.

Note that every $x_d(T_i)$ determines a unique $x_d(t_1)$, given by

$$x_d(t_1) = \Phi_0(t_1, T_i)x_d(T_i) + h_0(t_1, T_i)$$

Hence, we can define the image of the subspace $\mathscr{L}_{u,0}$ as

$$\Phi_0(t_1, t_0) \circ \mathscr{L}_{u,0} = \{x : x = \Phi_0(t_1, t_0)y + h_0(t_1, t_0);\ y \in \mathscr{L}_{u,0}\}$$

which represents the linear variety composed by the points reachable at time t_1 with the constraint of $y(t) = y_d(t)$ for all $t \in [t_0, t_1)$.

To maintain exact tracking in the next interval $t \in [t_1, t_2)$, it is necessary that $x_d(t_1) \in \mathscr{L}_1$. The compatibility condition at time $t = t_1$ states that

$$x_d(t_1) \in \mathscr{L}_1 \cap \Phi_0(t_1, T_i) \circ \mathscr{L}_{u,0}$$

which is possible if and only if the linear variety

$$\mathscr{S}_1 = \mathscr{L}_1 \cap \Phi_0(t_1, T_i) \circ \mathscr{L}_{u,0}$$

is not empty, i.e. if and only if $\mathscr{L}_1$ intersects the image of $\mathscr{L}_{u,0}$ under the system flow. The same procedure can be repeated for the switching time $t = t_2$. Starting from $\mathscr{S}_1$, we can flow forwards in time. To achieve exact tracking in the interval $[t_2, t_3)$, the image of $\mathscr{S}_1$ must intersect $\mathscr{L}_2$, i.e. the set

$$\mathscr{S}_2 = \mathscr{L}_2 \cap \Phi_1(t_2, t_1) \circ \mathscr{S}_1$$

must be not empty and more generally, the exact tracking in $t \in [T_i, t_{k+1})$ is possible if and only if the image of $\mathscr{S}_{k-1}$ under the system flow $\Phi_{k-1}(t_k, t_{k-1})$ intersects $\mathscr{L}_k$, i.e. the set

$$\mathscr{S}_k = \mathscr{L}_k \cap \Phi_{k-1}(t_k, t_{k-1}) \circ \mathscr{S}_{k-1} \tag{10}$$

is non-empty for every $k = 1, \ldots, N$. However, to obtain a bounded solution for $t > T_f$, the final state at time $t = T_f$ must belong to the stable subspace of the system internal dynamics $\mathscr{L}_{s,N}$. Let

$$\mathscr{S}_{T_f} \triangleq \mathscr{L}_{s,N} \cap \Phi_N(T_f, t_N) \circ \mathscr{S}_N$$

Hence, we have proved an analogue of Lemma 1 in geometric terms.

Lemma 2: *The exact output tracking problem is solvable if and only if $\mathscr{S}_{T_f}$ is non-empty, i.e.*

$$\mathscr{S}_{T_f} \neq \varnothing \tag{11}$$

As the flow of a linear system is a homeomorphism, the dimension of a linear variety and that of its image are equal, and hence

$$\dim(\mathscr{S}_i) \geqslant \dim(\mathscr{S}_j), \quad j \geqslant i$$

This means that at each iteration (10) the set of possible solutions could reduce at each K and that no solution is possible if it becomes the empty set for some k, i.e. it is empty for every $j \geqslant k$.

2.6. *Switched systems with invariant internal-dynamics subspace*

We present below a particular case in which the given conditions considerably simplify. This exemplifies the obtained results and will be illustrated with an example in § 5.

Assumption 4: *The system* (1) *has constant relative degree* $r = r_k$ *for every* k, *and matrix* $C_k^* = C^*$ *is constant for every* k.

It follows from the previous assumption that the coordinates outside the internal dynamics Y_k are the same for every k, and thus the internal dynamics subspace is the same for every k. Note that the stable and unstable subspaces may still be different, and may switch around, but are constrained to belong to the same subspace.

As $Y_k = C^*x$, the continuity of x implies that the compatibility conditions are always satisfied.

Lemma 3: *If assumption* 4 *is satisfied, then the compatibility conditions are satisfied for every smooth enough* (C^r) *desired output trajectory* $y_d(t)$.

In addition, $\Phi_k(t_{k+1}, t_k) \circ \mathscr{S}_k \subset \mathscr{L}_{k+1}$ implies that

$$\mathscr{S}_{k+1} = \Phi_k(t_{k+1}, t_k) \circ \mathscr{S}_k$$

is non-empty because $0 \in \mathscr{S}_0$. Further $\dim(\mathscr{S}_n) = \dim(\mathscr{L}_{0,u})$.

The additional condition for boundedness of solutions for $t > T_f$ is met if and only if $\mathscr{S}_N$ intersects $\mathscr{L}_{s,N}$. The linear variety $\mathscr{S}_N$ can be expressed as

$$\mathscr{S}_N = \mathrm{Im}(S_N) + v$$

and the stable subspace of the internal dynamics can be expressed as

$$\mathscr{L}_{s,N} = \mathrm{Im}(L_{s,N})$$

From the previous considerations we have the following lemma.

Lemma 4: *If Assumptions* 1–4 *hold, then the exact output tracking problem with bounded solution is solvable if*

$$\mathrm{rank}\,[S_N \quad L_{N,s}] = n_z \tag{12}$$

where n_z *is the dimension of the system internal dynamics at* $t = T_f$.

As a last remark in this section, note that if not only do the internal dynamics subspace remain constant across the switchings, as ensured by Assumption 4, but its stable and unstable subspaces do too; then the condition (12) is always satisfied and the problem has a solution for every admissible $y_d(t)$. Moreover, this solution is

unique for every given $y_d(t)$. This implies that the exact-tracking problem for a system without switches is always solvable.

3. y_d given through an exosystem

In this section we consider how the preceding results can be specified when the reference trajectory is not completely general but is generated through a known linear exosystem, given by

$$\left.\begin{aligned} \dot{x}_e &= A_e(k)x_e \\ y_d &= C_e(k)x_e \end{aligned}\right\} \tag{13}$$

First we solve the tracking problem when the initial state of the exosystem (at time T_i) is known in advance, hence the obtained result will be valid for the particular reference trajectory determined by the initial condition. Later, we will extend the approach to the case of unknown initial conditions. In this case, we look for asymptotic tracking of the reference trajectories for arbitrary initial conditions of the exosystem.

We begin by studying the case where the state of the exosystem $x_e(T_i)$ is known. The system equation (4) becomes

$$\dot{x}_d(t) = A_y(k)x(t) + B_y(k)C_e^*(k)x_e(t) \tag{14}$$

with $y_d^{(r_k)}(t) \triangleq C_e^*(k)x_e(t)$, because all the time derivatives of the output can be written in terms of x_e by using (13).

The system evolution can then be rewritten as

$$x(t) = \Psi_{k,0}(t, T_i)x(T_i) + \hat{H}_{k,0}(t, T_i)x_e(T_i) \tag{15}$$

where

$$\hat{H}_{k,i}(t, t_i) = \hat{h}_k(t, t_k) + \sum_{j=i}^{k-1} \Psi_{k-1,j}(t_{k-1}, t_j)\hat{h}_j(t_{j+1}, t_j)$$

$$\hat{h}_k(t, t_k) = \int_{t_k}^{t} \exp\left[A_y(k)(t-\tau)\right] B_y(k)C_e^*(k)\hat{\Psi}_{k,0}(\tau, T_i)\, d\tau$$

and $\hat{\Psi}_{k,0}(\tau, T_i)$ is the evolution of the exosystem (analogous to (7)). A solution to the exact tracking problem exists if Lemma 2 is satisfied. The compatibility condition is satisfied for all initial conditions $x_d(T_i) \in \mathscr{L}_0$ if $C_e^* = C^*$. The stability condition becomes

$$0 = s_1 z_{u,0}(T_i) + s_2 x_e(T_i) \tag{16}$$

where

$$s_1 = Z_{uN}\Psi_{N,0}(T_f, T_i)Q_0^{-1}\begin{bmatrix} 0 \\ 0 \\ I \end{bmatrix}$$

$$s_2 = Z_{uN}\hat{H}_{N,0}(T_f, T_i)$$

In what is to follow, we will assume that the above equation has a unique solution (iff s_1 is invertible). This yields a one-to-one relationship between the plant's state and the exosystem, as follows:

$$x_d(T_i) = Q_0^{-1}\begin{bmatrix} 0 \\ 0 \\ z_{u,T_i}(T_i) \end{bmatrix}$$

$$= Q_0^{-1}\begin{bmatrix} 0 \\ 0 \\ -s_1^{-1}s_2 x_e(T_i) \end{bmatrix} \triangleq G(T_i)x_e(T_i)$$

What is interesting is that we can also write the desired exact tracking state trajectory in terms of the exosystem state. By substituting the above expression into (15) we obtain

$$x_d(t) = G(t)x_e(t)$$

where

$$G(t) \triangleq [\Psi_{k,T_i}(t, T_i)G_{(T_i)} + \hat{H}_{k,T_i}(t, T_i)C_e^*]\hat{\Psi}_{k,0}^{-1}(N, T_i)x_e(t) \tag{17}$$

It may be verified that $G(t)$ satisfies the differential equation

$$\dot{G}_k(t) = A_y(k)G_k(t) - G_k^T(t)A_e(k) + C_e^*$$

In the case of no switching, a constant solution always exists for the above Lyapunov equation provided that the eigenvalues of the exosystem A_e are different from the zeros of the plant eigenvalues of A_y. The above equation also provides a control strategy when the exosystem states are not known. We estimate the state of the exosystem as $\hat{x}_e$ and regulate the trajectory $\hat{x}_d = G(t)\hat{x}_e$. The stability of such a controller is studied in the next section.

4. Stabilization

If the state of the exosystem x_e is not known, then we could estimate it as $\hat{x}_e$ with $\|x_e(t) - \hat{x}_e(t)\|_2 \leqslant K_e\, e^{\alpha_e t}\|x_e(0) - \hat{x}_e(0)\|_2$. We use $\hat{x}_d(t) = G(t)\hat{x}_e(t)$ as the estimated desired state trajectory, and stabilize this trajectory by using the control scheme shown in Fig. 3. Note that the feedforward used (see (3)) is completely specified in terms of the exosystem's state estimate, as follows:

$$\begin{aligned} u_d &= F_{k,1}x_d(t) + F_{k,2}\, y_d^{(r_k)}(t) \\ &= F_{k,1}G(t)\hat{x}_e(t) + F_{k,2}C_e^*\hat{x}_e(t) \\ &\triangleq F_k\hat{x}_e(t) \end{aligned}$$

The state equations are of the form

$$\dot{x} = A_k x + B_k(F_k\hat{x}_e + K(x - G(t)\hat{x}_e))$$

We require that the system in each interval is either stable or stabilizable. For simplicity, we assume that $A(k) + B(k)K$ is Hurwitz for all k; the arguments remain valid if the system is stabilized through any other feedback control scheme.

The desired trajectory satisfies

$$\dot{x}_d = A_k x_d + B_k F_k x_e$$

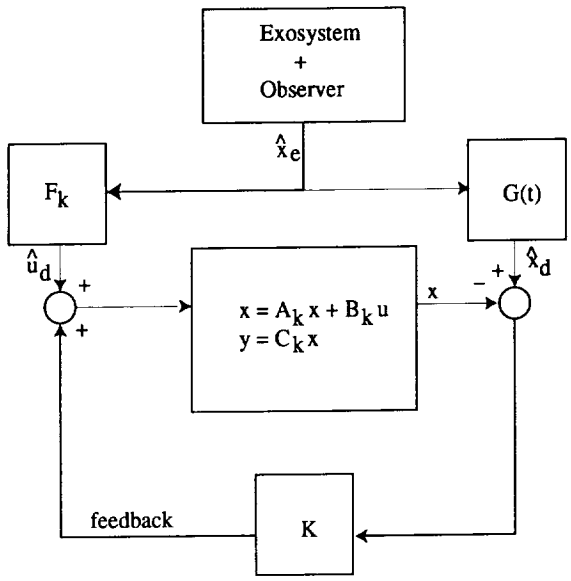

Figure 3. Trajectory tracking with exosystem.

Let $e := x - x_d$. Then the difference between the last two equations yields

$$\dot{e} = (A_k + B_k K)e + (B_k F_k + B_k K G(t))(\hat{x}_e - x_e)$$

The exponential stability of the error dynamics system follows from the next lemma.

Lemma 5: *Given the system* $\dot{e} = Ae + v(t)$, *where* $K_1 e^{\alpha_1 t} < \|e^{-At}\|_2 < K_2 e^{\alpha_2 t}$ *and* $\|v(t)\|_2 < K_3 e^{-\alpha_3 t}$, *with* K_1, K_2, K_3 *positive, then* $e = 0$ *is an exponentially stable equilibrium point, provided that* $\alpha_3 > \alpha_2 > 0$.

Proof: Using the variation of constants formula

$$\begin{aligned}
\|e^{-At}e(t)\|_2 &\leqslant \left\| e(0) + \int_0^t e^{-A\tau} v(\tau)\, d\tau \right\|_2 \\
&\leqslant \|e(0)\|_2 + \left\| \int_0^t e^{-A\tau} v(\tau)\, d\tau \right\|_2 \\
&\leqslant \|e(0)\|_2 + \int_0^t \|e^{-A\tau} v(\tau)\|_2\, d\tau \\
&\leqslant \|e(0)\|_2 + K_2 K_3 \int_0^t e^{\alpha_2 - \alpha_3}\, d\tau \\
&\leqslant \|e(0)\|_2 + K_2 K_3 \frac{1}{\alpha_3 - \alpha_2}
\end{aligned}$$

provided that $\alpha_3 > \alpha_2$. Hence

$$K_1 \|e^{\alpha_1 t} e(t)\|_2 \leqslant \|e^{-At} e(t)\|_2 \leqslant \|e(0)\|_2 + K_2 K_3 \frac{1}{\alpha_3 - \alpha_2}$$

the right-hand side being a constant. Therefore, for all $\epsilon > 0$ there exists a positive constant K such that

$$\|e(t)\|_2 < K\,\mathrm{e}^{-(\alpha_1-\epsilon)}$$

5. Example

Consider the flexible structure, cantilevered at the base and free at the top, shown in Fig. 4. It is modelled (with the finite-element method) with a single flexural element. The degrees of freedom are the translational motion at the base x_1, and the top x_2, and the rotation at the top x_3. The input is a translational force at the base and the system output is x_2. The structure is loaded with a mass m_t, which is changed at several instances. The flexural element has the following properties: mass 420; length 1; elastic modulus 1; and cross-sectional area moment of inertia 1. The objective is to maintain the top of the structure along a prescribed trajectory to facilitate the transfer of the load. The equations of motion can be described by

$$M\ddot{x} + Sx = \hat{B}u$$

where

$$M = \begin{bmatrix} 156 & 54 & -13 \\ 54 & 156 + m_t & -22 \\ -13 & -22 & 4 \end{bmatrix}, \quad S = \begin{bmatrix} 12 & -12 & 6 \\ -12 & 12 & -6 \\ 6 & -6 & 4 \end{bmatrix}$$

$x = [x_1 \;\; x_2 \;\; x_3]'$, and $\hat{B} = [1 \;\; 0 \;\; 0]'$.

In the standard form $x = [x' \;\; \dot{x}']'$ (abuse of notation) we have the dynamics as

$$\dot{x} = A_k x + B_k u$$

$$y_k = C_k x$$

where

$$A_k = \begin{bmatrix} 0 & I \\ -M^{-1}S & 0 \end{bmatrix}, \quad B_k = \begin{bmatrix} 0 \\ M^{-1}\hat{B} \end{bmatrix}, \quad C_k = [0 \;\; 1 \;\; 0 \;\; 0 \;\; 0 \;\; 0]$$

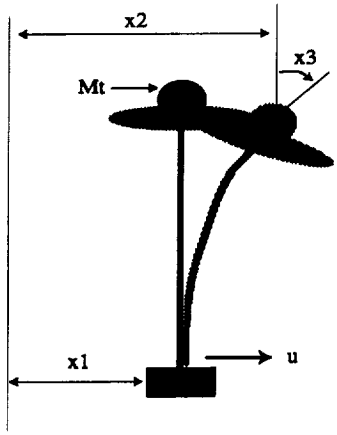

Figure 4. Example.

The desired trajectory is generated by an exosystem of the form $\dot{x}_e = A_e x_e$, where

$$A_e = \begin{bmatrix} 0 & 1 & 0 & 0 \\ -1 & 0 & 0 & 0 \\ 0 & 1 & 0 & 0 \\ 0 & 0 & 1 & 0 \end{bmatrix}$$

and the desired output is $y_d = [0\ 0\ 0\ 1]x_e \triangleq C_e x_e$. We also switch the exosystem to $A_e = 0^{4\times 4}$ at the initial and final times $T_i = 0$ and $T_f = 2pi$. The first two states of the exosystem form an oscillator and the second state is then integrated twice to obtain the desired output. Note that (A_e, C_e) is observable. Hence the exosystem states can be estimated. In our simulations we ensure that the output trajectories have a compact support $[0, 2\pi]$ by choosing initial conditions of the exosystem of the form $x_e(T_i) = [0; *; 0; 0]$.

We also switch the mass m_t on the structure (see Fig. 4) to take the values $m_t = 0$, $\forall t \in [0, \pi/2]$, $m_t = 100$, $\forall t \in (\pi/2, 1{\cdot}5\pi]$, and $m_t = 10$, $\forall t \in (1{\cdot}5\pi, 2\pi]$, which denotes the jumps in the system. Note that C_k^* remains constant through the switches and hence the compatibility conditions are always satisfied. As illustrated in § 3, the map $G(0) : x_e(T_i) \to x_d(T_i)$ is given as

$$G(0) = \begin{bmatrix} -4{\cdot}6715 & -3{\cdot}3239 & 0 & 0 \\ 0 & 0 & 0 & 1 \\ 6{\cdot}9406 & 2{\cdot}6672 & 0 & 0 \\ -0{\cdot}5935 & -1{\cdot}4710 & 0 & 0 \\ 0 & 0 & 1 & 0 \\ 2{\cdot}6851 & -0{\cdot}8211 & 0 & 0 \end{bmatrix}$$

As an example we simulate the forward dynamics with the initial condition for the exosystem as $[0\ 1\ 0\ 0]'$. The corresponding initial system state for exact output tracking is

$$x_d(T_i) = [-3{\cdot}3239 \quad 0 \quad 2{\cdot}6672 \quad -1{\cdot}471 \quad 0 \quad -0{\cdot}8211]'$$

The simulation results are shown in Fig. 5, where the exact tracking state trajectory is shown; this desired state trajectory yields the desired output with an error of 10^{-6} for a motion of two units. This error is believed to be due to the numerical integration schemes. Furthermore, the initial conditions are large and unrealistic. The initial conditions of the system are typically not the same as the initial conditions of the desired state trajectory; this results in initial transient errors. If the system is stabilized then these errors decay exponentially, even if the system dynamics has switches. This ability to maintain tracking across switches is a major advantage of our approach. Furthermore, preactuation techniques to achieve these initial conditions (with output error maintained at zero) has been developed by Devasia *et al.* (1996) and we expect to integrate the two approaches in the future.

6. Conclusions

The problem of achieving exact output tracking for linear systems that present jumps in a parameter's values has been analysed. We have established necessary and sufficient conditions for the existence of exact output-tracking bounded state trajectories. When the reference trajectory is generated through an exosystem, the

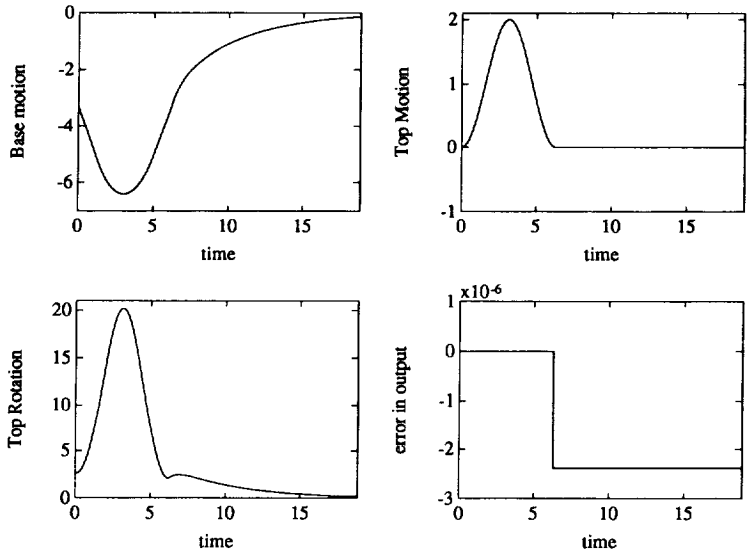

Figure 5. Simulation results.

feedforward action needed to maintain exact tracking can be written as a time-varying feedback. Furthermore, this time-varying feedback is related to a map from the state of the exosystem to the desired system state. The map is linear and is shown to satisfy an ordinary differential equation. For the case of systems without switches the presented theory reduces to the standard regulator theory. We also showed that the desired trajectory can be stabilized and presented the simulation results for an example flexible structure with switching mass.

Future work will attempt to remove the requirement of compact support for the output. There is also a need to address the tracking problem for systems whose internal dynamics may not be hyperbolic.

Acknowledgment

This work was supported through National Science Foundation grant MSS-9216690, NASA Ames Research Center Grant NAG 2-1042, and by the Astro Aerospace Corporation.

References

Basile, G., and Marro, G., 1992, *Controlled and Conditioned Invariants in Linear System Theory* (Prentice Hall).

Devasia, S., Chen, D., and Paden, B., 1996, Nonlinear inversion-based output tracking. *IEEE Transactions on Automatic Control*, **41**, 930–943.

Francis, B. A., 1977, The linear multivariable regulator problem. *Journal of Control and Optimization*, **15**, 486–505.

Hunt, L. R., Meyer, G., and Su, R., 1996, Noncausal inverses for linear systems. *IEEE Transactions on Automatic Control*, **41**, 608–611.

Isidori, A., 1989, *Nonlinear Control Systems: An Introduction* (Berlin: Springer-Verlag).

Marro, G., and Piazzi, A., 1993, Regulation without transients under large parameter jumps. *Proceedings of the 12th IFAC World Congress*, pp. 23–26.

MEYER, G., HUNT, L. R., and SU, R., 1995, Nonlinear system guidance. *Proceedings of the IEEE Conference on Decision and Control*, New Orleans, Louisiana, U.S.A., pp. 590–595.

WONHAM, W. M., 1985, *Linear Multivariable Control: a Geometric Approach* (Berlin: Springer-Verlag).